ISAS - INTERNATIONAL SCHOOL
FOR ADVANCED STUDIES

Study and Solution of the Five-Vertex Model

Thesis submitted for the degree of
"Doctor Philosophiæ"

CANDIDATE
Miklós Gulácsi

SUPERVISOR
Prof. Andrea C. Levi

October 1991

TRIESTE

SISSA - SCUOLA
INTERNAZIONALE
SUPERIORE
STUDI AVANZATI
TRIESTE
Strada Costiera 11

SISSA ISAS

Study and Solution of the Five-Vertex Model

Thesis submitted for the degree of

"Doctor Philosophiæ"

CANDIDATE

Miklós Gulácsi

SUPERVISOR

Prof. Andrea C. Levi

October 1991

Index

Introduction

After the solution of the Ising model and the dimer problem, the next class of statistical mechanical models to prove tractable was that of the *ice-type* models.

There exist in nature a number of crystals with hydrogen bonding. The most familiar example is ice, where the oxygen atoms form a lattice of coordination four, and between each adjacent pair of atoms is a hydrogen ion. Each ion is located near one or the other end of the bond in which it lies. On the basis of electrical neutrality the ions must satisfy the so-called *ice rule*: of the four ions surrounding each atom, two are close to it, and two are removed from it, on their respective bonds. All the systems or models which satisfy this rule are called *ice-type* models.

The hydrogen-ion bonds between atoms form electric dipoles, so can be conveniently represented by arrows placed on the bonds pointing toward the end occupied by the ion. The ice rule is then equivalent to stating that at each site (or vertex) of the lattice there are two arrows in and two arrows out. For this reason the ice-type models are known as *six-vertex* models. The general model includes three important models as special cases, the ice, F- and KDP-models.

Since the solution of these special cases by Lieb [1] and a more general model by Sutherland, Yang and Yang [2], the main effort concerning the ice-type models has been directed to analyzing the properties of these solutions, their connection to other statistical models and to quantum systems, or the finite-size effects. More recently, with the increasing development of theoretical studies on crystal growth, the need of a solution for a new type of vertex model on the square lattice has become imminent. This is the motivation of the present work.

Even though realistic models of crystal growth are complex, perhaps beyond any hope of an exact solution, some variants of the terrace-ledge-kink model [3] (TLK) can be solved exactly. The TLK model, where growth and evaporation take place only by attachment and detachment of atoms at kink sites along steps, is appropriate for a crystal of rectangular (in particular, cubic) symmetry. Assuming the steps to run up and to the right exclusively on the crystal surface, a special case of the TLK model was mapped by Garrod, Levi and Touzani [4] onto the well-known six-vertex model [5,6].

Let us consider the line representation [5,6] of the allowed arrow configurations of the six-vertex model in terms of *fermion* lines. Performing the mapping procedure of Ref. [4], the step lines on the crystal surface can be identified with such *fermion* lines. An important observation, however, is that no crossing of lines will occur. That is, vertex two (see Fig. 1.1.c) is actually absent from the surface model used in Ref. [4] to describe crystal growth. This seemingly strange result becomes evident if we keep in mind that vertex two would imply multiple steps to develop, and cavities to appear, which is not allowed in the terrace-ledge-kink growth model. Based on these physical motivations we were led to look for an exact solution of the five-vertex model.

This model has a relatively long history. The non-interacting case, and only this one, was solved by the Pfaffian method by Wu [7], using the equivalence of the five-vertex model on a square lattice (called *modified* KDP model by Wu) to that of close-packed dimers on a hexagonal lattice. However, it was known already from the works on dimer statistics of Kasteleyn [8] and Fisher [9] that a phase transition exists. The correlation functions of the dimers, and consequently of the arrows in the five-vertex model, were recently computed by Garrod [10].

The only way to get some insight in the five-vertex case starting from the six-vertex model, is to consider the latter in a direct field. However, it turns out (see § **2.11**) that, if such limits are performed, the *free-fermion* condition is fulfilled. The traditional solution of the six-vertex model applies to the five-vertex model only in the non-interacting case. Here we present a general solution of the model based on the Bethe Ansatz.

The organization of the thesis is as follows. In Chap. **1** all the known exact solvable vertex models of statistical mechanics are reviewed, emphasizing the common properties and algebraic identity of the solutions of different models. In Chap. **2** the solution of the five-vertex model is given in a very comprehensive manner. Chap. **3** is devoted to applications. After a general description of the spin-spin correlation function of the integrable models, we give the connection of the height-height correlation (more exactly, the mean square height difference) of a surface with the vertex models and compute the relevant quantities for our case.

Chapter 1

Exactly Solvable Vertex Models in Statistical Mechanics

1.1 Introduction

One aspect of statistical mechanics is the study of models. It should be accepted that almost all Hamiltonians, even those regarded as fundamental, are really models. One of the main reasons that models are introduced is the attempt to understand one of the most striking phenomena of nature, namely phase transitions. Various studies of models in statistical mechanics show that only a few of them are solvable, and even fewer are completely solvable. The two dimensional lattice models of interacting systems which were exactly solved are as follows

i) Ising model, solved by Onsager [11],

ii) spherical model, Berlin and Kac [12],

iii) dimer model, Kasteleyn [8] and Fisher [9],

iv) six-vertex model, Lieb [1],

v) eight-vertex model, Baxter [13],

vi) triangular three-spin model, Baxter and Wu [14],

vii) self-dual Potts model, Baxter [15],

viii) hard hexagon model, Baxter [16].

The spherical model is distinct from the others in that it can be solved in any dimension, but it has the non-physical feature that it introduces interactions between spins infinitely far apart. Due to this feature its solution differs from the others. The only three dimensional model which has been solved exactly, up to date is the

i) Zamolodchikov model [17].

The solution of which initially was conjectured by Zamolodchikov [17] and verified to be exact by Baxter [18].

All these models can be regarded as special cases of a more general (and in general unsolved) model of the "Interaction-Round-a-Face" (IRF) model. Moreover these can be regarded as extensions of the Ising model. Thus all of them can be solved also by the transfer matrix method (for the Ising and dimer models the transfer matrix reduces to Pfaffians). Subsequently it was realized [19,20] that models vi) and viii) are special cases of the eight-vertex model and model vii) is equivalent to the six-vertex model [21]. We are then left with two distinct vertex models to be studied, that is the six- and the eight-vertex model. Note, that the six-vertex model without an external electric field can be related to a critical limit of the eight-vertex model [22].

The vertex models define a statistical mechanics on a (for simplicity) square lattice as follows. On each link there is a degree of freedom taking two values which is represented (traditionally) by an arrow, i.e. $\rightarrow$ and $\leftarrow$. To each vector therefore there corresponds $2^4 = 16$ possible configurations. To each of these we associate a Boltzmann weight $\omega_i = \exp(-\beta\varepsilon_i)$. This general model is referred to as the sixteen-vertex model. It is equivalent to an Ising model with two, three and four body interactions and with an external magnetic field[23]. The exact solution of this general ferroelectric model is not known. Only in two cases we know that the system will exhibit an Ising like transition. These two cases are obtained[24] by a specific choice of the Boltzmann weights which leads inevitably to an Ising model with only two body interactions.

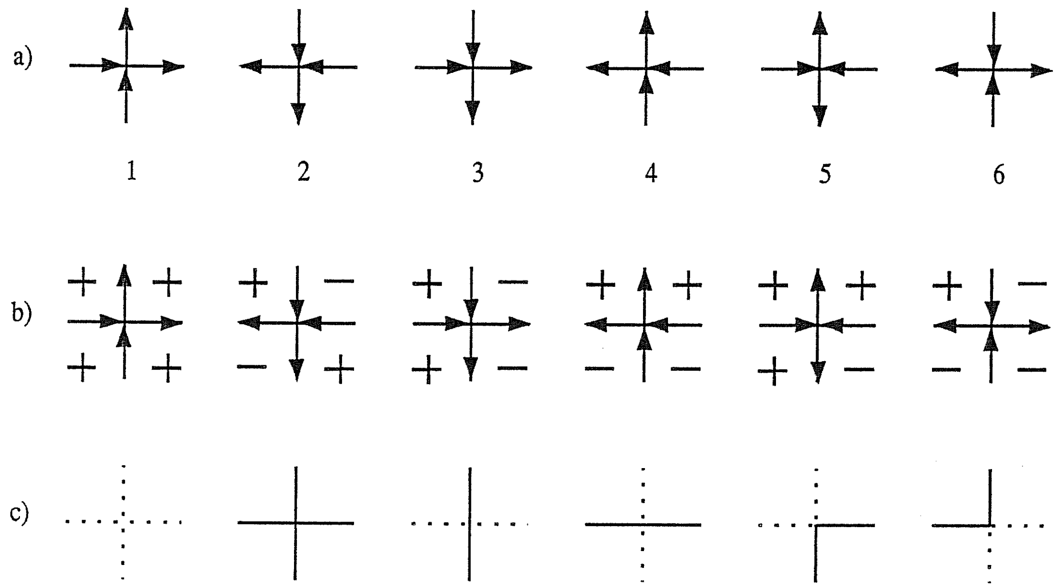

Fig. 1.1: a) The six arrow configurations allowed at a vertex in the case of the six-vertex model, b) the corresponding Ising spin configurations and c) the corresponding line configurations.

If we choose the Boltzmann weights, so that six vertices with two entering and two exiting arrows (or eight vertices including also the cases where four or zero arrows exit) have finite weight, then we define the six- or eight-vertex models. The corresponding vertices of the six-vertex model are shown in Fig. 1.1 a), while the two additional vertices of the eight-vertex model are presented in Fig. 1.2.

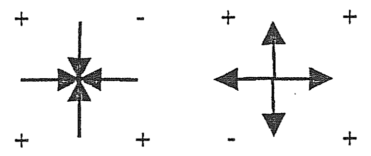

7 8

Fig. 1.2: The additional two arrow configurations of the eight-vertex model, with the corresponding Ising spin configurations.

In terms of the transfer matrix to each vertex there corresponds an Ising spin configuration, shown in Fig. 1.1 b) and Fig. 1.2. The correspondence is defined by the relation: an arrow points up (down) or right (left), if the two adjacent Ising spins have the same (opposite) sign. Thus, the Boltzmann weights $\omega_1, \ldots, \omega_6$ can be denoted in a convenient way by $W(a,b,c,d)$, where $a, \ldots, d = \pm 1$ are the Ising spins at the sites of an elementary cell of the two dimensional square lattice. As an example, let us consider this transformation in the case of vertex one (performing also a rotation by $\pi/4$)

$$\begin{array}{ccc} & \uparrow & \\ \rightarrow & & \rightarrow \\ & \uparrow & \end{array} \equiv \begin{array}{ccc} \searrow & & \nearrow \\ & & \\ \nearrow & & \searrow \end{array} \equiv \begin{array}{ccc} & +1 & \\ +1 & & +1 \\ & +1 & \end{array}$$

The Boltzmann weight is

$$W(a,b,c,d) \equiv W\left(\begin{array}{ccc} & c & \\ d & & b \\ & a & \end{array} \right) \equiv W\left(\begin{array}{ccc} & +1 & \\ +1 & & +1 \\ & +1 & \end{array} \right) .$$

The partition function in the language of the Ising spins becomes

$$Z = \prod_{cells} W(a,b,c,d) \quad , \tag{1.1}$$

In the general model of IRF to each site of an elementary cell (face) is associated a spin σ and only interactions between spins situated on a common face is taken into account. This model can be easily generalized to three dimensions (Zamolodchikov model). In this case all possible interactions within each elementary cube must be considered. The partition function will be

$$Z = \prod_{cubes} W(a, \ldots, h) \quad , \tag{1.2}$$

where $a, \ldots, h$ are the eight corner spins of a cube. Considering the conditions [17] in which the solution of the Zamolodchikov model was found, we obtain a corresponding eight-vertex model in three dimensions. These vertices are built up by combining the first four two dimensional vertices of Fig. 1.1 a) with two vertical arrow configurations. Four of these three dimensional vertices are presented in Fig. 1.3. The remaining four are obtained from Fig. 1.3 by inverting the vertical arrows.

In all these cases we are interested in computing the free energy. With the exception of the Zamolodchikov model, the free energy is obtained using the transfer matrix. Suppose that the square lattice has M rows and N columns, and impose cyclic (i.e. toroidal) boundary conditions (some models, like the symmetric six-vertex model can be solved also for rotating boundary conditions [25]). Consider two successive rows of vertical bonds with an intervening row of horizontal bonds. The transfer matrix, defined by mapping a state of one row into the successive one, is given by

$$T_{\{a\}}^{\{c\}} = \sum_{d_1, \ldots, d_N} \prod_{i=1}^{N} W(a_i, d_{i+1}, a_{i+1}, d_i) \quad , \tag{1.3}$$

where $\{a\} \equiv a_1, \ldots, a_N$, similarly for c. In terms of the transfer matrix, from

Eq. (1.1) we find

$$Z = \mathrm{Tr}\, T^M \equiv \sum \Lambda^M \quad , \tag{1.4}$$

where Λ are the eigenvalues of the transfer matrix. Since the free energy per site is

$$f = -k_B T \lim_{M,N\to\infty} \frac{1}{MN} \ln Z \quad , \tag{1.5}$$

If the largest eigenvalue Λ_0 is separated from the others by a gap, we find immediately

$$f = -k_B T \lim_{N\to\infty} \frac{1}{N} \ln \Lambda_0 \quad , \tag{1.6}$$

The other eigenvalues are suppressed in the thermodynamic limit.

In the following paragraphs we will analyze in detail the solution of the six-vertex model, without analyzing the resulting spectrum. This is needed, in order to analyze the specific limits of the six-vertex model which can be related to the five-vertex case. For completeness, we present briefly the solution of the eight-vertex and Zamolodchikov models.

1.2 The Asymmetric Six-Vertex Model

The eigenvalues of the six-vertex model can be obtained in several ways. We will follow the method of the algebraic Bethe Ansatz. The following analysis is mainly based on Baxter [5], Gaudin [26], Lieb [1], Lieb and Wu [6] and the Yangs [2]. The maximum number of vertices which can be solved by the algebraic Bethe Ansatz is six. For all $\omega_1, \ldots, \omega_6$ independent, the eigenvalue in terms of fugacities ($z = \exp ik$) is

$$\Lambda = \omega_1^{N-n} \prod_{i=1}^{n} [\omega_3 + \frac{\omega_5 \omega_6 z_i}{\omega_1 - \omega_4 z_i}] + \omega_4^{N-n} \prod_{i=1}^{n} [\omega_2 - \frac{\omega_5 \omega_6}{\omega_1 - \omega_4 z_i}] \quad , \tag{1.7}$$

where the fugacities must satisfy

$$z_i^N = (-1)^{n-1} \prod_{j=1}^{n} \frac{\omega_1\omega_3 + \omega_2\omega_4 z_i z_j - (\omega_1\omega_2 + \omega_3\omega_4 - \omega_5\omega_6) z_i}{\omega_1\omega_3 + \omega_2\omega_4 z_i z_j - (\omega_1\omega_2 + \omega_3\omega_4 - \omega_5\omega_6) z_j} \quad . \tag{1.8}$$

For a derivation, see Appendix A. Eqs. (1.7) and (1.8) describe the solution of the general six-vertex model with six independent variables. However, it is enough to consider only four independent variables [6]. This is because the zero of energy can be chosen arbitrarily and the ice rule implies $\omega_5 = \omega_6$. In this situation the model is called asymmetric six-vertex model [2], in opposition to the symmetric six-vertex model [1,5] where the number of independent variables is two. However, the approach to solve the asymmetric six-vertex model is to find another parameter family of weights with two independent variables such that the original transfer matrix commutes with the transfer matrix of the initial problem. This is actually the basic idea of the quantum inverse scattering method [27,28]. Thus, the problem of solving the asymmetric six-vertex model is reduced to a known result. This way of reducing the number of variables is common also in other solvable models, e.g. the Heisenberg chain or the Hubbard chain.

The parametrization which is introduced in the six-vertex models is given in Eq. (B.1), see Appendix B

$$a = \sqrt{\omega_1\omega_2} \quad , \qquad b = \sqrt{\omega_3\omega_4} \quad , \qquad c = \sqrt{\omega_5\omega_6} \quad . \tag{1.9}$$

The symmetric case is obtained by $\omega_1 = \omega_2$, $\omega_3 = \omega_4$ and $\omega_5 = \omega_6$. For the asymmetric six-vertex model we are left with five independent variables $\omega_1, \omega_2, \omega_3, \omega_4$ and $\omega_5 = \omega_6$. From these, we define four new variables (see, Eqs.(B.2) - (B.5) from Appendix B) as

$$\eta = \frac{a}{b} \equiv e^{\beta\delta} \quad , \tag{1.10}$$

$$\Delta_6 \; = \; \frac{a^2 + b^2 - c^2}{2ab} \; \equiv \; \frac{1}{2} \left(\eta + \frac{1}{\eta} - \xi\right) \quad , \tag{1.11}$$

where $\xi = c^2/ab \equiv \exp(2\beta\epsilon)$, and

$$H \; = \; \sqrt{\frac{\omega_1 \omega_3}{\omega_2 \omega_4}} \; \equiv \; e^{2\beta h} \quad , \qquad V \; = \; \sqrt{\frac{\omega_1 \omega_4}{\omega_2 \omega_3}} \; \equiv \; e^{2\beta v} \quad . \tag{1.12}$$

These variables become complete by imposing the condition [2,26]

$$\omega_1 \; \omega_2 \; \omega_3 \; \omega_4 \; = \; 1 \quad . \tag{1.13}$$

That is, from the original five independent variables four independent variables are obtained [2,26]. The reason to choose these variables, i.e. η, Δ_6, h, v as new variables, is that the transfer matrix obtained will depend only on the variables η, Δ_6. Thus it will commute (actually it turns out to be identical) with the transfer matrix of the symmetric six-vertex model. (V appears as a factor which multipies the transfer matrix, the effect of H is slightly more complicated.)

Let us treat the $\Delta_6 < 1$ region (if $\Delta_6 > 1$ the eigenvalue equations reduce to a very simple form, see Eq. (B.38) of Appendix B). Making the dummy variable change $z_i^0 = Hz_i$ in Eq. (1.7) and introducing the spectral parameter ϕ as in Eqs. (B.18) of Appendix B, the parametrization, Eq. (B.20), is obtained:

$$\begin{aligned}
a \; &= \; \begin{cases} \sin \frac{\mu+\phi}{2} \, , & \text{if } \Delta_6 = -\cos\mu \; ; \\ \sinh \frac{\lambda+\phi}{2} \, , & \text{if } \Delta_6 = -\cosh\lambda \; , \end{cases} \\
b \; &= \; \begin{cases} \sin \frac{\mu-\phi}{2} \, , & \text{if } \Delta_6 = -\cos\mu \; ; \\ \sinh \frac{\lambda-\phi}{2} \, , & \text{if } \Delta_6 = -\cosh\lambda \; , \end{cases} \\
c \; &= \; \begin{cases} \sin\mu \, , & \text{if } \Delta_6 = -\cos\mu \; ; \\ \sinh\lambda \, , & \text{if } \Delta_6 = -\cosh\lambda \; . \end{cases}
\end{aligned} \tag{1.14}$$

This parametrization is identical with that of the symmetric six-vertex model [5], or the Heisenberg-Ising chain [29] one. A similar parametrization can also be given for the Hubbard chain [30], in which case $a = 1$, $b = i\sin k/(i\sin k + U)$ and $c = U/(i\sin k + U)$. The free energy per site [Eq. (1.6)] becomes

$$\begin{aligned} f &= \min\{ -k_BT/N\ln\Lambda_L - h - vp_v \,, \\ &\qquad -k_BT/N\ln\Lambda_M + h - vp_v \} \quad , \end{aligned} \tag{1.15}$$

where $p_v = 1 - 2n/N$ is the vertical polarization. The largest eigenvalues are obtained, see Eqs. (B.27) and (B.28) of Appendix B, to be equal to

$$\Lambda_L = \begin{cases} \sin^N \frac{1}{2}(\mu+\phi) \prod_{i=1}^n \frac{\sin\frac{1}{2}(\phi-\phi_i-2\mu)}{\sin\frac{1}{2}(\phi-\phi_i)} \,, & \text{if } \Delta_6 = -\cos\mu \,; \\ \sinh^N \frac{1}{2}(\lambda+\phi) \prod_{i=1}^n \frac{\sinh\frac{1}{2}(\phi-\phi_i-2\lambda)}{\sinh\frac{1}{2}(\phi-\phi_i)} \,, & \text{if } \Delta_6 = -\cosh\lambda \,, \end{cases} \tag{1.16}$$

and

$$\Lambda_M = \begin{cases} \sin^N \frac{1}{2}(\mu-\phi) \prod_{i=1}^n \frac{\sin\frac{1}{2}(\phi-\phi_i+2\mu)}{\sin\frac{1}{2}(\phi-\phi_i)} \,, & \text{if } \Delta_6 = -\cos\mu \,; \\ \sinh^N \frac{1}{2}(\lambda-\phi) \prod_{i=1}^n \frac{\sinh\frac{1}{2}(\phi-\phi_i+2\lambda)}{\sinh\frac{1}{2}(\phi-\phi_i)} \,, & \text{if } \Delta_6 = -\cosh\lambda \,. \end{cases} \tag{1.17}$$

At this level it can be seen, that not only the algebraic parametrization is identical with the other known exact solutions, but also the algebraic form of the eigenvalues Λ_L and Λ_M from Eqs. (1.16) and (1.17) is equivalent with that of the eigenvalues of the symmetric six-vertex model [5], the Heisenberg-Ising chain [29], and even the Hubbard chain [30]. Due to this reason all these models can be treated on a common ground by the quantum inverse scattering method.

1.3 Relationship of the Six-Vertex Model and the Quantum Spin Chain

The fact that the algebraic forms of the eigenvalues are identical in different models suggests an equivalence between these models. Hereafter we will deal only with the equivalence between the six-vertex model and the Heisenberg (more generally

Heisenberg-Ising) one dimensional quantum spin system. The equivalence with the Hubbard chain is rather complicated and needs the introduction of two sublattices.

The configurations of up and down arrows on a vertical bond of the vertex models are evidently isomorphic to the state of a chain of spin 1/2 particles. In order to prove this isomorphism, first we must write up the transfer matrix of the vertices in terms of the Pauli spin operators and secondly, find a non-trivial linear Hamiltonian which commutes with the transfer matrix. For a special case of the six-vertex model [31] and of the eight-vertex model [32] this equivalence was shown to exist. This calculations were extended for the general six- and eight-vertex model by Barouch [6] and Gaudin [26]. The detailed calculations for the general six-vertex model are given in Appendix C.

If all the six vertices are considered to be independent, and all of the ω_i strictly positive, then the Hamiltonian corresponding to the general eigenvalues of Eq. (1.7) is

$$\mathcal{H} = \frac{1}{2}\frac{\omega_1\omega_3+\omega_2\omega_4}{\sqrt{\omega_1\omega_2\omega_3\omega_4}}\sum_{i=1}^{N}[(1+\gamma)\sigma_i^+\sigma_{i+1}^- + (1-\gamma)\sigma_i^-\sigma_{i+1}^+ + \tilde{\Delta}\sigma_i^z\sigma_{i+1}^z] \quad , \tag{1.18}$$

where

$$\gamma = \frac{\omega_2\omega_4-\omega_1\omega_3}{\omega_2\omega_4+\omega_1\omega_3} \quad ,$$

and the general anisotropy constant

$$\tilde{\Delta} = \frac{\omega_1\omega_2+\omega_3\omega_4-\omega_5\omega_6}{\omega_1\omega_3+\omega_2\omega_4} \quad ,$$

defined in Eq. (A.32) of Appendix A, appears in a natural way also in the Hamiltonian representation. Notice that $\tilde{\Delta}$ and Δ_6 are not identical. For the asymmetric six-vertex case, with the notations of Eqs. (1.11), (1.12), the corresponding Hamiltonian becomes

$$\begin{aligned}\mathcal{H} &= H\sigma_i^+\sigma_{i+1}^- + \frac{1}{H}\sigma_i^-\sigma_{i+1}^+ + \Delta_6\sigma_i^z\sigma_{i+1}^z \quad , \\ &= \cosh(2\beta h)\,(\sigma_i^+\sigma_{i+1}^- + \sigma_i^-\sigma_{i+1}^+) \\ &+ \sinh(2\beta h)\,(\sigma_i^+\sigma_{i+1}^- - \sigma_i^-\sigma_{i+1}^+) + \Delta_6\sigma_i^z\sigma_{i+1}^z \quad .\end{aligned} \tag{1.19}$$

The symmetric six-vertex case can easily be seen to reduce to the well-known Heisenberg-Ising form[29] ($\gamma = 0$). The Heisenberg-Ising chain reduces further to the Heisenberg chain for $\tilde{\Delta} = \pm 1$, to the XY chain for $\tilde{\Delta} = 0$ and to the Ising chain for $\tilde{\Delta} \rightarrow \pm\infty$.

1.4 The Quantum Inverse Scattering Method and the Eight-Vertex Model

In the following, we present briefly the way of obtaining the eigenvalues of Eqs. (1.16) and (1.17) by a different method than the algebraic Bethe Ansatz, which also holds[27,28] for the eight-vertex model[5,13]. Let us consider the eight-vertex model and denote the Boltzmann weights $\omega_1 = \omega_2 = a$, $\omega_3 = \omega_4 = b$, $\omega_5 = \omega_6 = c$ and $\omega_7 = \omega_8 = d$. The original transfer matrix $T(\omega_1, \omega_3, \omega_5, \omega_7)$ is transformed into the language of IRF by choosing a parametrization

$$T = \sum_{i=1}^{3} w_i\, \sigma^i_{j_1 j_3}\sigma^i_{j_4 j_2} = \sum_{i=0}^{3} w_i\, (\sigma^i \otimes \sigma^i)_{j_1 j_3, j_4 j_2} \quad , \tag{1.20}$$

where the subscript i labels the spin variable, the subscript j label the matrix element of the Pauli matrix σ and σ^0 is the 2×2 unity matrix. The Boltzmann weight of an elementary cell is defined as in Eq. (1.1) as $W(j_1, j_2, j_3, j_4)$. From

Eq. (1.20) the connection between the ω's and w's is obtained as $\omega_1 = w_3 + w_4$, $\omega_3 = w_3 - w_4$, $\omega_5 = w_1 + w_2$ and $\omega_7 = w_1 - w_2$. We are looking for the conditions for which the two transfer matrices commute[27,28], that is $[T(\omega_i), T(w_i)] = 0$. For the eight-vertex case this condition gives six equations, of which just three are independent. For the six-vertex case four equations are obtained with only two of them independent. Obviously, the solution of these equations depends on the initial values of $a, \ldots, d$. Baxter[5,13] defines the fundamental region by $c > a + b + d$, $a > 0$, $b > 0$ and $d > 0$. All other regions can be obtained from this fundamental region by elementary variable transformations.

In both eight- and six-vertex cases, the equations to be solved define an elliptic curve[27,28] written in parametric form, with three (let us call them μ, ϕ and q) or two (μ and ϕ) independent parameters. For the six-vertex case Eqs. (1.14) are verified

$$\begin{aligned} a &= \sin \frac{1}{2}(\mu + \phi) \ , \\ b &= \sin \frac{1}{2}(\mu - \phi) \ , \\ c &= \sin \mu \quad . \end{aligned} \tag{1.21}$$

While for the eight-vertex case the following results are obtained:

$$\begin{aligned} a &= w_3 + w_4 &= sn[\frac{1}{2}(\mu + \phi), q] \ , \\ b &= w_3 - w_4 &= sn[\frac{1}{2}(\mu - \phi), q] \ , \\ c &= w_1 + w_2 &= sn[\mu, q] \ , \\ d &= w_1 - w_2 &= q \ sn[\frac{1}{2}(\mu + \phi), q] \ sn[\frac{1}{2}(\mu - \phi), q] \ sn[\mu, q] \quad . \end{aligned} \tag{1.22}$$

Here $sn(u, v)$ denotes the elliptic sine[33] of modulus v. The derivation of Eqs. (1.21) and (1.22) is very tedious, but it can be found in Ref. [28]. The elliptic sine and cosine function have nearly the same properties as the trigonometric sin and cos functions, with the $\pi/2 \to \Pi$ change, where $\Pi = \int_0^{\pi/2} dt/\sqrt{1 - q^2 \sin^2 t}$.

In the process of calculating the commutator of two transfer matrices, it turns out that the sufficient condition for the commutator to be zero is the existence of two matrices, τ (the so-called monodromy matrix) and R, with the property $R(\tau \otimes \tau') = (\tau' \otimes \tau)R$. The R matrix can be any 4×4 matrix which satisfies the above equation, while τ is a 2×2 matrix, connected to the transfer matrix by $T = \mathrm{Tr}\ \tau$ and can be expressed as a product $\tau = \prod_{i=1}^{n} L_i$. The parametrization of L_i is identical with that of the transfer matrix, Eq. (1.20) with the $\phi \to \phi_i$ change. τ' is defined as a product of L'_i matrices, which are parametrized by w'_i in Eq. (1.20). The values of w'_i obtained are identical with those of w_i from Eqs. (1.21), provide ϕ is replaced by ϕ'. For the R matrix we can use again Eq. (1.20) with w''_i as a parameter. For w''_i the same equations, i.e. Eq. (1.20) are obtained with the variable change $\phi \to \phi - \phi' + \mu$.

For the symmetric six-vertex model ($d = 0$) the diagonal elements of τ which are obtained, during the calculation of the commutator of the two transfer matrices, are identical with Eqs. (1.16) and (1.17). Thus the eigenvalue of the transfer matrix will be

$$\begin{aligned}\Lambda &= \sin^N \frac{1}{2}(\mu + \phi) \prod_{i=1}^{n} \frac{\sin \frac{1}{2}(\phi - \phi_i - 2\mu)}{\sin \frac{1}{2}(\phi - \phi_i)} \\ &+ \sin^N \frac{1}{2}(\mu - \phi) \prod_{i=1}^{n} \frac{\sin \frac{1}{2}(\phi - \phi_i + 2\mu)}{\sin \frac{1}{2}(\phi - \phi_i)} \quad .\end{aligned} \tag{1.23}$$

The terms $\sin^N \frac{1}{2}(\mu+\phi)$, $\sin^N \frac{1}{2}(\mu-\phi)$ are the eigenvalues of the reference (vacuum) state. These for the symmetric six-vertex model are equal with a^N and b^N.

For the eight-vertex model the eigenvalues of the reference state are changed to $h^N[\frac{1}{2}(\mu + \phi)]$ and $h^N[\frac{1}{2}(\mu - \phi)]$. If we use the definition of the Jacobian elliptic sine function $sn(u, v)$ in terms of the generalized theta functions [33] $H(u, v)$ and $\Theta(u, v)$, as $sn(u, v) = \sqrt{v}H(u, v)/\Theta(u, v)$ then $h(u)$ is defined [5] to be $h(u) =$

$-i\Theta(0,v)\Theta(iu,v)H(iu,v)$ for any v. The eigenvalues of the total transfer matrix are obtained [34]

$$\begin{aligned}\Lambda &= h^N[\frac{1}{2}(\mu+\phi)]\; e^{C(\mu+\phi)} \prod_{i=1}^{n} \frac{h[\frac{1}{2}(\phi-\phi_i-2\mu)]}{h[\frac{1}{2}(\phi-\phi_i)]} \\ &+ h^N[\frac{1}{2}(\mu-\phi)]\; e^{C(\mu-\phi)} \prod_{i=1}^{n} \frac{h[\frac{1}{2}(\phi-\phi_i+2\mu)]}{h[\frac{1}{2}(\phi-\phi_i)]} \quad .\end{aligned} \tag{1.24}$$

If n is odd, then the $\mu \to \mu - 2i\Pi$ change should be made. C denotes a well defined constant dependent on n. As it can be seen from Eq. (1.24), the algebraic structure of the solution is identical with that of the six-vertex model, only instead of circular sine functions the elliptic sine functions occur. From Eq. (1.22) it results, that the $q \to 0$ limit must give back the symmetric six-vertex model solution, i.e. Eq. (1.23). By a systematic study [35], indeed it can be shown that the two eigenvalues are identical in the $q \to 0$ limit. For further information about the eigenvalues of the eight-vertex model see Ref. [34]. For the spectrum, thermodynamic properties and correlations, see Refs. [5,13] .

With the quantum inverse scattering method a general description of the integrable models emerged. It turned out that all integrable models possess an infinite set of commuting charges. The existence of this infinite number of conserved charges guarantees the integrability, but restricts the dynamics, in the sense that production of particles in a collision is absent. The colliding particles only undergo time delays and exchange quantum numbers. As a consequence, the scattering matrix is factorizable. This can be understood by considering a scattering of three particles, labelled by 1, 2 and 3. Factorizability of the scattering matrix means that $S(123) = S(12)\ S(13)\ S(23)$. As the particles are interchangeable, consistency requires

$$S(12)\ S(13)\ S(23) \ = \ S(23)\ S(13)\ S(12) \quad . \tag{1.25}$$

Eq. (1.25), known as the star-triangle[11] or Yang[36]-Baxter[13] relation, guarantees integrability. This is a consistency requirement for the scattering matrices. A number of new exactly solvable models have been found by only analyzing the different possible solutions of the Yang-Baxter equation. Even the free energy can be quickly calculated by the so-called inversion-relation trick[37] directly from the Yang-Baxter equation. However, the calculated free energy does depend on making some assumptions regarding its analyticity as a function of the spectral parameter (usually denoted by ϕ).

1.5 The Zamolodchikov Model

The inversion-relation can be easily generalized to three dimensions[38], as also the star-triangle (Yang-Baxter) relation can be generalized to three dimensions[38], as the tetrahedron relation. However, in three dimension there are 14 boundary spins. Thus, the tetrahedron relation will generate 2^{14} separate equations to satisfy. It seems unlike that this coupled system of equations can be solved in other than the trivial case. However, in 1980 Zamolodchikov[17] conjectured a solution. Using the three dimensional inversion relation Baxter[18] has proven that Zamolodchikov's conjecture was indeed correct.

The model seems to be a three dimensional free-fermion model[17], but it does not factor into independent two-dimensional checkboard Ising models[18]. From the symmetry point of view, it has the same symmetry properties as the two dimensional eight-vertex model. The original solution was given in terms of IRF corner spin variables. However, we have related it to three dimensional vertices and we obtained eight independent vertices. Thus, the Zamolodchikov model represents an eight-vertex model in three dimensions. From these eight vertices, four are given in Fig. 1.3. The next four vertices are obtained from these by reversing the arrows in the vertical direction. By inspection of Fig. 1.3, it can be seen that the projections of the four vertices shown here onto the (x, y) plane are identical to the first four vertices of the six-vertex model, see Fig. 1.1. The statistical system has four independent variables, which can be related to the Boltzmann weights of the eight vertices taken to be equal two-by-two.

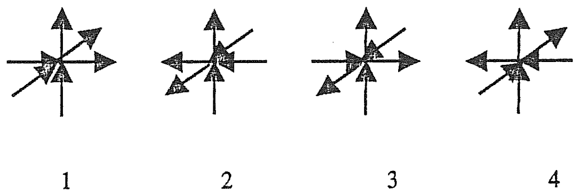

Fig. 1.3: Four arrow configurations of the Zamolodchikov model. The remaining four vertices can be obtained from these ones, by changing the up arrow of the vertical direction, in down arrows.

If we put a spin in the center of a cube, the model allows four independent spin interactions between the central spin and the cube site spins. These coefficients are related [18] to the three sides a_1, a_2, a_3 and the perimeter s of a spherical triangle, by which we built up the cube. Denoting $\alpha_0 = \pi - s$ and $\alpha_i = s - a_i$, the partition function in the thermodynamic limit is [17,18]

$$Z = \frac{1}{2} \prod_{i=0}^{4} G(\alpha_i) \quad , \tag{1.26}$$

where

$$\ln G(\alpha) = \frac{1}{2\pi} \int_0^{\alpha} \left[x \cot x + \frac{\pi}{2} \tan \frac{x}{2} - \ln(2 \sin x)\right] dx \quad . \tag{1.27}$$

From variational arguments [39] it seems that the model is always critical as an n-layer three-dimensional model, that is the correlation length is always infinite.

Chapter 2

The Five-Vertex Model

2.1 Definition of the Model

As we saw in Chap. **1**, the known exactly solvable models in two dimensional statistical mechanics are characterized by an even number of vertices. From these, the basic one is the six-vertex model, which is characterized by the six vertices presented in Fig. 1.1 a). Instead of vertices ω_5 and ω_6 we could also take ω_7 and ω_8 of Fig. 1.2. The six vertices ω_1, ω_2, ω_3, ω_4, ω_7 and ω_8 can be transformed into the usual vertices ω_1, ω_2, ω_3, ω_4, ω_5 and ω_6 by a unitary transformation applied on the transfer matrix, which makes the interchange $\sigma^+ \leftrightarrow \sigma^-$.

From these vertices, without restriction the condition $\omega_5 = \omega_6$ can be assumed to hold, as indicated in Chap. **1**. From Fig. 1.1 a) it is obvious that vertex five is a sink of horizontal arrows, while vertex six is a source. By imposing cylindrical boundary conditions, the number of sources and sinks must be equal. Thus, the vertices five and six will enter into the partition function only in the combination $\omega_5\omega_6$, so there is no loss of generality in choosing $\omega_5 = \omega_6$. Even if we had chosen them not to be equal, we could transform the transfer matrix by a similarity transformation $\exp(\alpha \sum_i \sigma_i^z)$ and chose α to make the coefficients of the two vertices equal. Such a transformation applied to the transfer matrix preserves linearity.

For the symmetric six-vertex model, the further conditions $\omega_1 = \omega_2$ and $\omega_3 = \omega_4$ are imposed. These ensure that the model is unchanged by reversing all dipole arrows. This one would expect to be the case for a model in zero external field. In these conditions, not only the algebraic form of the solution becomes identical with that of the Heisenberg-Ising chain, but the two transfer matrices commute, thus the two models are equivalent.

If an external field is present, however, that solution of the general six-vertex case should be taken [2] which continuously goes over into that of the Heisenberg-Ising chain, when the fields are varied and made to vanish. This is why, for the asymmetric six-vertex case the $\omega_1\omega_2\omega_3\omega_4 = 1$ condition is imposed. By this, we ensure that the model is unchanged by reversing simultaneously all arrows and the external electric fields. In this condition, see Chap. **1**, the algebraic form of the solution is identical with that of the symmetric six-vertex model and the model turns out to be equivalent with an extended XYZ model.

More recently [4], with the increasing development of theoretical studies on crystal growth, the need of a solution for a new type of vertex model on a square lattice has become imminent. It turns out that in this case only an odd number of vertices are allowed, see Chap. **3**. Since one of the six vertices is forbidden, the model was called [4] five-vertex model. As presented previously, within the six-vertex models $\omega_5 = \omega_6$ always. Thus, one of the remaining four vertices has strictly zero weight. In other words, we define a statistical mechanics on a square lattice with only five vertices with two entering and two exiting arrows. Similarly to the six-vertex model, the number of independent variables can be reduced by two, since $\omega_5 = \omega_6$ as discussed and the zero of energy can be chosen arbitrarily.

Thus, in the most natural way we will define the four equivalent five-vertex models by the Boltzmann weights

$$\begin{aligned}
a &= \omega_1 \,, \quad b = \omega_3 = \omega_4 \,, \quad c = \omega_5 = \omega_6 \,; \\
a &= \omega_2 \,, \quad b = \omega_3 = \omega_4 \,, \quad c = \omega_5 = \omega_6 \,; \\
b &= \omega_3 \,, \quad a = \omega_1 = \omega_2 \,, \quad c = \omega_5 = \omega_6 \,; \\
b &= \omega_4 \,, \quad a = \omega_1 = \omega_2 \,, \quad c = \omega_5 = \omega_6 \quad .
\end{aligned} \tag{2.1}$$

From the previous brief presentation of the symmetric and asymmetric six-vertex model, we can see that in both cases such a limit breaks the conditions in which the respective solutions were given. Those limits which still can be handled are presented in § **2.11**. The solution of the five-vertex model in the free-fermionic case, which could be obtained by means of the Pfaffian method, was already known[7,8].

2.2 The Bethe Ansatz Results

The eigenvalues of the four different cases of Eqs. (2.1) can be one-by-one constructed by the algebraic Bethe Ansatz, as presented in Appendix A. As an example, let us consider the $\omega_2 = 0$ case.

First we consider the vacuum (i.e. the reference state) to be the state with all vertical arrows pointing up, as it was done in Appendix A for the general six-vertex model. Thus, the eigenvalue is identical to Eq. (A.4), i.e. $\omega_1^N + \omega_4^N$. If we have one overturned arrow, the possible configurations are a, c and d of Fig. A.1 from Appendix A. Configuration b is prohibited as $\omega_2 = 0$. Summing up the geometric progressions from Eq. (A.5), for cases a, c and d, and imposing the boundary conditions the eigenvalue is obtained to be

$$\Lambda \;=\; \omega_1^N \, \frac{\omega_1\omega_3 + (\omega_5\omega_6 - \omega_3\omega_4)z}{\omega_1(\omega_1 - \omega_4 z)} \;-\; \omega_4^N \, \frac{\omega_5\omega_6}{\omega_4(\omega_1 - \omega_4 z)} \quad . \tag{2.2}$$

Furthermore, with two overturned arrows, the a, b, d and e configurations of Fig. A.3, and the a, c configurations of Fig. A.4 should be counted. Cancelling the *unwanted* terms, see Appendix A, the eigenvalue obtained is

$$\Lambda \;=\; \omega_1^N \prod_{i=1}^{2} \frac{\omega_1\omega_3 + (\omega_5\omega_6 - \omega_3\omega_4)z_i}{\omega_1(\omega_1 - \omega_4 z_i)} \;-\; \omega_4^N \prod_{i=1}^{2} \frac{\omega_5\omega_6}{\omega_4(\omega_1 - \omega_4 z_i)} \quad . \tag{2.3}$$

Continuing this procedure we obtain the eigenvalue and the consistency equations which can be directly linked to Eqs. (1.7) and (1.8). This is obvious, as Eqs. (1.7) and (1.8) were determined considering all the six vertices $\omega_1, \ldots, \omega_6$ independent. That is, any of the Boltzmann weights can be put equal to zero.

Secondly, let us consider the vacuum to be built up by down pointing arrows, the eigenvalue of which is ω_3^N (see Eq. (A.11)). If we have one overturned arrow the eigenvalue is given in Eq. (A.13). For $\omega_2 = 0$ we obtain

$$\Lambda \;=\; \omega_1\omega_3^{N-1} \;+\; \omega_3^{N-2}\omega_5\omega_6 \frac{1}{z} \quad . \tag{2.4}$$

The above eigenvalue, as it can be seen, describes only a state with four vertices. This is understandable, because the possible configurations left after imposing $\omega_2 = 0$ are very few (see Fig. A.2). Thus we conclude, that the eigenvalues should be constructed as in the previous case, i.e. Eq. (2.3).

The calculation proceeds in the following way. Eqs. (1.7) and (1.8) were determined writing up the algebraic Bethe Ansatz for the vertical down pointing arrows. That is, in Eqs. (1.7) and (1.8) we can put $\omega_2 = 0$ or $\omega_3 = 0$. With the parametrization of Eqs. (2.1) and (2.4) we obtain for the eigenvalues

$$\Lambda \;=\; a^N \prod_{i=1}^{n} \frac{ab - (b^2 - c^2)z_i}{a(a - bz_i)} \;+\; b^N \prod_{i=1}^{n} -\frac{c^2}{b(a - bz_i)} \quad , \tag{2.5}$$

for $\omega_2 = 0$, and

$$\Lambda = a^N \prod_{i=1}^{n} \frac{c^2 z_i}{a(a-bz_i)} + b^N \prod_{i=1}^{n} \frac{a^2 - c^2 + abz_i}{b(a-bz_i)} , \tag{2.6}$$

for $\omega_3 = 0$. From these eigenvalues the quantities $[ab - (b^2 - c^2)z_i] \;/\; [a(a-bz_i)]$ and $(a^2 - c^2 + abz_i) \;/\; [b(a-bz_i)]$ are algebraically identical with those occurring in the symmetric six-vertex model[5]. Let us call them in the same way

$$L(z) = \frac{ab - (b^2 - c^2)z}{a(a - bz)} , \tag{2.7}$$

and

$$M(z) = \frac{a^2 - c^2 + abz}{b(a - bz)} . \tag{2.8}$$

Thus we know, that they can be transformed into each other. The transformation is given in Eq. (A.56) of Appendix A. For the remaining two terms we use the notation

$$M'(z) = -\frac{c^2}{b(a - bz)} , \tag{2.9}$$

and

$$L'(z) = \frac{c^2 z}{a(a - bz)} , \tag{2.10}$$

underlying by this the origin of these terms. It can easily seen that these two terms, i.e. $M'(z)$ and $L'(z)$ also can be transformed one in each other by the same transformation. This means that e.g. the eigenvalues from Eq. (2.6) represent the reflection of those from Eq. (2.5) with respect to the $a = b$ plane.

If we want to consider a five-vertex case with $\omega_1 = 0$ or $\omega_4 = 0$, we must write the algebraic Bethe Ansatz for the vertical arrows pointing up. In this way we obtain an equation similar to Eq. (1.7) with the changes $\omega_1 \leftrightarrow \omega_2$, $\omega_3 \leftrightarrow \omega_4$, see Eq. (A.13) and (A.14) from Appendix A. From these equations, using the parametrization of Eqs. (2.1) we obtain Eqs. (2.5) or (2.6). Thus, all the four cases of the five-vertex model, reduces to the study of Eq. (2.5). For completeness, we will analyze the spectrum of both $L(z)$ and $M'(z)$ terms of Eq. (2.5).

Concerning the consistency equation for the fugacities, we can proceed in the same manner as for the eigenvalue equations. From Eq. (1.8) the $\omega_2 = 0$ and $\omega_3 = 0$ cases can be obtained. These are

$$z_i^N = (-1)^{n-1} \prod_{j=1}^{n} \frac{ab - (b^2 - c^2)z_i}{ab - (b^2 - c^2)z_j} \quad , \tag{2.11}$$

for the $\omega_2 = 0$ case, and

$$z_i^N = (-1)^{n-1} \prod_{j=1}^{n} \frac{ab - (a^2 - c^2)z_i}{ab - (a^2 - c^2)z_j} \quad , \tag{2.12}$$

for the $\omega_3 = 0$ case. In deriving Eq. (2.12) we used the fact that the choice of $z_i \leftrightarrow 1/z_i$ is arbitrary. For the other two cases, $\omega_1 = 0$ and $\omega_4 = 0$ we obtain the same equations, i.e. Eqs. (2.11) and (2.12), respectively. At this level, similarly to the six-vertex model we can define an *interaction* constant, which we will denote by Δ_5. For the definition of which, we use the interaction (anisotropy) constant of the general six-vertex model, see Eq. (A.36) of Appendix A or Eq. (1.18), i.e.

$$\tilde{\Delta} = \frac{\omega_1\omega_2 + \omega_3\omega_4 - \omega_5\omega_6}{\omega_1\omega_3 + \omega_2\omega_4} \quad ,$$

and the parametrization from Eqs. (2.1),

$$\Delta_5 = \begin{cases} (b^2 - c^2)/(a\,b) \ , & \text{if } \omega_1 = 0 \text{ or } \omega_2 = 0 \ ; \\ (a^2 - c^2)/(a\,b) \ , & \text{if } \omega_3 = 0 \text{ or } \omega_4 = 0 \end{cases} . \tag{2.13}$$

The consistency conditions for the fugacities, Eqs. (2.11) and (2.12) will have the form

$$z_i^N = (-1)^{n-1} \prod_{j=1}^{n} \frac{1 - \Delta_5 \, z_i}{1 - \Delta_5 \, z_j} \quad . \tag{2.14}$$

Thus the five-vertex models are characterized by an eigenvalue equation of the form of Eq. (2.5), with the consistency condition of Eq. (2.14).

2.3 Solution of the Consistency Relation and Properties of the Kernel

As for the asymmetric six-vertex model [2], in our case also we assume in Eq. (2.14) that for no j, $1 = \Delta_5 z_j$ is satisfied. In these conditions, Eq. (2.10) can be written as

$$\frac{(1 - \Delta_5 z_i)^n}{z_i^N} = (-1)^{n-1} \prod_{j=1}^{n} (1 - \Delta_5 z_j) \quad . \tag{2.15}$$

Eq. (2.11) written term by term gives

$$\begin{aligned} \frac{(1 - \Delta_5 z_1)^n}{z_1^N} &= (-1)^{n-1} \prod_{j=1}^{n} (1 - \Delta_5 z_j) \; ; \\ \frac{(1 - \Delta_5 z_2)^n}{z_2^N} &= (-1)^{n-1} \prod_{j=1}^{n} (1 - \Delta_5 z_j) \; ; \\ &\ldots ; \\ \frac{(1 - \Delta_5 z_n)^n}{z_n^N} &= (-1)^{n-1} \prod_{j=1}^{n} (1 - \Delta_5 z_j) \quad . \end{aligned} \tag{2.16}$$

Multiplying the left-hand-sides and the right-hand-sides of Eqs. (2.16), we obtain

$$\frac{\prod_{i=1}^{n} (1 - \Delta_5 z_i)^n}{\prod_{i=1}^{n} z_i^N} = (-1)^{n(n-1)} \prod_{j=1}^{n} (1 - \Delta_5 z_j)^n \quad . \tag{2.17}$$

As the term $(-1)^{n(n-1)}$ is always equal to unity, from Eq. (2.17) it results that

$$z_1 \, z_2 \, \ldots \, z_{n-1} \, z_n = \tau \quad , \tag{2.18}$$

with τ being an N-th root of unity. That is, for any N and n, z_i must be of the form

$$z_i \;=\; \exp(i\; k_i) \quad , \tag{2.19}$$

where the k_i's satisfy

$$N \sum_{i=1}^{n} k_i \;=\; 2\pi m \;, \quad m \;=\; 0,\; 1,\; \ldots,\; N-1 \quad . \tag{2.20}$$

These properties were expected to hold, as they hold in any integrable model [29].

In order to see the different solution types, let us analyze the two particle solution, that is $n = 2$. From Eq. (2.18) we have $(z_1 z_2)^N = 1$, from this the Perron-Frobenius theorem implies $z_1 z_2 = 1$. Combining this with the first two equations of Eqs. (2.16) we obtain

$$\Delta_5 \; (z_1^{N-1} \;+\; z_1) \;=\; z_1^N \;+\; 1 \quad . \tag{2.21}$$

Using Eq. (2.19) and a parametrization $r = N/2 - 1$, Eq. (2.21) becomes

$$\Delta_5 \;=\; \frac{\cos(r \;+\; 1)k}{\cos rk} \quad . \tag{2.22}$$

This equation is well known from the symmetric six-vertex model [5]. The plot of the right-hand-side of Eq. (2.22) is given in Fig. 2.1, as a function of k, for k real and for k pure imaginary. We can limit our further analysis to real values of k in the interval $[0,\; \pi/2r]$, or positive pure imaginary values. From Fig. 2.1, it can be seen, that for real k there exists one real solution for $\Delta_5 < 1$, while for k pure

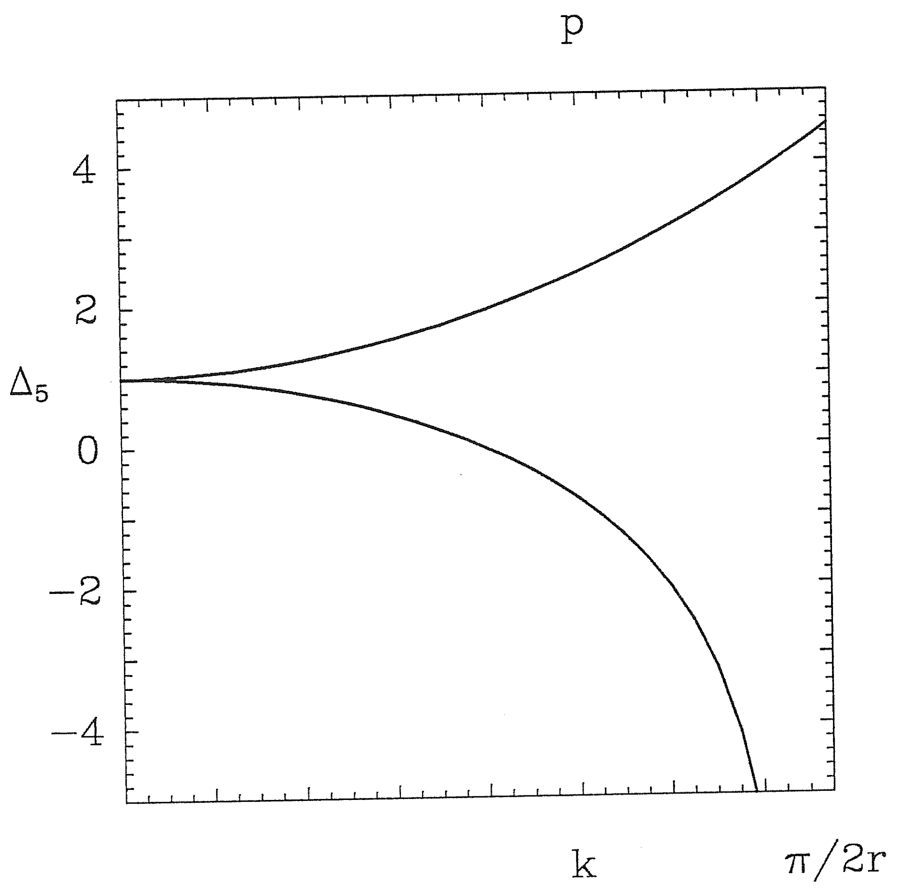

Fig. 2.1: The plot of the right-hand-side of Eq. (2.22) versus p (k=ip) the upper curve, and versus k the lower curve.

imaginary, e.g. $k = ip$, Eq. (2.22) has again a single real solution, but for $\Delta_5 > 1$. These results are again well known from the symmetric six-vertex model [5]. Thus we know that $\Delta_5 > 1$ will represent a frozen-in ferroelectric state.

For the cases for which $\Delta_5 < 1$ the following transformation [29] is performed

$$e^{-i\Theta(p,q)} = \frac{1 - \Delta_5 \, e^{ip}}{1 - \Delta_5 \, e^{iq}} \quad . \tag{2.23}$$

From this, it follows that

$$\begin{aligned} \cos\Theta(p,q) &= 1 - \Delta_5(\cos p + \cos q) + \Delta_5^2\cos(q-p) ; \\ \sin\Theta(p,q) &= \Delta_5(\sin p - \sin q) + \Delta_5^2\sin(q-p) \quad , \end{aligned} \tag{2.24}$$

and hence that

$$\Theta(p,q) = \arctan\frac{\Delta_5(\sin p - \sin q) - \Delta_5^2\sin(p-q)}{1 - \Delta_5(\cos p + \cos q) + \Delta_5^2\cos(p-q)} \quad , \tag{2.25}$$

so $\Theta(p,q)$ is a real function. We recall the symmetric six-vertex form [5], where

$$e^{-i\Theta(p,q)_{\text{six-vertex model}}} = \frac{1 - 2\Delta_6\, e^{ip} + e^{ip+iq}}{1 - \Delta_5\, e^{iq} + e^{ip+iq}} \quad ,$$

and finally

$$\Theta(p,q)_{\text{six-vertex model}} = 2\arctan\frac{\Delta_6\sin\frac{1}{2}(p-q)}{\cos\frac{1}{2}(p+q) - \Delta_6\cos\frac{1}{2}(p-q)} \quad .$$

It seems that the five-vertex case is more complicated than the six-vertex one, but it turns out that not to be the case.

Let us study the analytic properties of the $\Theta(p,q)$ function. Notice that $\Theta(-p,-q) = -\Theta(p,q) = \Theta(q,p)$ and $\Theta(0,0) = 0$. Concerning its definition interval, $\Theta(p,q)$ is a single valued real analytic function of Δ_5, p and q, if the latter two lie in the open interval of the variation range of the k_i's, which is the following

$$\begin{aligned} -(\pi - \nu) < k_i < \pi - \nu \,, &\quad \text{for } \Delta_5 \leq -1 ; \\ -(\pi - \mu) < k_i < \pi - \mu \,, &\quad \text{for } -1 < \Delta_5 < 1 \quad . \end{aligned} \tag{2.26}$$

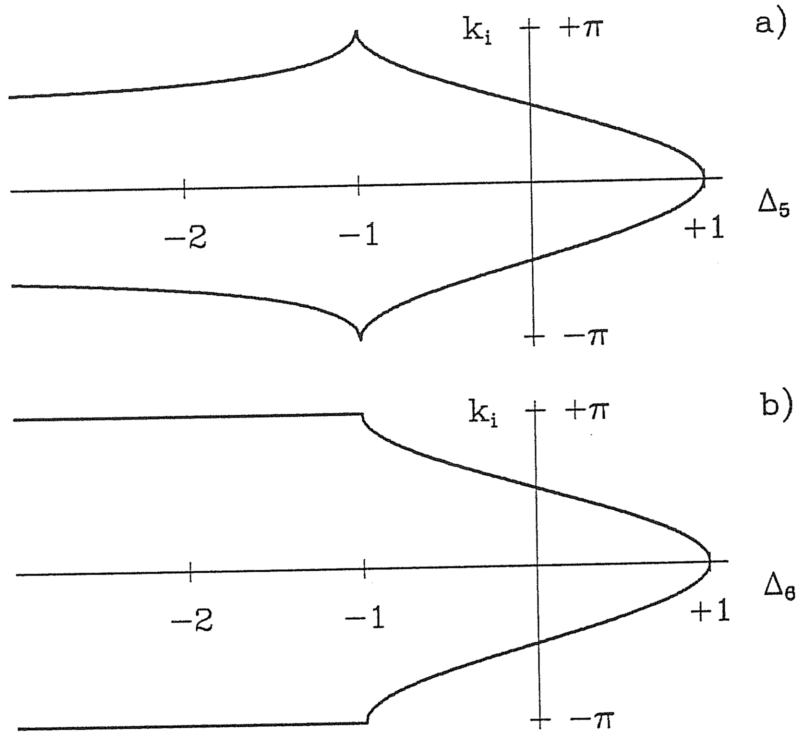

Fig. 2.2: The variation domain of k_i is bordered by the thick curves for the five-vertex a), and six-vertex b) cases.

The parametrization which is defined by the form of $\Theta(p,q)$, corresponding to Eqs. (2.26) is

$$\begin{aligned} \Delta_5 &= -\sec\nu\ , \quad 0 \leq \nu < \pi/2\ ; \\ \Delta_5 &= -\cos\mu\ , \quad 0 < \mu < \pi\ . \end{aligned} \tag{2.27}$$

These conditions are very important, because they define uniquely the branch of the arctan function in Eq. (2.25). The variation range of the k_i's which satisfy Eqs. (2.26) are plotted in Fig. 2.2 a). In Fig. 2.2 b) the variation range of the momenta k_i is given for the case of the symmetric six-vertex model[29]. In the case $\Delta_5 \leq -1$ the two domains are not equivalent. This is also reflected in the parametrization which should be taken for this domain, see Eqs. (2.27).

Under the conditions of the $\Delta_5 \leq -1$ case, see Eqs. (2.26) and (2.27) we have

$$-|\pi - 2\nu| < \Theta(p,q) < |\pi - 2\nu| \quad , \tag{2.28}$$

and $\Theta(p,q)$ has a discontinuity at those p and q values at which

$$\Xi(p,q) = 1 - \Delta_5(\cos p + \cos q) + \Delta_5^2 \cos(p-q) \quad , \tag{2.29}$$

is zero. $\Xi(p,q)$ is the denominator of the right-hand-side of Eq. (2.25). On the other hand, if $-1 < \Delta_5 < 1$ then

$$-|\pi - 2\mu| < \Theta(p,q) < |\pi - 2\mu| \quad , \tag{2.30}$$

and there are no singularities. This behaviour of the $\Theta(p,q)$ function in the intervals $\Delta_5 \leq -1$ and $-1 < \Delta_5 < 1$ is identical[29] with the behaviour of the symmetric six-vertex kernel in the intervals $\Delta_6 \leq -1$ and $-1 < \Delta_6 < 1$.

By direct differentiation of Eq. (2.25) it can be seen that

$$\frac{\partial \Theta(p,q)}{\partial p} = \frac{\Delta_5(\cos p - \Delta_5)}{1 - 2\Delta_5 \cos p + \Delta_5^2} \quad , \tag{2.31}$$

and

$$\frac{\partial \Theta(p,q)}{\partial q} = -\frac{\Delta_5(\cos q - \Delta_5)}{1 - 2\Delta_5 \cos q + \Delta_5^2} \quad . \tag{2.32}$$

That is, the kernel of the five-vertex model is degenerate. Thus, we have a simpler case than that of the symmetric six-vertex model. Obviously, Eqs. (2.31) and (2.32) define the analytic form of the kernel. Integrating

$$\Theta(p,q) = \theta(q) - \theta(p) + \phi(q,p) \quad , \tag{2.33}$$

with

$$\theta(\xi) = \arctan \frac{\sin \xi}{\cos \xi - 1/\Delta_5} \quad , \tag{2.34}$$

where the algebraic identity

$$\frac{\xi}{2} + \arctan[\frac{\Delta_5 + 1}{\Delta_5 - 1} \tan\frac{\xi}{2}] = \arctan\frac{\sin\xi}{\cos\xi - 1/\Delta_5}$$

was used ($\eta \neq \pi$). At first sight $\phi(p,q)$ seems to be a rather complicated function of p and q. However, it turns out in fact to be a piecewise constant. Its form is obtained in the easiest way by equating Eq. (2.34) with Eq. (2.25), and using the relations [33]

$$\begin{aligned}\arctan\frac{x-y}{1+xy} &= \arctan x - \arctan y\,, \quad \text{if } xy > -1\,;\\ &= \arctan x - \arctan y - \pi, \quad \text{if } x > 0 \text{ and } xy < -1\,;\\ &= \arctan x - \arctan y + \pi, \quad \text{if } x < 0 \text{ and } xy < -1\,.\end{aligned} \tag{2.35}$$

Thus we obtain

$$\begin{aligned}\theta(\xi,\eta) &= +\pi, \quad \text{if } \xi < 0\,,\ \eta > 0 \text{ and } \Xi(\xi,\eta) < 0\,;\\ &= -\pi, \quad \text{if } \xi > 0\,,\ \eta < 0 \text{ and } \Xi(\xi,\eta) < 0\,;\\ &= 0, \quad \text{otherwise}\,,\end{aligned} \tag{2.36}$$

where $\Xi(p,q)$ was defined in Eq. (2.29). This simple form of the kernel will call forth for a considerable simplification of the eigenvalue.

2.4 The Thermodynamic Limit

Using Eqs. (2.19) and (2.23), from Eq. (2.14) we obtain

$$\exp(iNk_l) = (-1)^{n-1} \prod_{j=1}^{n} \exp[i\Theta(k_l,k_j)] \quad . \tag{2.37}$$

As both sides of this equation are unimodular, we can take the logarithms and divide by i, obtaining

$$Nk_l = 2\pi I_l - \sum_{j=1}^{n} \Theta(k_l,k_j) \quad , \tag{2.38}$$

where I_l must be an integer if n is odd and half integer if n is even. The form of $\Theta(p,q)$ being rather simple, the method of Yang and Yang [29] can be easily applied to prove that Eq. (2.38) has a unique solution with $I_l = l - (n+1)/2$, where $l = 1, \ldots, n$.

As the algebraic Bethe Ansatz was constructed, the vertical down arrows were counted explicitly by n. Thus, the ratio n/N is the proportion of down arrows in each row of the lattice. In other words, it is the probability to find a vertical arrow to be down. This means that in the limit of n and N large, n/N remains fixed. Let us consider that in this limit the momenta $k_1, \ldots, k_n$ become densely packed in some fixed interval, denoted by $(-Q, Q)$, so they effectively form a continuous distribution. If we denote the number of k_i's lying between k and $k + dk$ w by $N\rho(k)dk$, with $\rho(k)$ being the distribution function, then as the total number of k_i's is n, $\rho(k)$ must satisfy

$$\int_{-Q}^{+Q} \rho(k)\, dk = \frac{n}{N} \quad . \tag{2.39}$$

From Eq. (2.28) it results that the thermodynamic limit can be taken as $\sum_{j=1}^{n} \to N \int \rho(k)\, dk$. With this, Eq. (2.38) becomes

$$Nk = -\pi(n+1) + 2\pi N \int_{-Q}^{k} \rho(k')\, dk' - N \int_{-Q}^{+Q} \Theta(k,k')\, \rho(k')\, dk' \quad . \tag{2.40}$$

Differentiating Eq. (2.40) with respect to k and dividing by N we obtain the well known linear integral equation [5,29] for $\rho(k)$

$$2\pi\rho(k) = 1 + \int_{-Q}^{+Q} \frac{\partial\Theta(k,k')}{\partial k}\, \rho(k')\, dk' \quad . \tag{2.41}$$

The solution of Eq. (2.41) can be easily found. Using Eq. (2.31) and (2.39) we can immediately write

$$
\begin{aligned}
2\pi\rho(k) &= 1 + \frac{\Delta_5(\cos k - \Delta_5)}{1 - 2\Delta_5\cos k + \Delta_5^2}\int_{-Q}^{+Q}\rho(k')\,dk' \;; \\
&= 1 + \frac{n}{N}\frac{\Delta_5(\cos k - \Delta_5)}{1 - 2\Delta_5\cos k + \Delta_5^2} \quad .
\end{aligned}
\tag{2.42}
$$

As mentioned previously, n/N represents the number of vertical down arrows on a row. Thus, it also defines the so-called vertical polarization p_v as

$$
p_v \equiv \frac{n_1 + n_4 - n_3}{N} = 1 - 2\frac{n}{N} \quad . \tag{2.43}
$$

Here n_i is the number of vertices i in a row. With Eq. (2.43), the form of the distribution function from Eq. (2.42) becomes

$$
\rho(k) = \frac{1}{2\pi}\,[1 + \frac{1-p_v}{2}\frac{\Delta_5(\cos k - \Delta_5)}{1 - 2\Delta_5\cos k + \Delta_5^2}] \quad . \tag{2.44}
$$

As it can be seen from Eq. (2.44) the distribution function has the same algebraic form for any $\Delta_5 < 1$. This property is a direct consequence of the form of the kernel and not of its analytic properties. Thus, it is not dependent on the parametrization introduced in Eq. (2.27), which, furthermore, we will not use.

The vertical polarization p_v can be also easily determined with the use of Eqs. (2.39), (2.43) and (2.44) and using the algebraic identity of Eq. (2.34)

$$
\begin{aligned}
p_v &= 1 - 2Q\,\{\pi + \frac{Q}{2} + \arctan[\frac{\Delta_5+1}{\Delta_5-1}\tan\frac{Q}{2}]\}^{-1} \;; \\
&= 1 - 2Q\,[\pi + \arctan\frac{\sin Q}{\cos Q - 1/\Delta_5}]^{-1} \quad .
\end{aligned}
\tag{2.45}
$$

In the variation range of the k given in Eqs. (2.26) we have $-\pi \le Q \le +\pi$ and $-1 \le p_v \le +1$. The first form of Eq. (2.45) is valid for any Q in the above range, however, the second form should be used only for $-\pi < Q < +\pi$.

Concerning the free energy, as for the symmetric and asymmetric six-vertex model, we denote

$$\Lambda_L = a^N \prod_{i=1}^{n} L(z_i) \quad , \tag{2.46}$$

and

$$\Lambda_{M'} = b^N \prod_{i=1}^{n} M'(z_i) \quad , \tag{2.47}$$

where $L(z)$ and $M'(z)$ was defined in Eq. (2.7) and (2.9), respectively. In the limit of N large, both terms of the right-hand-side grow exponentially, the larger dominating the smaller. From Eq. (1.6) the free energies are therefore given

$$\begin{aligned} f_L &= \min \{ \varepsilon_1 - \frac{k_B T}{N} \sum_{i=1}^{n} \ln[L(z_i)] \} ; \\ f_{M'} &= \min \{ \varepsilon_4 - \frac{k_B T}{N} \sum_{i=1}^{n} \ln[M'(z_i)] \} \quad . \end{aligned} \tag{2.48}$$

In the thermodynamic limit

$$\begin{aligned} f_L &= \min \{ \varepsilon_1 - k_B T \int_{-Q}^{+Q} \ln[L(e^{ik})] \, \rho(k) \, dk \} ; \\ f_{M'} &= \min \{ \varepsilon_4 - k_B T \int_{-Q}^{+Q} \ln[M'(e^{ik})] \, \rho(k) \, dk \} \quad . \end{aligned} \tag{2.49}$$

Since $\rho(k)$ is an even function of k, see Eq. (2.44), these integrals are real.

2.5 The Free Energy

For further considerations, we introduce the

$$x = \frac{a}{c} \quad , \qquad y = \frac{b}{c} \tag{2.50}$$

notations. As in the symmetric six-vertex case [5], the phase diagram can be conveniently drawn in the (x,y) plane. The Boltzmann weights a, b and c were defined in Eqs. (2.1) From Eq. (2.13) it results

$$\Delta_5 \;=\; \begin{cases} (y^2 \;-\; 1)/xy \;, & \text{if } \omega_1 = 0 \text{ or } \omega_2 = 0 \;; \\ (x^2 \;-\; 1)/xy \;, & \text{if } \omega_3 = 0 \text{ or } \omega_4 = 0 \quad . \end{cases} \tag{2.51}$$

If we wanted to use the second equation, as presented in the discussion following Eqs. (2.5) and (2.6), the free energy would be obtained from a reflection of Eq. (2.49) with respect to the $x = y$ plane, thus we would have had the eigenvalues $M(z)$ and $L'(z)$. In the following, we will work with the first equation of Eq. (2.51).

With the notations of Eq. (2.50) the integrands from Eq. (2.49) are

$$\begin{aligned} L(e^{ik}) \;&=\; \frac{xy \;-\; (y^2-1)e^{ik}}{x(x \;-\; ye^{ik})} \;; \\ &=\; \frac{y(x^2+y^2-1) \;-\; x(2y^2-1)\cos k}{x(x^2+y^2-2xy\cos k)} \\ &+\; i\,\frac{x\sin k}{x(x^2+y^2-2xy\cos k)} \;; \\ &=\; \sqrt{\frac{y^2}{x^2} \;+\; \frac{1-2y^2+2xy\cos k}{x^2(x^2+y^2-2xy\cos k)}} \\ &\times\; \exp[i\;\arctan\frac{x\sin k}{y(x^2+y^2-1) \;-\; x(2y^2-1)\cos k}] \;; \\ &\equiv\; \sqrt{L(k)}\;\exp[i\,\chi_L(k)] \quad , \end{aligned} \tag{2.52}$$

and

$$\begin{aligned} M'(e^{ik}) \;&=\; \frac{-1}{y(x \;-\; ye^{ik})} \;; \\ &=\; \frac{-x+y\cos k}{y(x^2+y^2-2xy\cos k)} \;-\; i\,\frac{y\sin k}{y(x^2+y^2-2xy\cos k)} \;; \\ &=\; \sqrt{\frac{1}{y^2(x^2+y^2-2xy\cos k)}}\;\exp[i\;\arctan\frac{y\sin k}{x-y\cos k}] \;; \\ &\equiv\; \sqrt{M'(k)}\;\exp[i\,\chi_M(k)] \quad . \end{aligned} \tag{2.53}$$

The notations used in Eqs. (2.52) and (2.53) are obvious. From Eq. (2.44) it can be seen that $\rho(k)$ is an even function of k. As $\chi_L(k)$ and $\chi_M(k)$ are odd functions of k, their integral over a symmetric interval is vanishing. Using the forms given in Eqs. (2.52) and (2.53) the two free energies, f_L and $f_{M'}$ will have the following form

$$\begin{aligned} f_L &= \varepsilon_1 - k_B T \int_0^Q \ln[L(k)]\, \rho(k)\, dk \; ; \\ &= \varepsilon_1 - k_B T \int_0^Q \ln|\frac{1}{x^2}(y^2 + \frac{1-2y^2+2xy\cos k}{x^2+y^2-2xy\cos k})|\, \rho(k)\, dk \quad , \end{aligned} \tag{2.54}$$

and

$$\begin{aligned} f_{M'} &= \varepsilon_4 - k_B T \int_0^Q \ln[M'(k)]\, \rho(k)\, dk \; ; \\ &= \varepsilon_4 - k_B T \int_0^Q \ln|\frac{1}{y^2}\frac{1}{x^2+y^2-2xy\cos k}|\, \rho(k)\, dk \quad . \end{aligned} \tag{2.55}$$

Since the arrow-reversal symmetry of the system is broken, we anticipate that the horizontal polarization will not always equal the vertical one. Therefore, we also compute the horizontal polarization, which can be defined similarly to the vertical polarization p_v of Eq. (2.43) as

$$p_h \equiv \frac{n_1 + n_3 - n_4}{N} \quad . \tag{2.56}$$

Using the notations from Eq. (2.50) the expression of the horizontal polarization reduces to

$$p_h = -\frac{2\,x}{k_B T}\frac{\partial f}{\partial x} - p_v \quad , \tag{2.57}$$

where f denotes f_L or $f_{M'}$. We will use Eq. (2.57) to determine the horizontal polarization.

The thermodynamic quantities which we will compute besides the free energy are the internal energy

$$u = -T^2 \frac{\partial}{\partial T}(\frac{f}{T}) \quad , \tag{2.58}$$

and the specific heat

$$c = \frac{\partial u}{\partial T} \quad . \tag{2.59}$$

2.6 The Free-Fermion Solution

We will consider first the non-interacting limit, i.e. the $\Delta_5 = 0$ case which was solved [7] already, but not thoroughly analyzed. The non-interacting case corresponds to $y = 1$ due to Eq. (2.51). In this case, Eqs. (2.44), (2.45), (2.52) and (2.53) simplify considerably,

$$\ln|L(k)| = \ln|M'(k)| = -\frac{1}{2} \ln|1 + x^2 - 2x\cos k| \quad , \tag{2.60}$$

with $\rho(k) = 1/2\pi$ and $Q = \pi(1-p_v)/2$. The integral entering in the expression of the free energy is sensitively dependent on the value of x. For large values of x it is always negative, independently of Q. The free energy for $x \to \infty$ ($T \to 0$ limit) is

$$f_L = \varepsilon_1 + k_B T \frac{1-p_v}{2} \ln x \quad . \tag{2.61}$$

To obtain the minimum value, (i.e. ε_1) $p_v = 1$ must be considered. Eq. (2.57) implies $p_h = p_v = 1$ for $x \geq 1$. Thus, the system at $T = 0$ is in a completely polarized state. To leave this ferroelectric state, the obvious condition

$$1 + x^2 - 2x\cos k \geq 1 \tag{2.62}$$

is required. In Eq. (2.62) the equality defines the transition for $p_v = 1$. A remarkable feature of this phase transition, as it was noted already by Kasteleyn [8], is that up to the transition point the system shows a perfect ordering, i.e. the transition is a second order phase transition of a rather unusual kind. In the usual case, e.g. at the Curie point of a ferromagnet, the order parameter vanishes on both sides of the transition; here, on the contrary, it is maximal. The second order phase transition occurs at $x = 2$, a relation which defines the critical transition temperature, $k_B T_c = (\varepsilon_4 - \varepsilon_1)/\ln 2$. This result was also obtained by W u [7]. It should be noted that a frozen-in ferroelectric state is obtained in this $\Delta_5 = 0$ case which is distinct from that for $\Delta_5 > 1$ indicated above.

The free energy is ε_1 for $x > 2$, and is equal to

$$f_L = \varepsilon_1 + \frac{k_B T}{2\pi} \int_0^{Q_0} \ln(1 + x^2 - 2x\cos k)\, dk \quad , \tag{2.63}$$

for $1 \leq x \leq 2$. Here, $Q_0 = \cos^{-1}(x/2)$ which, due to $Q_0 = \pi(1 - p_v)/2$, defines also the polarization per vertex. The form of the free energy given in Eq. (2.63) is identical with that one obtained by Wu [7]. It is found that the vertical polarization does not vanish in zero field. p_v is a smooth function of x, being equal to unity for $x = 2$ ($T = T_c$), and reaches the $p_v = 1/3$ value at $x = 1$ ($T \to \infty$). This is in contradiction with the six-vertex results, where at infinite temperature all vertices are equally probable ($p_v = 0$). In the present case, however, we have $n_1 = 1/3$ and $n_3 = n_4 = n_5 = n_6 = 1/6$. The internal energy is a continuous function of x, thus also of T. The specific heat $c = 0$ for $x > 2$, i.e. $T < T_c$. Near the transition

$$c[x \to 2_{(-)}] = \frac{\sqrt{2}\ln^2 2}{\pi\sqrt{1 - x/2}} \quad , \tag{2.64}$$

that is

$$c[T \to T_{c(+)}] = \frac{\sqrt{2}T_c \ln^2 2}{\pi\sqrt{\varepsilon_4 - \varepsilon_1}\sqrt{T - T_c}} \quad . \tag{2.65}$$

The critical exponent α is thus, $\alpha = 1/2$.

The $x \to 1$ limit has a major significance, because it corresponds to $T \to \infty$. The specific heat smoothly decreases as x decreases, vanishing for $x = 1$ as

$$c[x \to 1_{(+)}] = (x - 1)^2 \frac{5 + \pi\sqrt{3}}{3\pi\sqrt{2}} \quad .$$

The same behaviour is obtained in the $x \leq 1$ variation range. In this case the free energy is given by

$$f_{M'} \; = \; \varepsilon_4 \; + \; \frac{k_B T}{2\pi} \int_0^{Q_0} \ln(1 \; + \; x^2 \; - \; 2x \cos k) \; dk \quad , \tag{2.66}$$

This means that the specific heat approaches zero at infinite temperature in both limits as

$$c(T \to \infty) \; = \; q \, \frac{(\varepsilon_4 - \varepsilon_1)^2}{T^2} \quad , \tag{2.67}$$

where $q = (5 + \pi\sqrt{3})/3\pi\sqrt{2}$. The entropy in the same limit is equal to the known value [4]

$$S(T \to \infty) \; \equiv \; S_\infty \; = \; \frac{Cl_2(\pi/3)}{\pi} \; \simeq \; 0.323 \quad , \tag{2.68}$$

where $Cl_2(z) \; = \; -\int_0^z \ln[2\sin(x/2)]dx$ is Clausen's integral [33]. This value is considerably smaller than the entropy density of the six-vertex model, where [6] $S_6 = 3[\ln 2 - (1/2)\ln 3] \simeq 0.431$. In the same limit, the free energy behaves as

$$f(T \to \infty) \; = \; \text{const.} \; - \; TS_\infty \; - \; \frac{q}{2} \, T \quad . \tag{2.69}$$

At this point, we must mention that the free energy can be written in a compact form (even in the $\Delta_5 \neq 0$ case) using Clausen's integral, e.g. Eq. (2.63) becomes [40]

$$f_L \; = \; \varepsilon_1 \; + \; \frac{k_B T}{2\pi} \, [Cl_2(2Q_0 + 2\eta) \; - \; Cl_2(2Q_0) \; - \; Cl_2(2\eta) \; - \; 2\eta \ln x] \quad , \tag{2.70}$$

where η has the form of the kernel (interestingly), see Eq. (2.34), i.e.

$$\eta \; = \; -\arctan \frac{\sin Q_0}{\cos Q_0 \; - \; 1/x} \quad .$$

However, for further analysis we will not use this special function representation, because the behaviour of Clausen's integral has not been comprehensively studied.

As we mentioned at the beginning, the free energy of this non-interactive case was already known due to Wu [7]. In the following we show the equivalence of the free energies from Eq. (2.63) or (2.67) with those obtained by Wu.

The expression of the free energy for the free-fermion case of the general eight-vertex model can be obtained by the method of dimers [41]

$$\begin{aligned} f \ = \ -\frac{k_B T}{8\pi^2} \int_{-\pi}^{+\pi} d\theta \int_{-\pi}^{+\pi} d\phi \ \ln[a_1 \ + \ 2a_2 \cos\theta \ + \ 2a_3 \cos\phi \\ + \ 2a_4 \cos(\theta - \phi) \ + \ 2a_5 \cos(\theta + \phi)] \quad , \end{aligned} \tag{2.71}$$

where

$$\begin{aligned} a_1 &= \omega_1^2 \ + \ \omega_2^2 \ + \ \omega_3^2 \ + \ \omega_4^2 \ ; \\ a_2 &= \omega_1\omega_3 \ - \ \omega_2\omega_4 \ ; \\ a_3 &= \omega_1\omega_4 \ - \ \omega_2\omega_3 \ ; \\ a_4 &= \omega_3\omega_4 \ - \ \omega_7\omega_8 \ ; \\ a_5 &= \omega_1\omega_2 \ - \ \omega_5\omega_6 \quad , \end{aligned}$$

and the free-fermion condition reads as

$$\omega_1\omega_2 \ + \ \omega_3\omega_4 \ = \ \omega_5\omega_6 \ + \ \omega_7\omega_8 \quad .$$

In the case, e.g $x < 1$, obviously $\omega_2 = \omega_7 = \omega_8 = 0$ and $\omega_3 = \omega_4 = \omega_5$, integrating over ϕ, Eq. (2.71) gives

$$f \ = \ -\frac{k_B T}{4\pi} \int_{-\pi}^{+\pi} d\theta \ \ln \ \max\,[\omega_4^2, \ \omega_4^2(1 \ + \ x^2 \ - \ 2x\cos\theta)] \quad . \tag{2.72}$$

The minimum value of the right-hand-side of Eq. (2.72) is obtained to be identical with Eq. (2.66).

The dimer method also allows an easy calculation of the correlation functions. In the case of the non-interacting five-vertex model the correlations of two and three edges of the associated hexagon lattice was determined by Garrod [10].

2.7 Phase Diagram of f_L

Hereafter, we will study the analytic properties and the phase diagram of the free energy f_L obtained in Eq. (2.54), i.e. given by

$$f_L = \varepsilon_1 - k_B T \int_0^Q \ln|\frac{1}{x^2}(y^2 + \frac{1-2y^2+2xy\cos k}{x^2+y^2-2xy\cos k})|\ \rho(k)\ dk \quad . \tag{2.73}$$

We borrow the computing procedure from the non-interacting case, see § **2.6**. That is, in order to obtain the minimum value of f_L we must require for the integrand of Eq. (2.73) to be positive. This implies, that the condition

$$\frac{1}{x^2}\ (y^2 + \frac{1-2y^2+2xy\cos k}{x^2+y^2-2xy\cos k}) \geq 1 \quad , \tag{2.74}$$

will determine the variation range of k. In Eq. (2.74) the equality defines the maximum value of k, i.e. the integration limit. For which, using the notation Q_L, we obtain from Eq. (2.74)

$$Q_L = \arccos\frac{x^2 + y^2 - 1}{2xy} \equiv \arccos q_L \quad , \tag{2.75}$$

where the argument of the arccos function was denoted by q_L. Thus, we know that for any $x > 0$ and $y > 0$ the minimum of f_L is given by

$$f_L = \varepsilon_1 - k_B T \int_0^{Q_L} \ln[\frac{1}{x^2}(y^2 + \frac{1-2y^2+2xy\cos k}{x^2+y^2-2xy\cos k})]\ \rho(k)\ dk \quad . \tag{2.76}$$

The vertical and horizontal polarizations can be determined using Eq. (2.45) and Eq. (2.57), respectively. It turns out that the vertical polarization (this is true also for the horizontal one) with Q_L defined in Eq. (2.75) and Δ_5 given in the first line of Eq. (2.51) is always a positive definite or a vanishing constant, that is $p_v \geq 0$. This observation is very important. Because, the value of p_v enters directly in the expression of the distribution, see Eq. (2.44), the property $p_v \geq 0$ ensures that indeed the free energy given in Eq. (2.76) is always the minimum possible. As we will see in § **2.8**, this property of the vertical polarization is not always satisfied in the case of $f_{M'}$. As a consequence of this, the behaviour of $f_{M'}$ is different close to $p_v \sim 0$.

In order to calculate the thermodynamic quantities, of Eqs. (2.58) and (2.59), we perform the transformation

$$\frac{\partial}{\partial T} = -\frac{(\varepsilon_5 - \varepsilon_1)}{T^2}\, x\, \frac{\partial}{\partial x} - \frac{(\varepsilon_5 - \varepsilon_4)}{T^2}\, y\, \frac{\partial}{\partial y} \quad , \tag{2.77}$$

where we used the definition from Eq. (2.50) and put $k_B = 1$. As mentioned in § **2.2**, we are analyzing the first case of Eqs. (2.1), as all other cases are equivalent or can be transformed to the present case. By direct computation it can be verified that

$$\{\ \rho(k)\ \ln \frac{1}{x^2}(y^2 + \frac{1 - 2y^2 + 2xy\cos k}{x^2 + y^2 - 2xy\cos k})\ \}_{[k\,=\,Q_L]} = 0 \quad . \tag{2.78}$$

Thus the internal energy from Eq. (2.58), with the use of Eqs. (2.77) and (2.78) becomes

$$\begin{aligned} u_L(x,y) &= \varepsilon_1 \\ - (\varepsilon_5 - \varepsilon_1)\, x \int_0^{Q_L} &\{\ \frac{\partial}{\partial x}\ [\ \rho(k)\ \ln \frac{1}{x^2}(y^2 + \frac{1 - 2y^2 + 2xy\cos k}{x^2 + y^2 - 2xy\cos k})\ ]\ \}\ dk \\ - (\varepsilon_5 - \varepsilon_4)\, y \int_0^{Q_L} &\{\ \frac{\partial}{\partial y}\ [\ \rho(k)\ \ln \frac{1}{x^2}(y^2 + \frac{1 - 2y^2 + 2xy\cos k}{x^2 + y^2 - 2xy\cos k})\ ]\ \}\ dk \quad . \end{aligned} \tag{2.79}$$

The specific heat, defined in Eq. (2.59), with the use of Eqs. (2.77), (2.78) and (2.79) will contain ten terms. These terms can be put in two separate groups

$$c_L(x,y) = C_{L,1}(x,y) + C_{L,2}(x,y) \quad , \tag{2.80}$$

as a consequence of their analytic behaviour. If we use the notation

$$F_L(x,y,k) = \rho(k)\ \ln \frac{1}{x^2}(y^2 + \frac{1 - 2y^2 + 2xy\cos k}{x^2 + y^2 - 2xy\cos k}) \quad , \tag{2.81}$$

then these terms are

$$
\begin{aligned}
C_{L,1}(x,y) &= \frac{(\varepsilon_5 - \varepsilon_1)^2}{T^2}\; x \int_0^{Q_L} [\frac{\partial}{\partial x}\, F_L(x,y,k)]\; dk \\
&+ \frac{(\varepsilon_5 - \varepsilon_1)^2}{T^2}\; x^2 \int_0^{Q_L} [\frac{\partial^2}{\partial x^2}\, F_L(x,y,k)]\; dk \\
&= \frac{(\varepsilon_5 - \varepsilon_1)(\varepsilon_5 - \varepsilon_4)}{T^2}\; xy \int_0^{Q_L} [\frac{\partial^2}{\partial y \partial x}\, F_L(x,y,k)]\; dk \\
&+ \frac{(\varepsilon_5 - \varepsilon_1)(\varepsilon_5 - \varepsilon_4)}{T^2}\; xy \int_0^{Q_L} [\frac{\partial^2}{\partial x \partial y}\, F_L(x,y,k)]\; dk \\
&= \frac{(\varepsilon_5 - \varepsilon_4)^2}{T^2}\; y \int_0^{Q_L} [\frac{\partial}{\partial y}\, F_L(x,y,k)]\; dk \\
&+ \frac{(\varepsilon_5 - \varepsilon_1)^2}{T^2}\; y^2 \int_0^{Q_L} [\frac{\partial^2}{\partial y^2}\, F_L(x,y,k)]\; dk \quad ,
\end{aligned}
\tag{2.82}
$$

and

$$
\begin{aligned}
C_{L,2}(x,y) &= \frac{(\varepsilon_5 - \varepsilon_1)^2}{T^2}\; x^2\; \frac{\partial Q_L}{\partial x}\; [\frac{\partial F_L(x,y,k)}{\partial x}]_{[k\, =\, Q_L]} \\
&+ \frac{(\varepsilon_5 - \varepsilon_1)(\varepsilon_5 - \varepsilon_4)}{T^2}\; xy\; \frac{\partial Q_L}{\partial x}\; [\frac{\partial F_L(x,y,k)}{\partial y}]_{[k\, =\, Q_L]} \\
&+ \frac{(\varepsilon_5 - \varepsilon_1)(\varepsilon_5 - \varepsilon_4)}{T^2}\; xy\; \frac{\partial Q_L}{\partial y}\; [\frac{\partial F_L(x,y,k)}{\partial x}]_{[k\, =\, Q_L]} \\
&+ \frac{(\varepsilon_5 - \varepsilon_4)^2}{T^2}\; y^2\; \frac{\partial Q_L}{\partial y}\; [\frac{\partial F_L(x,y,k)}{\partial y}]_{[k\, =\, Q_L]} \quad .
\end{aligned}
\tag{2.83}
$$

Using the analytic form of Q_L from Eq. (2.75), we obtain

$$
C_{L,2}(x,y) \;=\; -\frac{1}{\sqrt{1\, -\, q_L^2}}\; \widetilde{C}_{L,2}(x,y) \quad . \tag{2.84}
$$

The form of $\widetilde{C}_{L,2}(x,y)$ is identical with that of $C_{L,2}(x,y)$ from Eq. (2.83) only $\partial Q_L \,/\, \partial x$ (or y) should be changed with $\partial q_L \,/\, \partial x$ (or y). By direct evaluation it can be seen that $\partial q_L \,/\, \partial x$ (or y) > 0, but $[\partial F_L(x,y,k) \,/\, \partial x$ (or y)$]_{[k\, =\, Q_L]} < 0$ thus, the specific heat from Eq. (2.80) is equal to

$$
c_L(x,y) \;=\; C_{L,1}(x,y) \;+\; \frac{1}{\sqrt{1\, -\, q_L^2}}\; |\widetilde{C}_{L,2}(x,y)| \quad . \tag{2.85}
$$

It turns out that the functions $C_{L,1}(x,y)$ and $\widetilde{C}_{L,2}(x,y)$ are analytic in the limit $q_L^2 = 1$, and the values $C_{L,1}(q_L^2 = 1)$ and $\widetilde{C}_{L,2}(q_L^2 = 1)$ can be easily calculated. Thus, for those values of (x,y) for which $q_L = \pm 1$, the calculated specific heat from Eq. (2.85) will have a square-root like divergence. This corresponds to a phase transition of the second order type. The expression of the specific heat from Eq. (2.85) has no other singular points. The internal energy, Eq. (2.79) and the free energy, Eq. (2.76) are continuous for $q_L = \pm 1$. Other singularities of any other type are not to be found in the analytic expression of Eq. (2.76).

The (x,y) values for which $q_L = \pm 1$ with the corresponding values of Q_L are

$$\begin{aligned} q_L &= +1\ , \quad x = y - 1 \text{ and } Q_L = 0\ ; \\ q_L &= -1\ , \quad x = 1 - y \text{ and } Q_L = \pi\quad . \end{aligned} \tag{2.86}$$

For the first line, for which $Q_L = 0$, the system will exhibit a ferroelectric ground state, as can be seen easily from the expression of the free energy, Eq. (2.76). For the second one, where $Q_L = \pi$ the value of the vertical polarization calculated from Eq. (2.45), is $p_v(Q_L = \pi) = 0$. We can say, that a $n = N/2$ ground state is to be expected.

Obviously, to determine the true phase diagram of the system, the region of physical validity of f_L must be determined. The expression of the free energy f_L is valid, as presented in the discussion following Eq. (2.22), for any (x,y) for which $\Delta_5 < 1$.

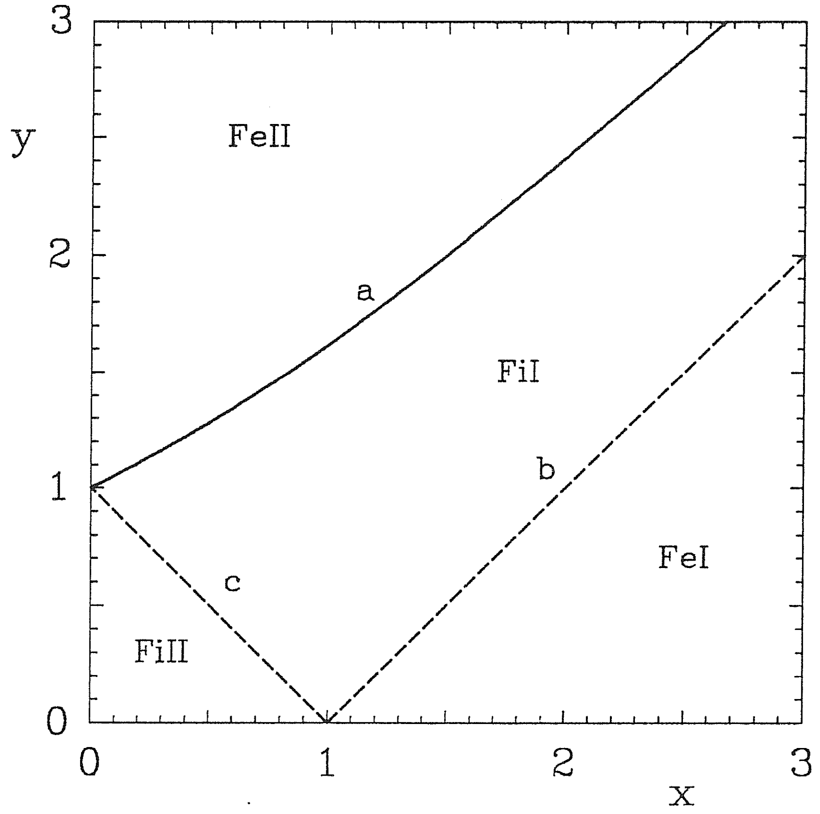

Fig. 2.3: The phase diagram of the f_L term in zero external field, in terms of the Boltzmann weights $x = a/c$ and $y = b/c$. The dashed curves represent continuous transitions of second order type, the solid curve a first order transition. Fe stands for a ferroelectric and Fi for a ferrielectric phase. The $x = y = 1$ point corresponds to the infinite temperature, while any point satisfying $x/y = 0$ or $y/x = 0$ corresponds to the zero temperature state.

2.7.1 The Ferroelectric Phases

For the values of (x, y), for which Δ_5 is larger than unity, the Bethe Ansatz gives a solution for the momenta k pure imaginary, see also Fig 2.1. Thus, for this parameter region the system exhibits a ferroelectric transition. The $\Delta_5 = 1$ condition defines the transition curve

$$x = y - \frac{1}{y} \quad , \tag{2.87}$$

denoted by **a** in Fig. 2.3. Eq. (2.87) defines also the transition temperature. All the region **FeII** of Fig. 2.3 is characterized by $\Delta_5 > 1$. Similarly to the symmetric six-vertex case[5], this region is trivial. To $\Delta_5 > 1$ corresponds $\varepsilon_3 = \varepsilon_4 < \varepsilon_1 < \varepsilon_5 = \varepsilon_6$. Thus, the lowest energy state is one in which all vertices are of type four or three. These two cases are reflected in the polarizations which can take the values $p_v = 1$, $p_h = -1$ or $p_v = -1$, $p_h = 1$, corresponding to vertices four or three. The **a** transition curve represents a first order transition, as the difference between the free energies is

$$\begin{aligned} f_L[x \to (y - 1/y)_{(-)}] - \varepsilon_4 &= 4(1 - \Delta_5) \frac{Q_{L\ (x=y-1/y)}}{\pi + Q_{L\ (x=y-1/y)}} \\ &\times \cot \frac{Q_{L\ (x=y-1/y)}}{2} \ln \frac{y^2}{y^2 - 1} \quad . \end{aligned} \tag{2.88}$$

Thus, $f_L(T \to T_{c(+)}) - \varepsilon_4 \sim -\text{const.}\ (T - T_c)/T_c$. The free energy is continuous on the whole transition curve, but its first derivative, i.e. the internal energy, has a step-like discontinuity. Also the polarization has a step discontinuity crossing this transition line. Due to this reasons, the **a** transition curve is similar to the ferroelectric transitions of the symmetric six-vertex model[5].

For large values of x there exists another ferroelectric phase. The minimum of the free energy is equal to ε_1, as in the non-interacting case. That is, in the

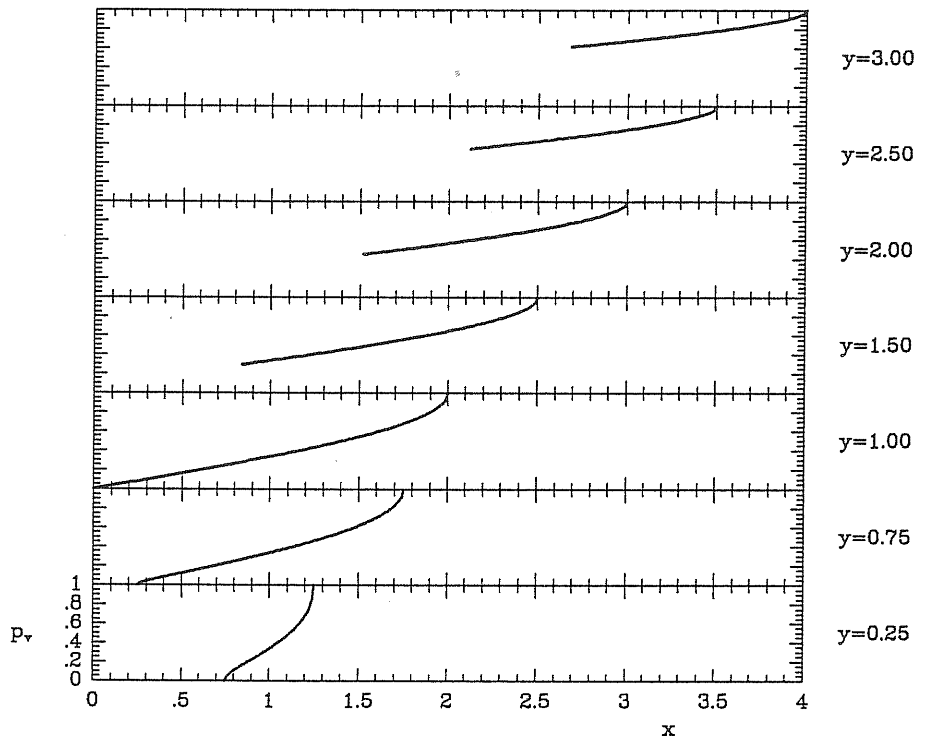

Fig. 2.4: Vertical polarization versus x for different fixed values of y. The plots are starting from the x values corresponding to the a and c transition curves of Fig. 2.3, and they finish at the x values corresponding to the b transition curve of Fig. 2.3.

region **FeI** of Fig. 2.3, the system is an ideal ferroelectric. The lowest energy state is one where all vertices are of type one. The phase separation line **b** of Fig. 2.3 is given by the second line of Eq. (2.86), i.e.

$$y = 1 + x \quad . \tag{2.89}$$

This ferroelectric phase remains stable on the whole region **FeI** of Fig. 2.3, even for low values of y, where $\Delta_5 < -1$. As we mentioned in the discussion following Eq. (2.86), there are no other singularities encountered by f_L. This result differs from that for the symmetric six-vertex model, where crossing the $\Delta_6 = -1$ line immediately led to an antiferroelectric state.

2.7.2 The Ferrielectric Phases

To the left of the **a** transition curve the vertical and horizontal polarizations p_v and p_h, as obtained from Eq. (2.45) and (2.51), respectively, are smooth functions of x and y. For some y values the vertical polarization is presented in Fig. 2.4. Since this domain, region **FiI** of Fig. 2.3, which is delimited by the **a**, **b** and **c** transition curves, has a nonvanishing polarization per vertex, it will correspond to a ferrielectric phase.

Approaching the **b** transition curve, both polarizations tend to unity. The internal energy is a continuous function on the whole transition line. The specific heat is zero to the right of curve **b**. From the left, the specific heat can be determined from Eq. (2.85). For $x \to (y+1)_{(-)}$ we have $\sqrt{1-q_L^2} \to \sqrt{1-[x/(y+1)]^2}/y$ and $\widetilde{C}_{L,2}[x \to (y+1)_{(-)}]$ from Eq. (2.83) is

$$\begin{aligned} \widetilde{C}_{L,2}[x \to (y+1)_{(-)}] &= -\frac{2}{\pi\, y\, (y+1)^2} \\ &\times \Big[\frac{(\varepsilon_5-\varepsilon_1)^2}{T^2}(y+1)^2 + \frac{(\varepsilon_5-\varepsilon_4)^2}{T^2}\, y^2 \\ &+ 2\,\frac{(\varepsilon_5-\varepsilon_1)(\varepsilon_5-\varepsilon_4)}{T^2}\, y(y+1) \Big] \quad . \end{aligned} \tag{2.90}$$

Thus, the specific heat behaves as

$$c[x \to (y+1)_{(-)}] = \frac{\sqrt{2}}{\pi}\,\frac{[(y+1)\ln(y+1) - y\ln y]^2}{(y+1)^2\sqrt{1-\frac{x}{y+1}}} \quad . \tag{2.91}$$

In terms of temperature

$$c[T \to T_{c(+)}] = \frac{\sqrt{2}}{\pi}\,\frac{[(\varepsilon_5-\varepsilon_1)e^{(\varepsilon_5-\varepsilon_1)/T_c} - (\varepsilon_5-\varepsilon_4)e^{(\varepsilon_5-\varepsilon_4)/T_c}]^2}{T_c e^{2(\varepsilon_5-\varepsilon_1)/T_c}\sqrt{\varepsilon_5-\varepsilon_1}\sqrt{T-T_c}} \quad . \tag{2.92}$$

Indeed, curve **c** of Fig. 2.3 represents a second order phase transition, with critical exponent $\alpha = 1/2$. From Eqs. (2.91) and (2.92), the results of the non-interacting case can be easily verified, for the $y = 1$ and $\varepsilon_5 = \varepsilon_4$ limit, respectively.

Close to the **c** curve the vertical polarization p_v tends to zero, in the realization of the first equation from Eq. (2.1) chosen here, while the horizontal polarization p_h tends to unity. This is due to the fact that the integration limit of Eq. (2.76) is approaching π. $Q_L = \pi$ defines the transition line, see Eq. (2.86), i.e

$$y = 1 - x \quad . \tag{2.93}$$

Thus, $Q_L = \pi$ on the whole **c** line, while $\Delta_5 = -(1+y)/y$. That is, we are leaving behind the $\Delta_5 = -1$ curve. Crossing the latter, due to the construction of the free energy f_L, no singularity is encountered. On the whole transition line the internal energy from Eq. (2.79) is a continuous function, but the specific heat, computed as in the previous case from Eq. (2.85), diverges as

$$c[x \to (1-y)_{(+)}] = \frac{\sqrt{2}}{\pi} \frac{[(1-y)\ln(1-y) - y\ln y]^2}{(1-y)^2\sqrt{\frac{x}{y-1} - 1}} \quad , \tag{2.94}$$

which in terms of temperature gives the same expression as Eq. (2.92). Thus, curve **c** also represents a second order phase transition, with critical exponent $\alpha = 1/2$.

Crossing the **c** curve the free energy in the region **FiII** of Fig. 2.3 is given by Eq. (2.76) with $Q_L = \pi$. The vertical polarization is equal to zero in the whole region, but the horizontal polarization is not. Due to this, the region **FiII** will be called a ferrielectric phase. In Fig. 2.5 we have given the value of the horizontal polarization in the vicinity of the transition line. Indeed, the value of p_h is very small already near the transition and decreases rapidly to zero. Thus, the **FiII** phase behaves like an antiferroelectric phase. The interesting feature of this phase

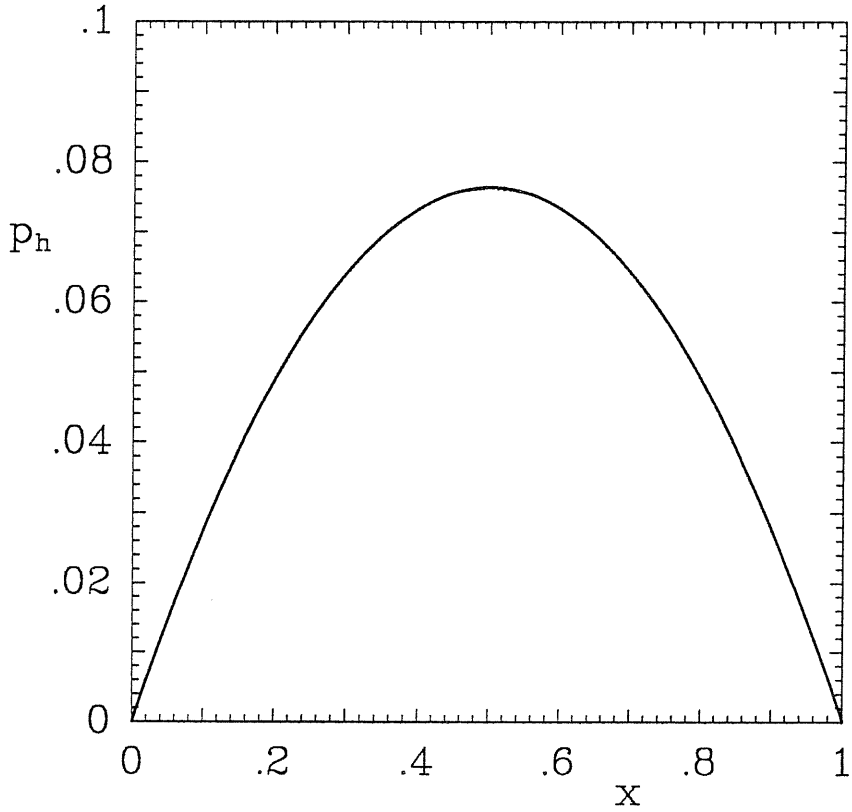

Fig. 2.5: Horizontal polarization versus x on the c transition curve of Fig. 2.3.

is that the vertical polarization is strictly zero. In terms of the vertices this means $n_1 + n_4 = n_3$, or $n = N/2$, in agreement with the conjecture presented in the discussions following Eq. (2.86).

The crossing point of the **a** (first order) and **c** (continuous) transition curves at $x = 0$ and $y = 1$ has a critical behaviour characteristic of a first order transition meeting a second order one.

2.8 Phase Diagram of $f_{\Lambda I'}$

We apply now the method used in § **2.7**, to study the analytic properties of the $f_{\Lambda I'}$ free energy, see Eq. (2.55), given by

$$f_{\Lambda I'} \;=\; \varepsilon_4 \;-\; k_B T \int_0^Q \ln \left| \frac{1}{y^2} \frac{1}{x^2 + y^2 - 2xy \cos k} \right| \rho(k)\; dk \quad . \tag{2.95}$$

We are looking for the minimum of $f_{\Lambda I'}$, for which we require the integrand function to be positive. That is

$$\frac{1}{y^2} \frac{1}{x^2 + y^2 - 2xy \cos k} \;\geq\; 1 \quad , \tag{2.96}$$

will determine the variation range of k in Eq. (2.95). The left-hand-side of Eq. (2.96) equal unity defines the integration limit, which in analogy to the previous case studied we denote by $Q_{\Lambda I'}$, thus

$$Q_{\Lambda I'} \;=\; \arccos \frac{x^2 \;+\; y^2 \;-\; 1/y^2}{2xy} \;\equiv\; \arccos q_{\Lambda I} \quad , \tag{2.97}$$

The argument of $Q_{\Lambda I'}$ was denoted by $q_{\Lambda I'}$. The vertical and horizontal polarizations can be calculated using Eq. (2.45) and (2.57). However, in this case, opposite to the previously studied f_L one, two new important results are found. First, with $Q_{\Lambda I'}$ defined in Eq. (2.97), the derivative $\partial f_{\Lambda I'} \;/\; \partial x$ is vanishing, thus $p_h = -p_v$, always. The easiest way to see this, is to introduce the external horizontal (h) and vertical (v) fields and calculated $p_{h\ (\text{or } v)} = -\partial f_{\Lambda I'} / \partial h$ (or v) $[h = v = 0]$. Secondly, the value of p_v obtained from Eq. (2.45), with $Q_{\Lambda I'}$ being equal to Eq. (2.97) and Δ_5 equal to the first line of Eq. (2.51), is $-1 \leq p_v \leq +1$. Both of these results, are not to be found in the behaviour of the f_L free energy.

From the second property it results immediately that there must be a curve at which p_v crosses the zero value. By a numerical computation this curve was found, and is presented in Fig. 2.6 as a dashed curve.

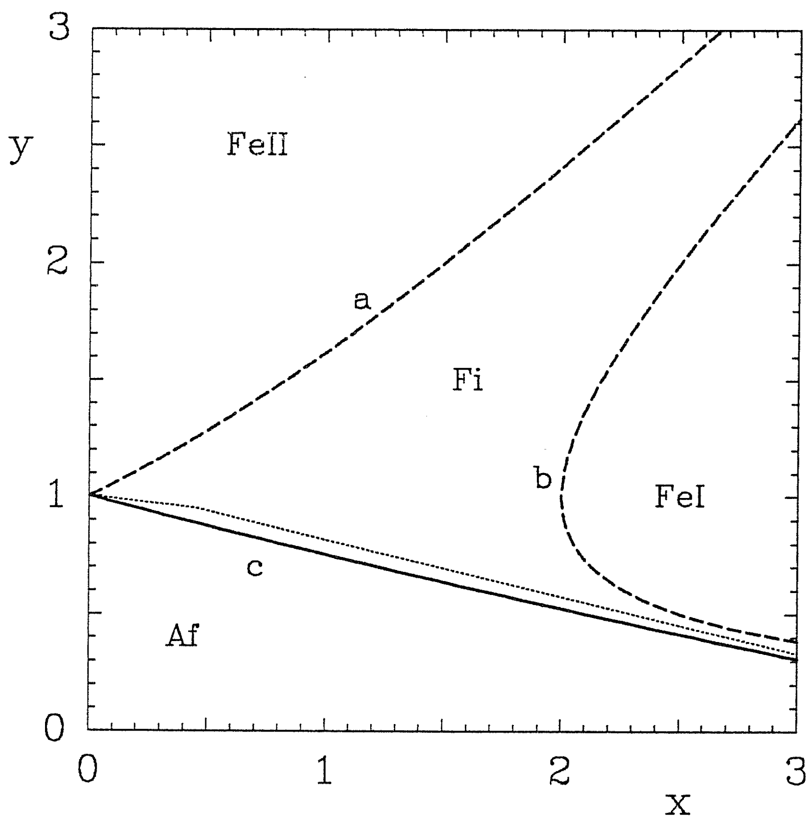

Fig. 2.6: The phase diagram of the $f_{\Lambda\Gamma'}$ term in zero external field, in terms of the Boltzmann weights x = a/c and y = b/c. The dashes curves represent continuous transitions of second order type, the solid curve first order transition. On the dotted curve the vertical polarization is zero. Fe stands for a ferroelectric, Fi for a ferrielectric and Af for antiferroelectric phase. The x = y = 1 point corresponds to the infinite temperature, while any point satisfying x/y = 0 or y/x = 0 corresponds to the zero temperature state.

Below this curve $p_v < 0$ and $\Delta_5 \ll -1$. These values will have a drastic effect on the behaviour of the distribution function from Eq. (2.44) and thus, also of the free energy from Eq. (2.95). It turns out that below this curve, the free energy $f_{\Lambda\Gamma'}$ is not always reaching its minimum value with the integration limit taken to be equal with $Q_{\Lambda\Gamma'}$. In consequence, this case must be analyzed separately.

However, for any (x, y) values for which p_v is positive the minimum of $f_{M'}$ is given by

$$f_{M'} \;=\; \varepsilon_4 \;-\; \frac{k_B T}{N} \int_0^{Q_M} \ln[\frac{1}{y^2} \frac{1}{x^2 + y^2 - 2xy \cos k}] \; \rho(k) \; dk \quad . \tag{2.98}$$

In this case also, the thermodynamic quantities can be determined in the same way as for f_L. Using Eq. (2.77) it can be verified that

$$\{ \; F_{M'}(x, y, k) \;\equiv\; \rho(k) \; \ln \frac{1}{y^2} \frac{1}{x^2 + y^2 - 2xy \cos k} \; \}_{[k \,=\, Q_{M'}]} \;=\; 0 \quad . \tag{2.99}$$

With the notation $F_{M'}(x, y, k)$ the free energy is identical with Eq. (2.79)

$$\begin{aligned} u_{M'}(x, y) \;&=\; \varepsilon_4 \\ - (\varepsilon_5 - \varepsilon_1) \; x \; &\int_0^{Q_{M'}} \{ \; \frac{\partial}{\partial x} \; [\; F_{M'}(x, y, k) \;] \; \} \; dk \\ - (\varepsilon_5 - \varepsilon_4) \; y \; &\int_0^{Q_{M'}} \{ \; \frac{\partial}{\partial y} \; [\; F_{M'}(x, y, k) \;] \; \} \; dk \quad . \end{aligned} \tag{2.100}$$

The specific heat will be given by a relation similar to Eq. (2.85)

$$c_{M'}(x, y) \;=\; C_{M',1}(x, y) \;+\; \frac{1}{\sqrt{1 \;-\; q_{M'}^2}} \; |\widetilde{C}_{M',2}(x, y)| \quad , \tag{2.101}$$

where $C_{M',1}(x, y)$ and $\widetilde{C}_{M',2}(x, y)$ have the same algebraic form as $C_{L,1}(x, y)$ and $\widetilde{C}_{L,2}(x, y)$ from Eqs. (2.82) and (2.84), with the obvious changes $Q_L \rightarrow Q_{M'}$ and $F_L(x, y, k) \rightarrow F_{M'}(x, y, k)$.

Concerning the analytic properties of $C_{M',1}(x, y)$ and $\widetilde{C}_{M',2}(x, y)$, it turns out that they are analytic for $q_{M'} = \pm 1$. Thus, for those values of (x, y) for which $p_v \geq 0$ and $q_{M'} = \pm 1$, the calculated specific heat from Eq. (2.101) has a square root like divergence. The thermodynamic system will encounter a second order phase transition. The expression of the specific heat of Eq. (2.101) does not exhibit other singularities. The internal energy given in Eq. (2.100) and the free energy given in Eq. (2.98) are continuous for $q_{\Lambda I'} = 1$. Other singularities of any other type are not to be found in the analytic expression of Eq. (2.98) for $p_v \geq 0$.

All those (x, y) values for which $q_{\Lambda I'} = \pm 1$ and $p_v \geq 0$ actually corresponds to $q_{\Lambda I'} = 1$, that is $Q_{\Lambda I'} = 0$, are

$$\begin{aligned} x &= \frac{y^2 + 1}{y} \; ; \\ x &= \frac{y^2 - 1}{y} \quad . \end{aligned} \tag{2.102}$$

This curves are presented in Fig. 2.6. As for both curves $Q_{\Lambda I'} = 0$, the system will exhibit a ferroelectric ground state.

Let us analyze, furthermore, the $p_v < 0$ case. As mentioned previously, the expression of the free energy Eq. (2.98), due to the change in sign of the vertical polarization which affects drastically the distribution function, is not any more a global minimum for all the values of (x, y) for which $p_v < 0$. For values of $q_{\Lambda I'}$ close to -1 the integration limit $Q_{\Lambda I'}$ tends to π. Thus, the vertical and horizontal polarization both are strictly zero. The antiferroelectric ground state which emerges for $y < 1$ and any x will have the free energy given by

$$f_{\Lambda I'} = \varepsilon_4 - k_B T \int_0^{\pi} \ln[\frac{1}{y^2} \frac{1}{x^2 + y^2 - 2xy \cos k}] \, \rho(k) \, dk \quad . \tag{2.103}$$

As the free energy from Eq. (2.98), for $p_v < 0$ has a change in its curvature, for the same values of (x, y) Eq. (2.103) will represent the lowest free energy. The phase separation curve **c**, see Fig. 2.6, between the free energies given in Eqs. (2.98) and (2.103) was determined by a numerical evaluation of the two expressions. On the whole phase separation curve the free energy is a continuous function, while its first derivative, that is the internal energy has a step discontinuity. Thus, a first order transition emerges. Below and above this curve the free energy is given by Eq. (2.103) and by Eq. (2.93), respectively.

2.8.1 The Ferroelectric Phases

As mentioned previously, for the (x, y) values for which $Q_{M'} = 0$ the free energy reduces to $f_{M'} = \varepsilon_4$ or ε_3. This two phase are **FeI** and **FeII** from Fig. 2.6. The phase separation curves are corresponding to Eqs. (2.102), i.e. curve **a** is

$$x = y - \frac{1}{y} \quad , \tag{2.104}$$

and curve **b** is

$$x = y + \frac{1}{y} \quad . \tag{2.105}$$

As it can be seen Eq. (2.104) is identical with the $\Delta_5 = 1$ condition, thus region **FeII** is characterized by $\Delta_5 > 1$. Thus, the lowest energy state is one in which all the vertices are of type four or three. For the **FeI** phase also the energy given by $f_{M'}$ is ε_4 or ε_3. This, obviously, is unphysical, as for $x > y$ we have $\varepsilon_1 < \varepsilon_4 = \varepsilon_3$.

2.8.2 The Ferrielectric Phase

Between the **a** and **b** transition curves the vertical and horizontal polarizations p_v and p_h, as obtained from Eq. (2.45) and (2.51), respectively, are smooth functions of x and y. For some y values the vertical polarization is presented in Fig. 2.7. Since this domain, region **Fi** of Fig. 2.6, which is delimited by the **a**, **b** and **c** transition curves, has a nonvanishing polarization per vertex, it will correspond to a ferrielectric phase.

Approaching both curves **a** or **b** the vertical polarization tends to unity. Being exactly equal to unity on the whole transition curves. On both transition lines the internal energy from Eq. (2.100) is a continuous function. The specific heat can be determined from Eq. (2.101). Approaching the **a** transition line from the

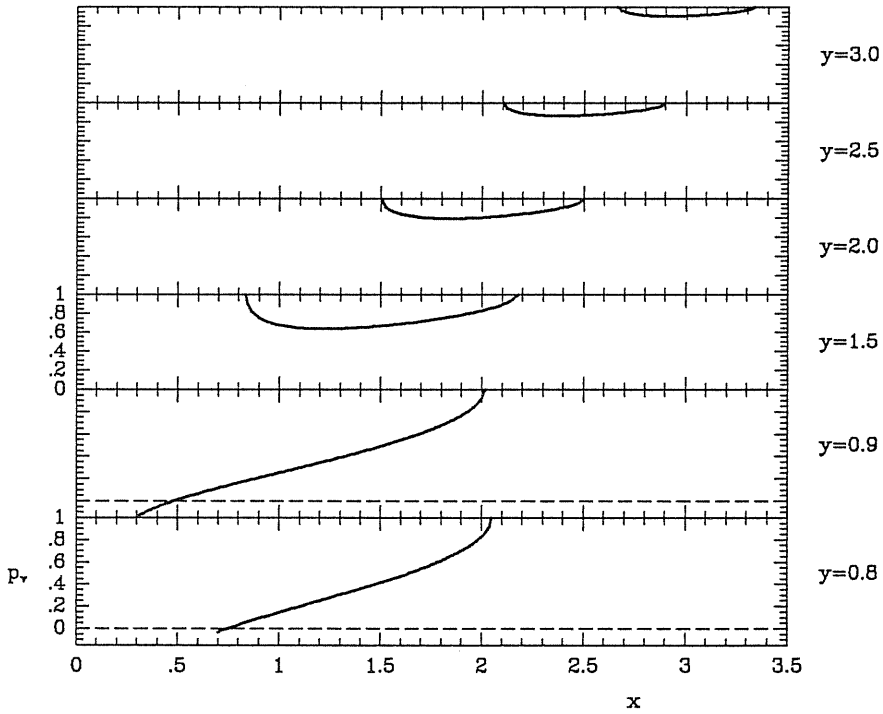

Fig. 2.7: Vertical polarization versus x for different fixed values of y. The plots are starting from the x values corresponding to the a and c transition curves of Fig. 2.6, and they finish at the x values corresponding to the b transition curve of Fig. 2.6. The dashed line is guide for the eye, it represents the $p_v = 0$ value. The $y = 1$ case is identical with Fig. 2.4.

left, the specific heat is zero. From the right, that is for $x \rightarrow [(y^2-1)/y]_{(+)}$ we have $\sqrt{1-q_{M'}^2} \rightarrow \sqrt{1-[xy/(y^2-1)]^2/y^2}$ and $\widetilde{C}_{M',2}\{x \rightarrow [(y^2-1)/y]_{(+)}\}$ from Eq. (2.84), with the obvious change $F_L(x,y,k) \rightarrow F_{M'}(x,y,k)$, is

$$
\begin{aligned}
\widetilde{C}_{M,2}[x \rightarrow (\frac{y^2-1}{y})_{(+)}] &= -\frac{1}{2\pi\,(y^2-1)} \\
&\times \; [\; \frac{(\varepsilon_5-\varepsilon_1)^2}{T^2}\,(\frac{y^2-1}{y})^2 + \frac{(\varepsilon_5-\varepsilon_4)^2}{T^2}\,y^2 \\
&- \; 2\,\frac{(\varepsilon_5-\varepsilon_1)(\varepsilon_5-\varepsilon_4)}{T^2}\,\frac{y^4-1}{y}\;] \quad .
\end{aligned} \tag{2.106}
$$

Thus, the specific heat behaves as

$$c[x \to (\frac{y^2-1}{y})_{(+)}] = \frac{1}{2\sqrt{2}\pi} \frac{[(y^2-1)\ln(y^2-1) - y(y+1)\ln y]^2}{(y^2-1)\sqrt{\frac{xy}{y^2-1}-1}} \quad , \tag{2.107}$$

that is,

$$\begin{aligned} c[T \to T_{c(+)}] &= \frac{e^{(\varepsilon_1-\varepsilon_4)/T_c}}{2\sqrt{2}\pi T_c} \\ &\times \frac{[(\varepsilon_5-\varepsilon_1)e^{(2\varepsilon_5-\varepsilon_1-\varepsilon_4)/T_c} - (\varepsilon_5-\varepsilon_4)(1+e^{2(\varepsilon_5-\varepsilon_4)/T_c})]^2}{\sqrt{\varepsilon_5-\varepsilon_1}\sqrt{T-T_c}} \quad . \end{aligned} \tag{2.108}$$

This means that the transition curve **a** represents a continuous transition with the critical exponent $\alpha = 1/2$.

Approaching the **b** transition curve we have

$$\begin{aligned} \widetilde{C}_{M,2}[x \to (\frac{y^2+1}{y})_{(-)}] &= -\frac{1}{\pi\, y(y^2+1)} \\ &\times [\frac{(\varepsilon_5-\varepsilon_1)^2}{T^2}(y^2+1)^2 + \frac{(\varepsilon_5-\varepsilon_4)^2}{T^2}(y^2-1)^2 \\ &- 2\frac{(\varepsilon_5-\varepsilon_1)(\varepsilon_5-\varepsilon_4)}{T^2}(y^4-1)] \quad . \end{aligned}$$

The specific heat will go like

$$c[x \to (\frac{y^2+1}{y})_{(-)}] = \frac{y}{\sqrt{2}\pi} \frac{[(y^2+1)\ln(y^2+1) - 2y^2\ln y]^2}{(y^2+1)\sqrt{1-\frac{xy}{y^2+1}}} \quad . \tag{2.109}$$

Which in terms of temperature gives

$$\begin{aligned} c[T \to T_{c(+)}] &= \frac{T_c e^{(\varepsilon_1-\varepsilon_5)/T_c}}{\sqrt{2}\pi} \\ &\times \frac{[(2\varepsilon_5-\varepsilon_1-\varepsilon_4)e^{(2\varepsilon_5-\varepsilon_1-\varepsilon_4)/T_c} - 2(\varepsilon_5-\varepsilon_4)e^{2(\varepsilon_5-\varepsilon_4)/T_c}]^2}{\sqrt{\varepsilon_5-\varepsilon_1}\sqrt{T-T_c}} \quad . \end{aligned} \tag{2.110}$$

As expected, also the **b** transition curve represents a continuous transition with the critical exponent $\alpha = 1/2$.

The crossing point of the **a** (continuous) and **c** (first order) transition curves at $x = 0$, and $y = 1$ has a different critical behaviour from the transition curves. Approaching the $x = 0$, $y = 1$ point from the **c**, $x \sim (1 - y^2)/y$ curve the polarization per vertex tends to zero, while the specific heat diverges like $\pi t^{-3/2} \ln^2 2$, where $t = (T - T_c)/T_c$. Thus, the critical exponent is $\alpha = 3/2$.

2.8.3 The Antiferroelectric Phase

The model exhibits an antiferroelectric phase, denoted by **Af** in Fig. 2.6. The vertical and horizontal polarizations are strictly zero in this region. Entering the **Af** phase from the **Fi** phase a first order transition is encountered. The vertical and horizontal polarizations have a step discontinuity. The free energy of the **Af** phase turns out to be independent of x. This means that the antiferroelectric phase is built up only with vertices three, four, five and six; vertex one is completely absent. Thus, we have the $n_3 = n_4$ symmetry ($n_5 = n_6$ always). Having in mind the definition of the vertical and horizontal polarization, the only possibility to obtain an antiferroelectric phase, i.e. $p_v = p_h = 0$ is $n_1 = 0$. This symmetry implies the emergence of an ordered antiferroelectric phase, in the same sense of the antiferroelectric phase of the symmetric six-vertex model.

2.9 Phase Diagram of $\mathrm{f} = min\ [\mathrm{f}_L,\ \mathrm{f}_{M'}]$

If we consider both eigenvalues from Eq. (2.5), then the free energy of the five-vertex model will be given by

$$f \;=\; \min \{\, f_L \;,\;\; f_{M'} \,\} \quad . \tag{2.111}$$

In § **2.7** and **2.8**, we analyzed the behaviour of the f_L and $f_{M'}$ terms on the whole (x, y) plane and obtained the phase diagrams of Fig. 2.3 and Fig. 2.6, respectively.

The two expressions of the free energies f_L and $f_{M'}$ are valid, as presented in the discussion following Eq. (2.22), for any (x, y) for which $\Delta_5 < 1$. For the values of (x, y), for which Δ_5 is bigger then unity, the Bethe Ansatz gives a solution for the momenta k being pure imaginary. Thus, for this parameter region the system exhibits a ferroelectric phase. The $\Delta_5 = 1$ condition defines the transition curve, which exists in both cases. The fact that this transition curve was obtained by two different methods, emphasizes the correctness of the procedures used in § **2.7** and **2.8**.

Below this transition curve, we match the two phase diagrams, i.e. Fig. 2.3 with Fig. 2.6. From Eq. (2.76) and (2.98), easily can be verified that for $x \gg y$ we have $f_L < f_{M'}$, while for $y \gg x$ $f_{M'} < f_L$. Unfortunately, the two free energy expressions are not equal for $x = y$ (contrary to what happens for the six-vertex model), thus a numerical analysis of the two expressions is needed. The final phase diagram obtained in this way is presented in Fig. 2.8. This phase diagram we will analyze briefly in the following, as its parts were analyzed comprehensively in § **2.7** and **2.8**.

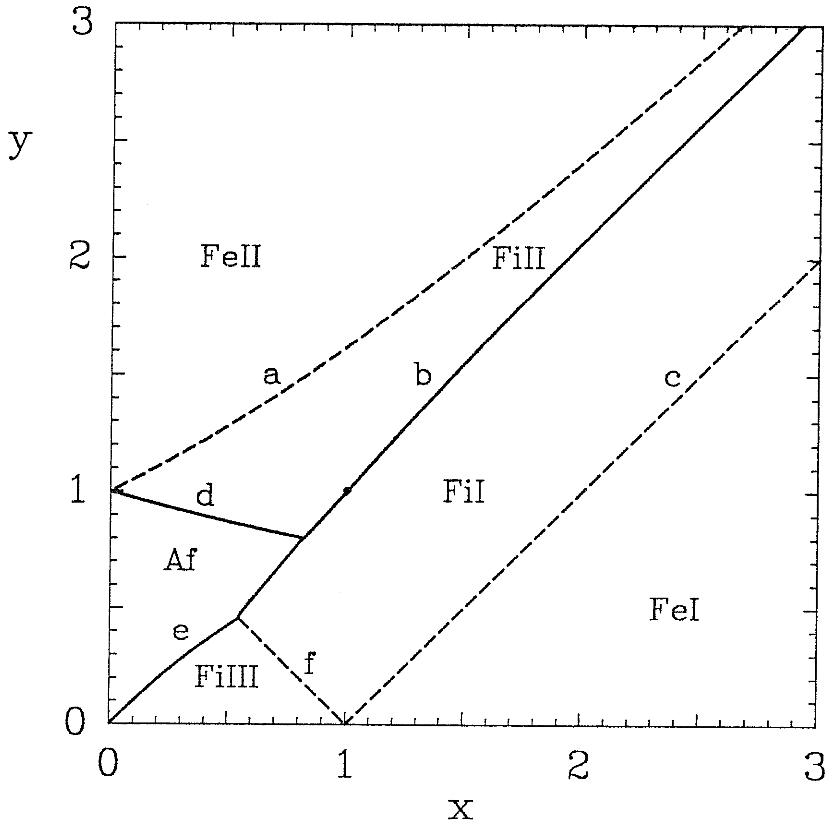

Fig. 2.8: The phase diagram of $f = min\ [f_L,\ f_{M'}]$ in zero external field, in terms of the Boltzmann weights x = a/c and y = b/c. The solid curves represent first order transition, the dashed curves continuous transitions. Fe stands for a ferroelectric, Fi for a ferrielectric and Af for an antiferroelectric phase. The x = y = 1 point corresponds to the infinite temperature, while any point satisfying x/y = 0 or y/x = 0 corresponds to the zero temperature state.

Some parts of the phase diagram (some phases) will be characterized by symmetry breaking, others not. For example, in the non-interacting case there is no symmetry breaking for $x > 1$, that is $p_h = p_v > 0$. But, there is symmetry breaking for $x < 1$, where two equivalent realizations are possible, one corresponding to $p_v > 0$, $p_h = -p_v < 0$, the other to $p_v < 0$, $p_h = -p_v > 0$.

Quite generally, since $p_v = (n_1 - n_3 + n_4)/N$ and $p_h = (n_1 + n_3 - n_4)/N$, and since exchanging rows with columns n_3 and n_4 are interchanged, it is clear that if a macroscopic state (realization) exists with $p_v = Y$, $p_h = X$, $Y \neq X$ then there is symmetry breaking, i.e. there exists another equivalent realization with $p_v = X$, $p_h = Y$.

2.9.1 The Ferroelectric Phases

In the six-vertex model the behaviour of the $\Delta_6 = 0$ case is actually typical for the entire region $-1 < \Delta_6 < 1$, i.e. the disordered phase. In our case, this is not entirely true. Due to the fact that the arrow-reversal symmetry is broken by construction, the model lacks the $x \leftrightarrow y$ reflection symmetry, as it was shown in § **2.2**. Such behaviour applies to both terms f_L and $f_{M'}$. If we start from large values of x, the minimum free energy is equal to ε_1, as in the non-interacting case. That is, in the region **FeI** of Fig. 2.8, the system is an ideal ferroelectric. The lowest energy state is one where all vertices are of type one. The phase transition line **c** of Fig. 2.8, is given by f_L. In our case, for $\Delta_5 < -1$ and $x > y+1$, there is a competition between a ferroelectric and an antiferroelectric phase, see Fig. 2.3 and Fig. 2.6. It turns out that f_L is always lower than $f_{M'}$. The horizontal polarization p_h is also unity on the whole region **FeI**. This is obvious, because the only choice for this region is to be built up of vertex one.

For small values of x there exists another ferroelectric phase. This is bounded by the $\Delta_5 = 1$ curve, denoted by **a** in Fig. 2.8. The free energy is ε_4 in region **FeII** of Fig. 2.8. All this region is characterized by $\Delta_5 > 1$. Notice that the **FeII** phase, contrary to the **FeI** phase, is symmetry breaking.

2.9.2 The Ferrielectric Phases

Crossing the line **c** the smallest free energy is f_L. The vertical and horizontal polarizations p_v and p_h, are smooth functions of x and y. Both of them are equal to unity on the $x = y + 1$, **c** line, tend to unity as $x, y \to \infty$ and at fixed y are decreasing as x decreases up to the **b** curve. The vertical polarization p_v is zero on the $x = 1 - y$, **f** line of Fig. 2.8, while the horizontal polarization p_h is equal to unity on the same **f** transition line (or viceversa).

As we know, close to the **f** curve the vertical polarization tends to zero, while the horizontal polarization tends to unity, or viceversa. Due to the existence of more realization, the symmetry is broken in the **FiI** phase. Curve **f** corresponds to curve **c** from Fig. 2.3, crossing of which, the lowest free energy in region **FiIII** is still given by f_L.

The phase separation curve **e** of Fig. 2.8, between the **FiIII** ferrielectric and **Af** antiferroelectric phases was determined by a numerical evaluation of Eq. (2.76) with $Q_L = \pi$ and Eq. (2.103). On the whole curve the free energy is a continuous function, while its first derivative, that is the internal energy, has a step discontinuity. This means that curve **e** represents a first order transition. The crossing point of the **e** first order and **f** continuous transition curves does not bring about a different critical behaviour.

The ferrielectric region **FiI** is bordered on its left side by curve **b**. Crossing this curve the lowest free energy in the whole region **FiII** is $f_{\Lambda I'}$. The two polarizations are different from the polarizations in region **FiI**. They, however, are still smooth functions of x and y. The vertical polarization p_v is equal to unity on the **a** transition curve, while the horizontal polarization $p_h = -1$, corresponding to vertex four (or viceversa, corresponding to vertex three). For the horizontal polarization always the $p_h = -p_v$ relation holds. Using the definition of the polarizations, this means that there is no vertex one present in this phase, i.e. $n_1 = 0$, contrary to the **FiI** phase which contains all the five vertices. The transition curve **b**, containing the infinite temperature point, corresponds to a disorder line.

This disorder line represents a first order transition. As mentioned at the beginning of § **2.9**, the exact form of the curve **b** was obtained by a numerical comparison of f_L and $f_{\Lambda I'}$. The two expressions for the free energy become identical crossing the $y = 1$ line. The free energy is continuous, of course, on the whole **b** curve, but its first derivative, i.e. the internal energy, has a step discontinuity. Also the polarization (both vertical and horizontal) has a step discontinuity crossing this transition line.

The **FiII** ferrielectric phase is bounded by a second transition curve of the first order type. This corresponds to the **d** curve, which was obtained also by a numerical analysis, corresponds to curve **c** from Fig. 2.6. Along the whole curve the internal energy has a step discontinuity. Crossing curve **d** leads to an antiferroelectric phase; both polarizations have a step like discontinuity.

The crossing point of the transition curves **b** and **d**, both first order transitions, represents a triple point.

2.9.3 The Antiferrolectric Phase

The free energy of the phase **Af** is given by $f_{\Lambda I'}$ from Eq. (2.103). The antiferroelectric phase can be approached from all the ferrielectric regions **FiI**, **FiII** and **FiIII**. Entering the **Af** antiferroelectric phase from any of these ferrielectric phases we encounter a first order transition. The vertical and horizontal polarization per vertex have a step discontinuity on all the **b**, **d** and **e** transition curves. Approaching the **Af** phase from **FiI**, close to the **b** curve the vertical polarization p_v varies continuously from zero up to the 0.256 value corresponding to the $x = 0.82$, $y = 0.80$ triple point. If we move in the neighbourhood of the **d** transition curve, inside the **FiII** phase, the vertical polarization per vertex vanishes at $x = 0$ and $y = 1$, reaches its minimum value of $-1/3$ close to this point, and increases as we approach the triple point, always remaining negative (being below the dotted curve of Fig. 2.6) while the horizontal polarization is positive. Or, the two polarizations are interchanged, as in the **FiII** phase the symmetry is broken.

2.9.4 Conclusions on the Phase Diagram

As we saw both f_L and $f_{\Lambda I'}$ exhibits first order transitions and continuous transitions with the specific heat critical exponent $\alpha = 1/2$. Several aspects of this second order phase transitions are unusual, because the order parameter is equal to unity on one side of the transition, instead of vanishing as in the normal Curie point of ferromagnets. The high temperature phases have a non-vanishing polarization per vertex, that is ferrielectric phases are emerging. In fact in Fig. 2.8 three such phases appear, all of them exhibiting different properties. One (**FiI**), in which the vertex one is dominant, a second one (**FiII**), in which vertices three and four are in majority, and vertex one is missing and the third one (**FiIII**), where the vertical polarization p_v (or the horizontal polarization p_h) is always zero. The **FiI** and **FiII** ferrielectric phases are separated by a disorder line, corresponding to a first order transition, while the **FiI** and **FiIII** ferrielectric phases are separated by a second order transition line. The phase **FeII** and all three ferrielectric phases break the symmetry (they present two realizations differing by exchange of the vertices three and four, i.e. by a reflection with respect to the $x = y$ plane), while the phases **FeI** and **Af** do not. Notice the different situation in the six-vertex model, where both ferroelectric phases are symmetry-breaking, but not the antiferroelectric phase, nor the disordered phase.

Before closing this paragraph, let us briefly study the possible thermal trajectories. Thus, we fix the energy of the vertices and change the temperature, i.e. move on the thermal trajectories. For $\varepsilon_5 - \varepsilon_4 \geq 0$ and $\varepsilon_5 - \varepsilon_1 \geq 0$ at low temperatures we always encounter a ferroelectric phase, **FeI** or **FeII**. Increasing the temperature we cross a second order transition curve, either **a** or **c**. At very high temperatures we can also cross the disorder curve, i.e. curve **b** of Fig. 2.8, if we are situated in the $0.88 < (\varepsilon_5 - \varepsilon_4)/(\varepsilon_5 - \varepsilon_1) < 1.00$ region.

If we consider the $\varepsilon_5 - \varepsilon_4 < 0$, $\varepsilon_5 - \varepsilon_1 < 0$ case at low temperatures the system is an antiferroelectric or ferrielectric, see the thermal trajectories **1**, **2** and **3** of Fig. 2.9. The variation of the vertical and horizontal polarizations is presented in Fig. 2.10, 2.11 and 2.12, corresponding to the thermal trajectories **1**, **2** and **3** of Fig. 2.9. For $(\varepsilon_5 - \varepsilon_4)/(\varepsilon_5 - \varepsilon_1) > 1.30$ the thermal trajectories are always of type **1**, that is at high temperatures we encounter a first order transition. As it can be see from Fig. 2.10 both polarizations have a step-like discontinuity at the transition temperature T_c corresponding to this phase transition. Below the transition both polarizations are strictly zero.

However, if the condition $(\varepsilon_5 - \varepsilon_4)/(\varepsilon_5 - \varepsilon_1) < 1.12$ is satisfied the thermal trajectories are of type **3**, in which case a second order phase transition takes place. One of the two polarizations (e.g. the vertical polarization), as seen in Fig. 2.12, is continuous at the transition and is strictly zero below. The other (e.g. horizontal) polarization has a step - like discontinuity, and is vanishingly small as $T \rightarrow 0$ in the **FiIII** ferrielectric phase.

Between these two limits an interesting situation seems to appear, corresponding to trajectory **2** of Fig. 2.9. Increasing the temperature first a first order transition is encountered from the **FiIII** ferrielectric phase to an antiferroelectric phase (**Af**), after which a second transition emerges which is again of the first order type, from the antiferroelectric phase into the **FiI** ferrielectric phase. At the lower temperature transition one horizontal polarization (e.g. p_h) has a step-like discontinuity, see Fig. 2.11, while at the high temperature transition both polarizations (p_v and p_h) exhibit a step-like discontinuity. This numerical analysis, however, is very delicate and trajectory **2** is only tentative.

In conclusion, we have constructed the eigenvalue of a five-vertex model, see Eq. (2.5). This equation describes in principle all the four cases of a five-vertex model. We have analyzed separately and together the two free energy terms which emerge from the eigenvalue equation. Due to the unusual properties of the phases given by the $f_{M'}$ term, like exhibiting symmetry breaking and being an effective four vertex solution, in the following we consider the f_L to be the free energy term of the five-vertex model, i.e., we consider the right-hand, lower half of the phase diagram.

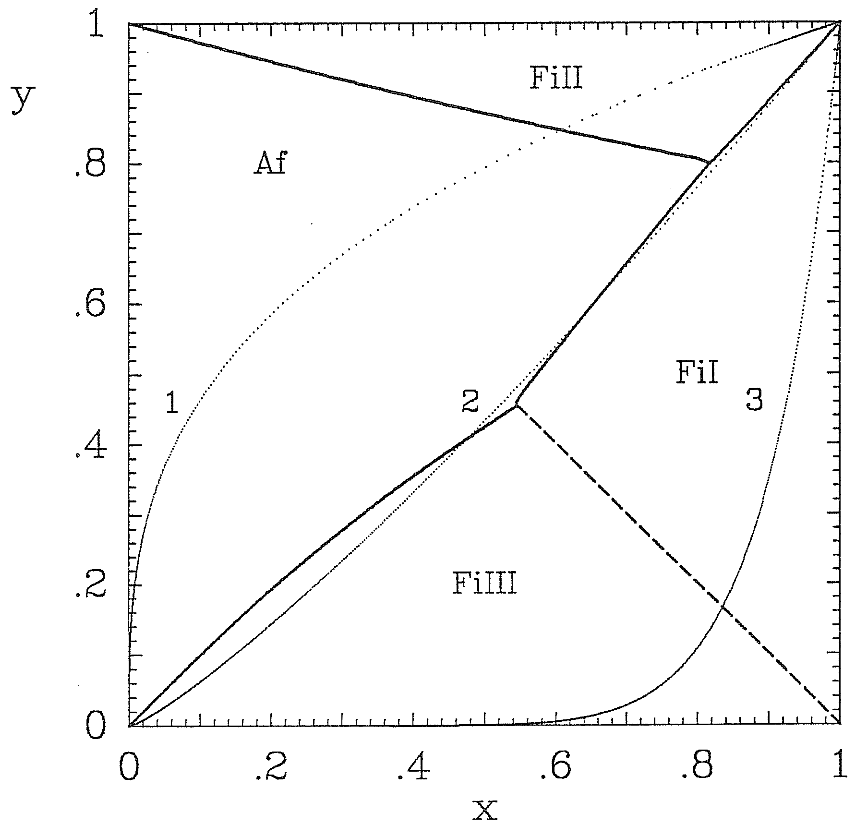

Fig. 2.9: Details of the Fig. 2.8 phase diagram, for the ε_5 - ε_4 < 0 and ε_5 - ε_1 < 0 case. The dotted curves 1, 2 and 3 represent thermal trajectories from x = y = 0 (T = 0) to x = y = 1 (T = ∞).

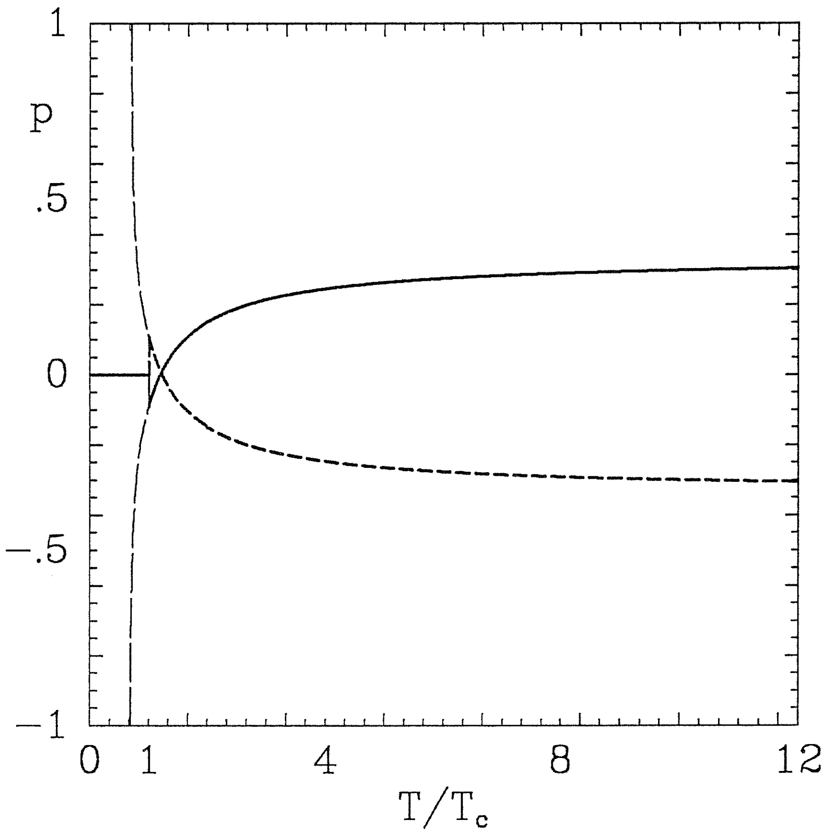

Fig. 2.10: Vertical polarization p_v (solid curve) and horizontal polarization p_h (short dashed curve) as functions of temperature for the thermal trajectory 1 of Fig. 2.9. The long-dashed curves represent the analytic continuation of the two expression for the polarization below the phase transition.

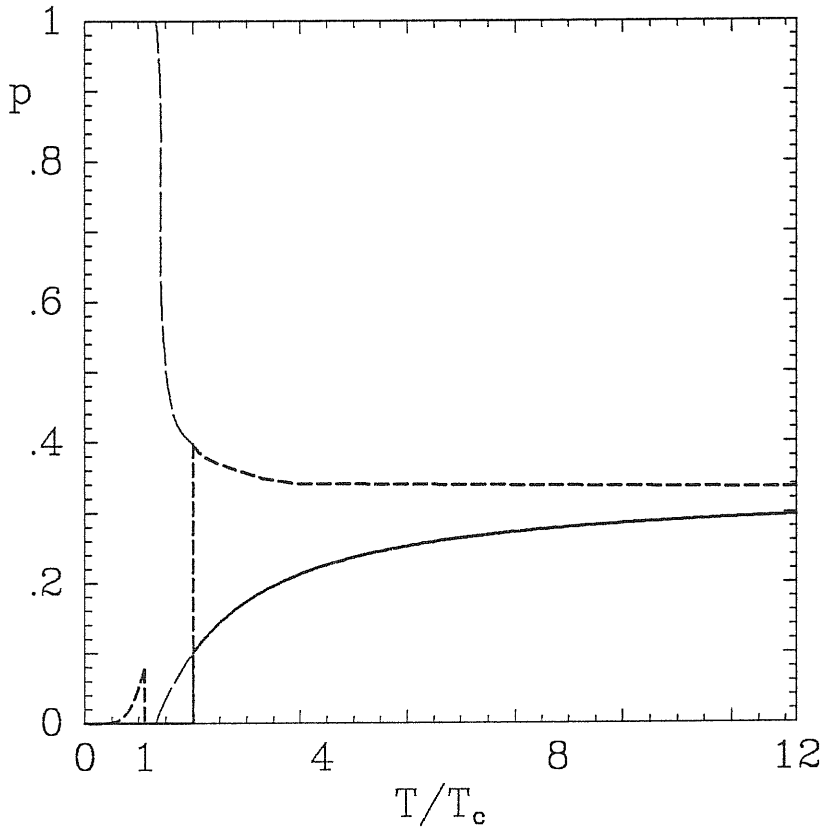

Fig. 2.11: Vertical polarization p_v (solid curve) and horizontal polarization p_h (short dashed curve) as functions of temperature for the thermal trajectory 2 of Fig. 2.9. The lower transition temperature between the FiIII phase and the Af phase was denoted by T_c. The second, higher transition temperature between the Af phase and FiI phase is equal with 1.82 T_c. The long-dashed curves represent the analytic continuation of the two expression for the polarization of the FiI phase below the phase transition.

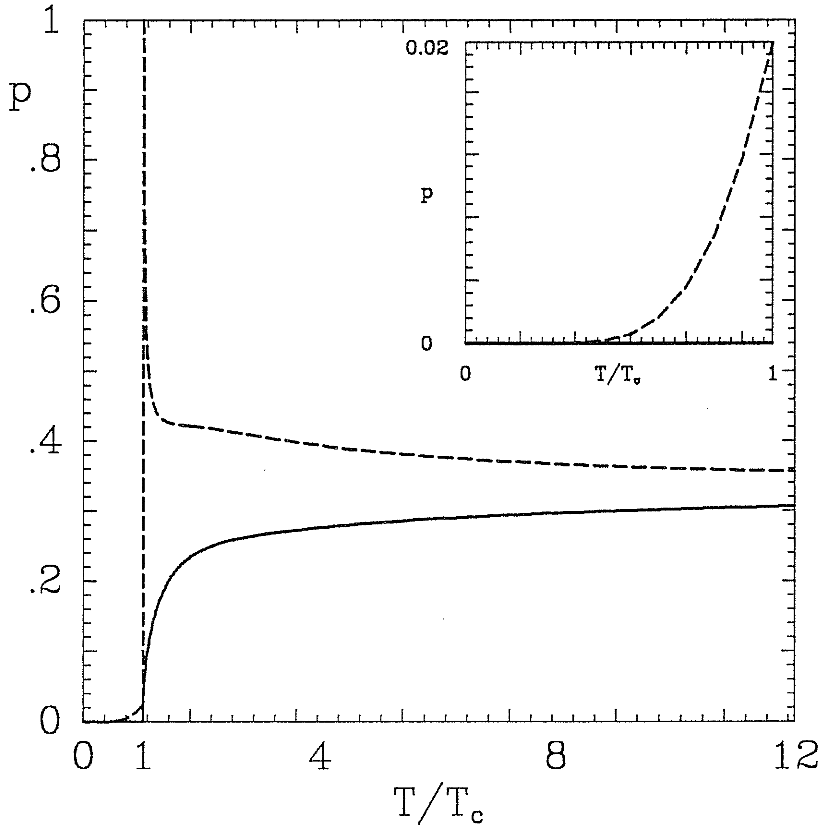

Fig. 2.12: Vertical polarization p_v (solid curve) and horizontal polarization p_h (short dashed curve) as functions of temperature for the thermal trajectory 3 of Fig. 2.9. In the inset, the detailed picture of the polarization below the transition temperature.

2.10 Five-Vertex Model in a Field

As was repeatedly said the arrow-reversal symmetry is already broken in the system by construction. Thus, we expect that a direct external field will not change the behaviour of the model. Therefore, we might apply a vertical (v) and a horizontal (h) field on every site. In fact, however, the physics of the five-vertex model only depends on the difference $h - v$ (changing the sum $h + v$ is in fact equivalent to changing the energy ε_1 of vertex one). Thus it is not essentially restrictive to take $h = 0$. Rather than incorporating the vertical field into the vertex energies, let us keep $\omega_1 = a$, $\omega_3 = \omega_4 = b$ and $\omega_5 = \omega_6 = c$ still valid. Using the $V = \exp(-2v/k_B T)$ notation, we obtain for the $L(k)$ function defined in Eq. (2.52)

$$L(k) = \frac{V^2}{x^2} [y^2 + \frac{1 - 2y^2 + 2xy\cos k}{x^2 + y^2 - 2xy\cos k}] \quad . \tag{2.112}$$

$\rho(k)$ is still given by Eq. (2.44) and Δ_5 by Eq. (2.51). In the non-interacting case, i.e $y = 1$, the free energy becomes

$$f_L = \varepsilon_1 - v - k_B T \frac{Q_0}{\pi} \ln V + \frac{k_B T}{4\pi} \int_{-Q_0}^{+Q_0} \ln(x^2 + 1 - 2x\cos k)\, dk \quad , \tag{2.113}$$

The integration limit is $Q_0 = \arccos[(x^2 + 1 - V^2)/(2x)]$. Two continuous phase transitions appear for $x = 1 + V$ and $x = 1 - V$ with critical exponent $\alpha = 1/2$. That is, the specific heat $c[T \to T_{c(+)}] \sim (T - T_c)^{-1/2}$, and it turns out that also the susceptibility has the same behaviour in both cases. This means that the critical exponent of the susceptibility is $\gamma = 1/2$. The vertical p_v, and the horizontal p_h polarization per vertex can be easily computed, obtaining

$$\begin{aligned} p_v &= 1 - \frac{2}{\pi} Q_0 \; ; \\ p_h &= \pm [1 + \frac{2}{\pi} \arctan(\frac{\sin Q_0}{\cos Q_0 - x})] \quad . \end{aligned} \tag{2.114}$$

Note, the presence again of a function with algebraic form identical with that of the kernel, see Eq. (2.34). The two sign $(+,-)$ in Eq. (2.114) corresponds to $x < 1$, and $x \geq 1$, respectively. In particular it is obtained from Eq. (2.114) that in zero field, for $x \geq 1$ the polarization per vertex is $p_v = p_h = 1-(2/\pi)\arccos(x/2)$, while for $x < 1$ it is $p_v = -p_h = \pm[1-(2/\pi)\arccos(x/2)]$, identical with that obtained in § **2.6**. Both p_v and p_h approach unity in both $x = 1-V$ and $x = 1+V$ transitions as $\sqrt{T-T_c}$.

Away from the free-fermion condition ($\Delta_5 = 0$) we use the same method as in § **2.7**. As a result of the presence of the external field the ferrielectric and antiferroelectric phases will shrink. Curve **b** from Fig. 2.3 will be changed to

$$x \;=\; \frac{y}{2}(1+V) \;+\; [y^2(1-V)^2/4 \;+\; V]^{1/2} \quad , \tag{2.115}$$

curve **c** will become

$$x \;=\; -\,\frac{y}{2}(1+V) \;+\; [y^2(1-V)^2/4 \;+\; V]^{1/2} \quad . \tag{2.116}$$

All these phase separation curves will remain of the continuous type, with critical exponents $\alpha = 1/2$ and $\gamma = 1/2$. That is, both the specific heat and the susceptibility diverge like $(T-T_c)^{-1/2}$. The phase separation curve **a** of Fig. 2.3 will remain of the first order type. We recall that the **a** transition curve was determined by the condition $\Delta_5 = 1$, which is not changed by the presence of the external field. The zero field phase diagram from Fig. 2.3, for different values of the external field, is given in Fig. 2.13. Note that the **c** curve from Eq. (2.116) for any V and $x = 0$ has the only solution $y = 1$, while curves **b** and **c** are crossing for any V at $y = 0$ and $x = \sqrt{V}$, see Fig. 2.13.

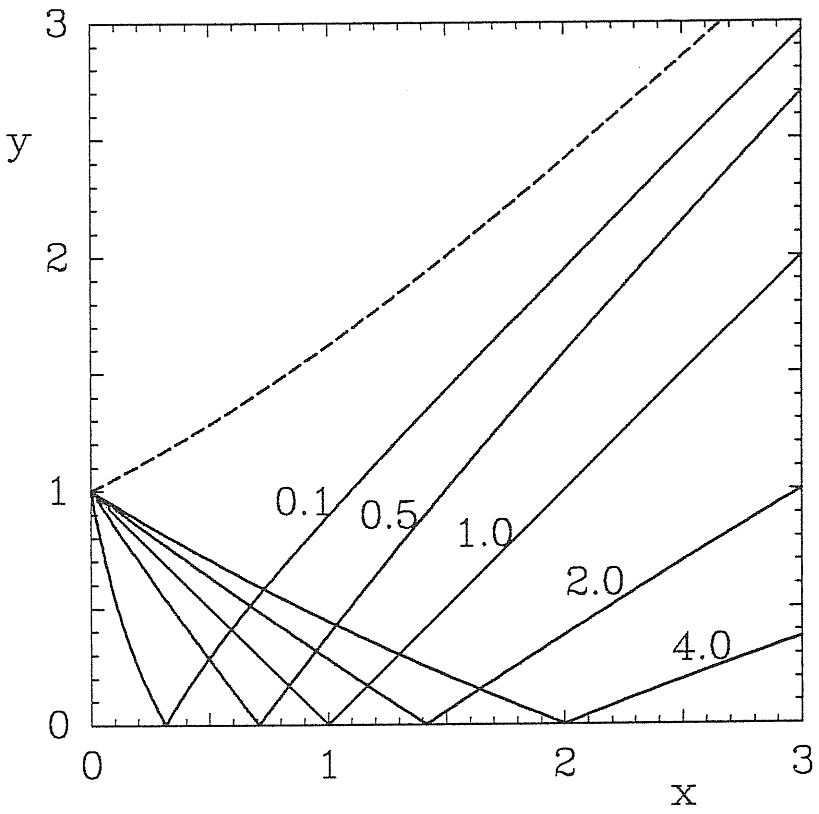

Fig. 2.13: The phase diagram of the five-vertex model in external field, in terms of the Boltzmann weights x = a/c and y = b/c, for five constant values of V. The corresponding phase diagram in zero external field is given in Fig. 2.3. V = 1 corresponds to no field.

For the ferrielectric phase, **FiI** of Fig. 2.3 the limit of integration entering in the expression of the free energy will be given by

$$Q_L \;=\; \arccos \frac{x^4/V^2 \;-\; (y^2-1)^2 \;+\; x^2y^2(1/V^2-1)}{2xy(1 \;-\; y^2 \;+\; x^2/V^2)} \quad . \tag{2.117}$$

The polarizations per vertex can be easily computed. However, in the following we give only the expressions for the vertical polarization, because these can be written in a short, compact form. p_v for the **FiI** phase is given by

$$\begin{aligned} p_v &= 1 - (2Q_L + \ln V \frac{\partial Q_L}{\partial V}) \\ &[\pi + \frac{Q_L}{2} + \arctan[\frac{\Delta_5 + 1}{\Delta_5 - 1} \tan \frac{Q_L}{2}] + \frac{1}{2} \ln V \frac{\partial Q_L}{\partial V} R_L]^{-1} \quad , \end{aligned} \tag{2.118}$$

where

$$R_L = \frac{y^2 - 1}{2x^2} \frac{x^2(x^2+2) + (y^2-1)^2 V^2 - x^2 y^2 (1 + V^2)}{x^2 - y^2 + 1} \quad , \tag{2.119}$$

In the limit of vanishing external field, the expression of the polarization known from Eq. (2.45) is recovered. Below the transition curve given in Eq. (2.116), Q_L is equal to π. As it can be seen from Eq. (2.118), this implies $p_v = 0$. That is, the vertical polarization of the **FiII** phase will be zero also in external field.

2.11 Relation between the Five-Vertex Model and the Asymmetric Six-Vertex Model

In the following we show that from the asymmetric six-vertex model in the strict limit of five vertices only the non-interacting case can be recovered. This is due to the method of calculating the free energy, i.e. to the transformation to new variables (rapidities) which make the equations symmetric.

The method of obtaining the equations in the asymmetric six-vertex case is presented in Appendix B. Briefly we review the calculations. The solution of the general six-vertex model, Eqs. (1.7) and (1.8) is given as a function of five variables, as ω_1, ω_2, ω_3, ω_4 and $\omega_5 = \omega_6$. These are transformed to

$$\eta = \sqrt{\frac{\omega_1 \omega_2}{\omega_3 \omega_4}} \equiv e^{\beta \delta} \quad , \tag{2.120}$$

$$\xi = \frac{\omega_5^2}{\sqrt{\omega_1\omega_2\omega_3\omega_4}} \equiv e^{2\beta\epsilon} \quad , \tag{2.121}$$

$$\Delta_6 = \frac{1}{2}\,(\eta + \frac{1}{\eta} - \xi) \quad , \tag{2.122}$$

$$H = e^{2\beta h} = \sqrt{\frac{\omega_1\omega_3}{\omega_2\omega_4}} \quad , \tag{2.123}$$

and

$$V = e^{2\beta v} = \sqrt{\frac{\omega_1\omega_4}{\omega_2\omega_3}} \quad . \tag{2.124}$$

Transformations are given in Eqs. (B.1) - (B.5) or Eqs. (1.9) - (1.12). With the condition $\omega_1\omega_2\omega_3\omega_4 = 1$ the number of independent variables is reduced to four

$$\begin{aligned}
\omega_1 &= \exp\beta(\frac{\delta}{2} + h + v) \; ; \\
\omega_2 &= \exp\beta(\frac{\delta}{2} - h - v) \; ; \\
\omega_3 &= \exp\beta(-\frac{\delta}{2} + h - v) \; ; \\
\omega_4 &= \exp\beta(-\frac{\delta}{2} - h + v) \; ; \\
\omega_5 &= \exp\beta\epsilon \; ; \\
\omega_6 &= \exp\beta\epsilon \quad .
\end{aligned} \tag{2.125}$$

It is possible to reduce the variables to three by the following transforms, see Eqs. (B.17) and (B.18)

$$\begin{aligned}
H\,e^{ik} &= \frac{e^{\nu} - e^{-i\alpha}}{-e^{\nu-i\alpha}+1} \, , \quad \text{if } \Delta_6 > 1 \, , \quad \Delta_6 = \cosh\nu \, , \quad \nu > 0 \; ; \\
&= \frac{e^{i\mu} - e^{\alpha}}{e^{i\mu+\alpha}-1} \, , \quad \text{if } |\Delta_6| \le 1 \, , \quad \Delta_6 = -\cos\mu \, , \quad 0 \le \mu \le \pi \; ; \\
&= \frac{e^{\lambda} - e^{i\alpha}}{e^{\lambda-i\alpha}-1} \, , \quad \text{if } \Delta_6 < -1 \, , \quad \Delta_6 = -\cosh\lambda \, , \quad \lambda > 0 \quad .
\end{aligned} \tag{2.126}$$

Furthermore, the rapidity ϕ is defined in the following

$$
\begin{aligned}
e^{\phi} &= \frac{e^{\nu}\eta - 1}{\eta - e^{\nu}} , \quad \text{for } \Delta_6 > 1 ; \\
e^{i\phi} &= \frac{1 + e^{i\mu}\eta}{e^{i\mu} + \eta} , \quad \text{for } |\Delta_6| \leq 1 ; \\
e^{\phi} &= \frac{e^{\lambda}\eta + 1}{\eta + e^{\lambda}} , \quad \text{for } \Delta_6 < -1 \quad .
\end{aligned}
\tag{2.127}
$$

We are considering the $\eta > 1$, case as in Ref. [2] and contrary to the rest of this thesis (this change is irrelevant). The original Boltzmann weights are given in terms of these new variables as

$$
\begin{aligned}
\omega_1\omega_2 &= \sinh^2 \frac{1}{2}(\nu + \phi) , \quad \Delta_6 > 1 ; \\
&= \sin^2 \frac{1}{2}(\mu + \phi) , \quad |\Delta_6| \leq 1 ; \\
&= \sinh^2 \frac{1}{2}(\lambda + \phi) , \quad \Delta_6 < -1 \quad ,
\end{aligned}
\tag{2.128}
$$

$$
\begin{aligned}
\omega_3\omega_4 &= \sinh^2 \frac{1}{2}(\nu - \phi) , \quad \Delta_6 > 1 ; \\
&= \sin^2 \frac{1}{2}(\mu - \phi) , \quad |\Delta_6| \leq 1 ; \\
&= \sinh^2 \frac{1}{2}(\lambda - \phi) , \quad \Delta_6 < -1 \quad ,
\end{aligned}
\tag{2.129}
$$

and

$$
\begin{aligned}
\omega_5 &= \sinh\nu , \quad \Delta_6 > 1 ; \\
&= \sin\mu , \quad |\Delta_6| \leq 1 ; \\
&= \sinh\lambda , \quad \Delta_6 < -1 \quad .
\end{aligned}
\tag{2.130}
$$

Since these equations are valid for $\eta > 1$, as seen from Eq. (2.120) the $\omega_3 \to 0$ limit is suitable for this case (see the discussion following Eqs. (2.5) and (2.6)). The notation which we use in this case is given in Eq. (2.1), i.e.

$$
x = \frac{\omega_1}{\omega_5} = \frac{\omega_2}{\omega_5} , \quad y = \frac{\omega_4}{\omega_5} \quad . \tag{2.131}
$$

As $\omega_1 = \omega_2$ from Eqs. (2.120) - (2.124) it results

$$\eta = \frac{\omega_1}{\sqrt{\omega_3\omega_4}} \ , \ \xi = \frac{\omega_5^2}{\omega_1\sqrt{\omega_3\omega_4}} \ , \ H = \sqrt{\frac{\omega_3}{\omega_4}} = 1/V \quad . \tag{2.132}$$

To obtain a five-vertex model we must require that ω_1, ω_3, ω_4 and ω_5 to be independent variables. A weak dependence between vertices could also mimic a five-vertex situation. By weak dependence we require the vertices to behave only in the $\omega_3 \to 0$ limit as independent variables.

From Eq. (2.122), with the $\omega_3 \ll 1$ condition we obtain

$$\Delta_6 \cong \frac{1}{2\sqrt{\omega_3\omega_4}} \frac{\omega_1^2 - \omega_5^2}{\omega_1} \quad . \tag{2.133}$$

where Eq. (2.13) was used. Let us consider the $\Delta_6 < -1$ case, the $\Delta_6 > 1$ case give similar result. The free energy of the asymmetric six-vertex model is given in terms of λ and ϕ. Using Eq. (2.133) and the fact that $\Delta_6 = -\cosh\lambda$ we obtain

$$e^{\lambda} \cong \frac{1}{\sqrt{\omega_3\omega_4}} \frac{\omega_5^2 - \omega_1^2}{\omega_1} \quad , \tag{2.134}$$

while from the last equation of Eq. (2.127)

$$e^{\phi} \cong \frac{\omega_1}{\sqrt{\omega_3\omega_4}} \frac{\omega_5^2 - \omega_1^2}{\omega_5^2} \quad , \tag{2.135}$$

where in both cases the $\omega_3 \ll 1$ fact was used. From these we can obtain

$$e^{(\lambda+\phi)/2} \cong \frac{1}{\sqrt{\omega_3\omega_4}} \frac{\omega_5^2 - \omega_1^2}{\omega_5} \quad , \tag{2.136}$$

and

$$e^{(\lambda-\phi)/2} \cong \frac{\omega_5}{\omega_1} \quad . \tag{2.137}$$

Using the parametrizations given in Eqs. (2.128) - (2.130) we get

$$\omega_1 \cong \frac{1}{2\sqrt{\omega_3\omega_4}} \frac{\omega_5^2 - \omega_1^2}{\omega_5} \quad , \tag{2.138}$$

$$\omega_3\omega_4 \cong \frac{1}{4}\left(\frac{\omega_5^2-\omega_1^2}{\omega_1\omega_5}\right)^2 \quad , \tag{2.139}$$

and

$$\omega_5 \cong \frac{1}{2\sqrt{\omega_3\omega_4}}\,\frac{\omega_5^2-\omega_1^2}{\omega_1} \quad , \tag{2.140}$$

As it can be seen, after transforming to the rapidity ϕ, the Boltzmann weights are becoming strongly dependent on each other. The limit $\lim_{\omega_3\to 0}(\omega_3\omega_4) \neq 0$ obtained in Eq. (2.139) contradicts the limit of $\omega_3 \to 0$ within such a framework.

Conversely, from Eq. (2.140) ω_3 can vanish with finite ω_1, ω_4, ω_5 only if $\omega_1 = \omega_5$, i.e. the only possibility to satisfy all the constrains is to first consider $\omega_1 = \omega_5$ and thus, $\mu = \phi$ from Eqs. (2.128) - (2.130). But, such a condition gives us information only about the non-interacting case.

A simpler proff of the fact that Yang's transformations, when applied to the five-vertex model, imply the free-fermion condition is given in Appendix D.

Chapter 3

Vertex Models and the Surface Roughening Transition

3.1 Spin-Spin Correlation Functions in Integrable Models

One of the main unsolved problems of the Bethe Ansatz technique is the calculation of the correlation functions. Generally, for an N-site one dimensional quantum system or for a statistical mechanical problem defined on an $N \times N$ square lattice, the Bethe Ansatz wave function involves an $N! \times N!$ determinant. For such a wave function, even the calculation of the norm is a very involved problem. The norm was conjectured by Gaudin [42] in 1967, by what appears to be an extraordinary feat of intuition. Some simple elements of this norm were checked by McCoy, Wu and Gaudin [43], but the final demonstration was given in terms of the quantum inverse scattering method by Korepin [44].

In the case of a non-interacting system, the Bethe Ansatz wave function reduces to a Slater determinant. In this case, the calculation of a spin-spin correlation reduces to an integral over the Fermi sea. To be more explicit, let us consider the correlation function of two vertical arrows in a row, within the six-vertex type models. We are interested only in this correlation, as it will turn out below, see § **3.2**, because this one is strictly related to the height-height correlation of an SOS model. Thus, we define[45]

$$G(m) \;=\; \langle \sigma_0^z \sigma_m^z \rangle \quad , \tag{3.1}$$

as the correlation function of two vertical arrows in a row separated by m sites, where m is an integer. $G(m)$ was first calculated by Sutherland[45], but hereafter we present a new derivation of the correlation function $G(m)$.

Obviously, $\sigma_i^z = 2c_i^\dagger c_i - 1$, where $c_i^\dagger$ and c_i are fermionic creation and annihilation operators, and $\langle \ldots \rangle$ denote an average value defined with the unperturbed Fermi sea, i.e. a Slater determinant. The $G(m)$ correlation function from Eq. (3.1) is equal to

$$\begin{aligned} G(m) \;&=\; \langle\, (2c_0^\dagger c_0 \;-\; 1)(2c_m^\dagger c_m \;-\; 1)\,\rangle \\ &=\; 4\langle\; c_0^\dagger c_0 c_m^\dagger c_m \;\rangle \;+\; 1 \\ &-\; 2\langle\; c_0^\dagger c_0 \;\rangle \;-\; 2\langle\; c_m^\dagger c_m \;\rangle \quad . \end{aligned} \tag{3.2}$$

For the four operator average we apply the Wick theorem[46], while the last two terms $\langle c_0^\dagger c_0 \rangle = \langle c_m^\dagger c_m \rangle$ are the expectation value of the number operator[46], thus

$$\begin{aligned} G(m) \;&=\; 4(\langle c_0^\dagger c_0 \rangle\;)^2 \;-\; 4\langle c_0^\dagger c_0 \rangle \;+\; 1 \\ &-\; 4\langle c_0^\dagger c_m \rangle \langle c_m^\dagger c_0 \rangle \\ &=\; [2\langle c_0^\dagger c_0 \rangle \;-\; 1]^2 \;-\; [2\langle c_0^\dagger c_m \rangle]^2 \quad . \end{aligned} \tag{3.3}$$

A non-interacting quantum system has a Hamiltonian of the form

$$\mathcal{H} \;=\; \sum_{\mathbf{k}} \epsilon_{\mathbf{k}}\; c_{\mathbf{k}}^\dagger c_{\mathbf{k}} \quad , \tag{3.4}$$

where the band energy $\epsilon_{\mathbf{k}}$ is given by the following tight-binding expression

$$\epsilon_{\mathbf{k}} \;=\; \frac{1}{N} \sum_{i,j}\; e^{-i\mathbf{k}\mathbf{R}_{i,j}} \quad . \tag{3.5}$$

In one dimension this reduces to

$$\epsilon_k = -2\cos k \quad . \tag{3.6}$$

We first calculate the filling dependence of the Fermi energy ϵ_F. We introduce an additional parameter $0 \leq \delta \leq 1$, in such a way that $\epsilon_F = -2\delta$, that is, $\delta = 1$ for an empty band and $\delta = 0$ for a half-filled band. In the vertex model language this means no vertical arrows in a row ($n = N$), i.e. a ferroelectric state, and an antiferroelectric state, with $n = N/2$. The momentum distribution in the non-interacting system will become

$$\begin{aligned}\theta(\epsilon_F - \epsilon_k) &= \theta(-2\delta + 2\cos k) \\ &= \theta(-\delta + \cos k) \quad ,\end{aligned} \tag{3.7}$$

where $\theta(\xi)$ is the Heaviside step function. Thus, the density of the down arrows in a row n/N is the expectation value of the number operator

$$\begin{aligned}\frac{n}{N} &= \frac{1}{2\pi}\int_{-\pi}^{+\pi} dk\ \theta(\epsilon_F - \epsilon_k) \\ &= \frac{1}{2\pi}\int_{-\pi}^{+\pi} dk\ \theta(-\delta + \cos k) \\ &= \frac{1}{\pi}\arccos\delta \quad .\end{aligned} \tag{3.8}$$

The integral in Eq. (3.8) was taken in the first Brillouin zone. The matrix element of the one-particle density matrix $\langle c_0^\dagger c_m\rangle$ is

$$\begin{aligned}\langle c_0^\dagger c_m\rangle &= \frac{1}{2\pi}\int_{-\pi}^{+\pi} e^{ikm}\ \theta(\epsilon_F - \epsilon_k) \\ &= \frac{1}{\pi m}\sin(m\arccos\delta) \\ &= \frac{1}{\pi m}\sin(\pi m\frac{n}{N}) \\ &= \frac{1}{\pi m}\sin[\frac{\pi m}{2}(1-p_v)] \quad .\end{aligned} \tag{3.9}$$

The definition of the vertical polarization from Eq. (2.43) was used. Thus, the correlation function $G(m)$ from Eq. (3.3) with Eqs. (2.43) and (3.9) becomes

$$G(m) \;=\; p_v^2 \;-\; \{\frac{2}{\pi m}\; \sin[\frac{\pi m}{2}(1-p_v)]\}^2 \quad . \tag{3.10}$$

Eq. (3.10), as seen from the derivation, is valid for both the six- and five-vertex models. The asymptotic behaviour of Eq. (3.10) is easily obtained for the disordered phase ($p_v = 0$), to be equal to the arithmetic average between the odd and even m contributions

$$G(m) \;=\; -\frac{2}{\pi^2}\,\frac{1}{m^2} \quad . \tag{3.11}$$

In the case of an interacting system, as mentioned previously, the form of the Bethe Ansatz wave function does not allow a simple treatment of the correlation functions. However, the main task to determine the critical index of the correlation length, can be managed, due to the fact that only the asymptotic form of the correlations are needed. For its calculation we could use a decoupling scheme [46] (limit) applied to the entire band of complex next-largest eigenvalues of the Bethe Ansatz eigenfunction, as it was done by Johnson, Krinsky and McCoy [47]. However, since the work of Schultz, Mattis and Lieb [48], for the calculation of the asymptotics of the correlation functions, we can use the relationship between the two dimensional statistical models and the fermion gas in one dimension. Actually, by this we transform the original problem to a Luttinger model, as done by Luther and Peschel [49] or to a Tomonaga model, see Fogedby [50].

A major step towards the understanding of the integrable models and their behaviour, that is also of the correlation functions, was the quantum inverse scattering method [27,28], by whose results, two new ideas appeared to unify the theory of critical phenomena in two dimensions. By two dimensions here we mean two spatial or (1 + 1) quantum dimensions. These are the conformal invariance [51] and the notion that there exist general models to which specific models of physical interest can be related by an appropriate transformation [52]. Thus, the universality classes of two dimensional theories are constrained by conformal invariance [53]. We do not intend to enter into the details of this enormous field of conformal invariance, only to subtract the information which is needed to determine the asymptotic form of the spin-spin correlation function of interest.

The notions of central charge (c) and of dressed charge are introduced. The central charge represents the dimension of a *non-interactive* field [54] (this is the above mentioned general model) into which we can transform the two dimensional theory of interest at criticality (thus, $c \leq 1$). In the modern language of the conformal field theory, the central charge is equal with the conformal anomaly of the associated Virasoro algebra [51]. As an example, for the Ising model $c = 1/2$, for the three-state Potts model $c = 4/5$, for the eight-vertex, six-vertex, XXZ Heisenberg-Ising chain, XYZ Heisenberg chain, four-state Potts models $c = 1$.

The dressed charge [55] ($Z(p)$), which characterizes the energy of the elementary dressed excitations over the ground state, is directly linked to the critical exponent describing the power decrease of correlations at long distances. The zero value $Z(0)$, i.e. the "fractional charge" will be of interest for us. Let us denote, as usual this critical exponent by θ. The relation between $Z(0)$ and θ is formulated in the following way: for all integrable models (i.e. solvable with the Bethe Ansatz) the asymptotic behaviour of the $G(m) = \langle \sigma_0^z \sigma_m^z \rangle$ equal-time correlation function (of a row for the lattice systems), in any state with no antiferro long range order, is given by

$$G(m) = -\frac{K}{m^2} + (-1)^m K' \frac{\cos(\pi m p_v)}{m^\theta} , \qquad (3.12)$$

where

$$\theta = \begin{cases} 2\ Z(Q)^2\ , & v_c \geq v > 0\ ; \\ 2\ |Z(0)|\ , & v = 0\ . \end{cases} \tag{3.13}$$

and the dressed charge can be obtained from the solution of the equation

$$Z(p) - \frac{1}{2\pi} \int_{-Q}^{+Q} \frac{\partial\Theta(p,q)}{\partial p} Z(q)\ dq = 1\ . \tag{3.14}$$

The kernel $\Theta(p,q)$ is the one which defines the distribution function. Note that Eq. (3.14) is very similar to the integral equation for the distribution function. Actually, Eq. (3.14) is identical with Eq. (2.41) plus a numerical constant. This is a fortunate situation.

The K coefficient is also universally determined, $K = \pi^2\theta$. Using Eq. (3.13) it can be seen that it is given by $Z(Q)$ in the presence of an external field and by its zero value $Z(0)$, i.e. by the "fractional charge" [27,28], in zero field

$$K = \begin{cases} 2\ Z^2(Q)\ /\ \pi^2\ , & v_c \geq v > 0\ ; \\ 2\ |Z(0)|\ /\ \pi^2\ , & v = 0\ . \end{cases} \tag{3.15}$$

All the following results were demonstrated to exist by the quantum inverse scattering method [27,28], for details, see Ref. [56]. This universality property within the integrable models can be understood in the following way. In all the models which allow an exact solution with the Bethe Ansatz wave function the dependence on the distance, i.e. m only enters in the phase of the wave function. In the asymptotic behaviour, this eigenfunctions dependence on m will dominate independently of the algebraic form of the eigenvalues [27,28], for all values [56] of the external field $v_c \leq v < 0$.

We can give the following motivation for the form of Eq. (3.15): based on Ref. [56], we can see that the $v \to 0$ limit (where v is the vertical external field) for the $\langle \sigma_0^z \sigma_m^z \rangle$ correlation function is singular, in the sense that K depends weakly on the distance. Using the notation $\eta = \pi / \arccos \Delta_6$, two analytic domains can be distinguished

$$\begin{aligned} \eta v^{2(1-1/\eta)} \ll m v^{2(1-1/\eta)} &\ll \Delta_6^2 \ ; \\ m v^{2(1-1/\eta)} &\gg \Delta_6^2 \quad , \end{aligned} \tag{3.16}$$

corresponding to near and far asymptotic. The two limits correspond to the second and first formulas of Eq. (3.15). For any m large but fixed and any small v, the first form from Eq. (3.16) should be taken [56], which implies the first form from Eq. (3.15). However, if $v = 0$ then the second form of Eq. (3.15) is obtained.

From the correlation function $G(m)$ given in Eq. (3.12) only the first term will be of importance in the following paragraphs, see § **3.2**. Thus, hereafter we will study the form of K given in Eq. (3.15) for the six-vertex and the five-vertex model.

The solution of Eq. (3.14) can be obtained in a similar way as for the distribution function [5] of the symmetric six-vertex model. We are in the disordered phase, thus $p_v = 0$ and $\Delta_6 = -\cos\mu$. We transform to $p = k(\alpha)$ and $q = k(\beta)$, where the rapidities α and β are defined by Eq. (B.17) from Appendix B. Eq. (3.14) is transformed to [5]

$$Z(\alpha) - \frac{1}{2\pi} \int_{-\infty}^{+\infty} \frac{\sin 2\mu}{\cosh(\alpha - \beta) - \cos 2\mu} Z(\beta)\, d\beta = 1 \quad . \tag{3.17}$$

Define the Fourier transform

$$\tilde{Z}(\xi) = \frac{1}{2\pi} \int_{-\infty}^{+\infty} Z(\alpha)\, e^{(i\xi\alpha)}\, d\alpha \quad .$$

Multiplying both sides of Eq. (3.17) by $\exp(i\xi\alpha)$ and integrating over α, we obtain

$$\tilde{Z}(\xi) - \frac{\sinh(\pi - 2\mu)\xi}{\sinh \pi\xi} \tilde{Z}(\xi) = 2\pi\, \delta(\xi) \quad , \tag{3.18}$$

where $\delta(\xi)$ is the Dirac delta function. It immediately follows that

$$\widetilde{Z}\,(\xi) \;=\; 2\pi\,\frac{\delta(\xi)}{1-(\sinh(\pi-2\mu)\xi)/(\sinh\pi\xi)} \quad . \tag{3.19}$$

Applying the inversion of the Fourier transformation to Eq. (3.19) we easily see that $Z(p)$ is constant ($p \neq 0$), thus

$$\begin{aligned} Z(Q) \;&=\; \frac{\pi}{2\mu}\;; \\ &=\; -\,\frac{\pi}{2\arccos\Delta_6} \quad , \end{aligned} \tag{3.20}$$

where Eq. (B.17) from Appendix B was used. From Eq. (3.15) it results

$$K \;=\; \begin{cases} 1\;/\;[2\;(\arccos\Delta_6)^2]\;, & v_c\;\geq\;v\;>\;0\;; \\ 1\;/\;[\pi\;\;\arccos\Delta_6]\;, & v\;=\;0\quad . \end{cases} \tag{3.21}$$

in agreement with Ref. [56]. The non-interacting limit from Eq. (3.11) is recovered for $\Delta_6 = 0$ from any of the two forms of Eq. (3.21).

Comment. As mentioned previously, if the external field is strictly zero, in other words if we are in the case of the symmetric six-vertex model, the second form of Eq. (3.21) is only obtained. If we put a small field, the first form of Eq. (3.21) is the one which is analytically valid. In the previous calculations [47–50], as no dependence on the external field was studied, the second form was obtained, barring some obvious misprints in the formula (21) and (24) of Luther and Peschel (1975) [49] and formula (7.21) of Fogedby [50]. This second form was used in Ref. [57] to determine the coarse-grained correlations of ferroelectrics. This is also in agreement with the renormalization group approach [58] of the two dimensional discrete Gaussian model. There is no renormalization group approach in the presence of an external field. The behaviour of the two dimensional XY model is also non-analytic in the zero external field limit [59].

The critical exponent describing the power decrease of the correlations at long distance in zero external field, using Eq. (3.13) becomes

$$\theta = \frac{\pi}{\arccos \Delta_6} \quad , \tag{3.22}$$

in agreement with Johnston, Krinsky and McCoy [47].

For the five-vertex model, the solution of Eq. (3.14), interestingly, is more involved than for the six-vertex one. From Eq. (2.31) we saw that

$$\frac{\partial \Theta(p,q)}{\partial p} = \frac{\Delta_5(\cos p - \Delta_5)}{1 - 2\Delta_5 \cos p + \Delta_5^2} \equiv \vartheta(p) \quad .$$

The notation $\vartheta(p)$ will be further used. Thus, Eq. (3.14) will become

$$1 = Z(p) - \frac{1}{2\pi} \vartheta(p) \int_{-Q}^{+Q} Z(q)\, dq \quad .$$

Assume that there exists a function such that $\partial W(\xi) \,/\, \partial \xi = Z(\xi)$, then

$$\begin{aligned} 1 &= \frac{\partial W(p)}{\partial p} - \frac{1}{2\pi} \vartheta(p) \int_{-Q}^{+Q} \frac{\partial W(q)}{\partial q}\, dq \; ; \\ &= \frac{\partial W(p)}{\partial p} - \frac{1}{2\pi} \vartheta(p) \left[W(Q) - W(-Q)\right] \quad . \end{aligned} \tag{3.23}$$

Integrating Eq. (3.23) between $-Q$ and $+Q$, and using Eqs. (2.39) and (2.44), we get

$$W(Q) - W(-Q) = \pi(1 - p_v) \quad . \tag{3.24}$$

Integrating for the second time Eq. (3.23), but between 0 and a variable ξ, and using Eq. (3.24) we obtain the function $W(\xi)$, from which $Z(p)$ becomes

$$Z(p) = 1 + \frac{1 - p_v}{2} \left[2\vartheta(p) - \vartheta(0)\right] \quad . \tag{3.25}$$

The coefficient K from Eq. (3.15) is equal to

$$K = \begin{cases} \frac{2}{\pi^2} \left[1 + \frac{1-p_v}{2} \left(2\vartheta(Q) - \vartheta(0)\right)\right]^2 , & v_c \ge v > 0 \; ; \\ \frac{2}{\pi^2} \left[1 + \frac{1-p_v}{2} \frac{\Delta_5}{1-\Delta_5}\right] , & v = 0 \quad . \end{cases} \tag{3.26}$$

The non-interacting limit of Eq. (3.11) is easily reobtained from Eq. (3.26). The critical exponent θ for the five-vertex case will become

$$\theta \;=\; 2\,[1 \;+\; \frac{1-p_v}{2}\,\frac{\Delta_5}{1-\Delta_5}] \quad , \tag{3.27}$$

which is equal to that of the six-vertex model, see Eq. (3.22), only in the non-interacting case. Note that the behaviour of θ from Eq. (3.27) is similar to that of the six-vertex case from Eq. (3.22), and in the ferroelectric phase $\theta = 2$, as it should be [47,49].

3.2 Height-Height Correlation and the Vertex-Models

The most frequently used model for a crystal-vapor interface is the Solid-on-Solid (SOS) model [60]. There it is assumed that the atoms are densely-packed in a lattice; at the interface atoms may sit on top of each other but overhangs and vacancies are excluded. Since neither the bulk of the so-defined crystal nor the vapor contribute any degrees of freedom to the system, the model merely describes the interface crystal-gas in a simplified form. Its static properties are defined by a Hamiltonian whose simplest variant (Absolute Solid-on-Solid, or ASOS) is

$$\mathcal{H} \;=\; \text{const.} \sum_{\langle i,j\rangle} |h_i \;-\; h_j\,| \quad , \tag{3.28}$$

where the sum runs over all pairs of nearest-neighbour sites in a two dimensional lattice and h_i may take an all integer values between $\pm\infty$. The first argument for the existence of a singularity in the free energy of this system was given in Ref. [60]. For the crystal this would mean [61] that above this singularity the surface is rough, i.e. the nucleation barrier for two dimensional nucleation vanishes.

Our purpose in not to analyze the SOS models, which can be found in Ref. [62], see also Ref. [58]. In Ref. [62] it is shown, that an alternative way appears to characterize this singularity, mainly by the introduction of the height-height correlation function of the interface $g_{ij} = \langle [h(r_{ij}) - h(r_{00})]^2 \rangle$, where $r \equiv |r_{ij} - r_{00}|$ and the ensemble average is taken for the SOS system. Hereafter, we are calculating the height-height correlation in a row exactly, i.e.

$$g_j = \langle [h(r_{0j}) - h(r_{00})]^2 \rangle \quad , \tag{3.29}$$

in those cases in which the interface can be mapped to an exactly solvable vertex model.

3.2.1 Six-Vertex Case

The Body Centered Solid-on-Solid model (BCSOS) which was proposed by van Beijeren[63], is isomorphic to the six-vertex model. The model is suitable for the (001) facet of an bcc crystal. Extensions of this model exists for the (001), (011) [64] and (110) [65] facets of an fcc crystal. In order to calculate g_j from Eq. (3.29) we follow the method of Levi[66]. The height difference in BCSOS models being restricted, we can consider $h_{j+1} - h_j = \sigma_j$. With this, it easily can be shown easily that

$$g_{j+1} + g_{j-1} - 2g_j = 2 \langle \sigma_0 \sigma_j \rangle \quad . \tag{3.30}$$

The above equation is verified, quite generally, if we take

$$g_j = -j + 2 \sum_{j'=0}^{j-1} (j - j') \langle \sigma_0 \sigma_{j'} \rangle \quad . \tag{3.31}$$

Thus, g_j becomes

$$g_j = -j + 2j \sum_{j'=0}^{j-1} \langle \sigma_0 \sigma_{j'} \rangle - 2 \sum_{j'=0}^{j-1} j' \langle \sigma_0 \sigma_{j'} \rangle \quad . \tag{3.32}$$

The first two terms of Eq. (3.32) vanishes in the asymptotic $j \to \infty$ limit, since

$$\sum_{j'=0}^{\infty} \langle \sigma_0 \sigma_{j'} \rangle = \frac{1}{2} \quad .$$

Proof: $\sum_{j=-\infty}^{+\infty} \sigma_j = S$ is the total spin of a row. This is uncorrelated with any individual spin σ_0, otherwise the system would be ferroelectric. Thus,

$$\begin{aligned}
0 &= \langle \sigma_0 S \rangle ; \\
&= \langle \sigma_0 \sum_{j=-\infty}^{+\infty} \sigma_j \rangle ; \\
&= \sum_{j=-\infty}^{+\infty} \langle \sigma_0 \sigma_j \rangle ; \\
&= \sum_{j=-\infty}^{-1} \langle \sigma_0 \sigma_j \rangle + \langle \sigma_0^2 \rangle + \sum_{j=1}^{+\infty} \langle \sigma_0 \sigma_j \rangle ; \\
&= \langle \sigma_0^2 \rangle + 2 \sum_{j=1}^{+\infty} \langle \sigma_0 \sigma_j \rangle ; \\
&= 1 + 2 \sum_{j=1}^{+\infty} \langle \sigma_0 \sigma_j \rangle \quad .
\end{aligned}$$

From the above equation results

$$\sum_{j=1}^{+\infty} \langle \sigma_o \sigma_j \rangle = -\frac{1}{2} \ , \text{ and } \sum_{j=0}^{+\infty} \langle \sigma_0 \sigma_j \rangle = +\frac{1}{2} \quad .$$

The asymptotic form of g_j, using Eq. (3.12) with $p_v = 0$, will become

$$g_j = 2K \int_1^j \frac{1}{j'} \, dj' - 2K' \int_1^j \frac{\cos \pi j'}{j'^{\theta-1}} \, dj' \quad . \tag{3.33}$$

The second integral from Eq. (3.33) for $j \to \infty$ is a constant number [33] depending on θ, while the first one being divergent is the dominant one. Thus the asymptotic form of the height-height correlation in a row has the well-known form

$$g_j = 2 \, K \, \ln j \quad . \tag{3.34}$$

At the transition, as seen from Eq. (3.21), $K = 2/\pi$, again the well-known value[58,62]. The roughness constant $K(T)$ can be expressed from Eq. (3.21). In the symmetric six-vertex case, a Taylor expansions yields

$$K(T) = \frac{1}{\pi^2} + C_6 \sqrt{T - T_R} \quad , \tag{3.35}$$

where T_R is defined as the roughening temperature, i.e. $\Delta_6(T = T_R) = -1$ and C_6 is a constant value

$$C_6 = \frac{1}{\pi^3 T_R \sqrt{2k_B T_R}} \left[2\varepsilon_5 - \varepsilon_1 - \varepsilon_3 + e^{(\varepsilon_3-\varepsilon_1)/k_B T_R} + e^{(\varepsilon_1-\varepsilon_3)/k_B T_R}\right]^{1/2} \quad .$$

We have used the second form of Eq. (3.21), as in the presence of an external field there is no roughening transition in the six-vertex model.

3.2.2 Five-Vertex Case

The mapping procedure in this case was first described by Garrod, Levi and Touzani[4] (GLT). Since this is a rather new method, we briefly present it. This mapping procedure is suitable for surfaces of simple cubic crystals. Following closely Ref. [4], let us consider a rectangular $N_0 \times M_0$ table, see Fig 3.1. Let be L_0 steps, and let L be the total level difference between the upper and lower ends of the right side of the table. Thus, if s labels the steps and if the s-th step corresponds to a jump of Δm_s units $L = \sum_s \Delta m_s$. On the average the y coordinate of each step climbs by S from the left to the right end of the table. Then the Miller indices (hkl) of the vicinal surface $(h < 0; k, l > 0)$ obey the relation $|h|/k = S/N_0$ and $k/l = L/M_0$. The multiple steps can be reduced to single steps by sliding the crystal layers, see Fig. 3.2. The number of steps L_0, becomes L.

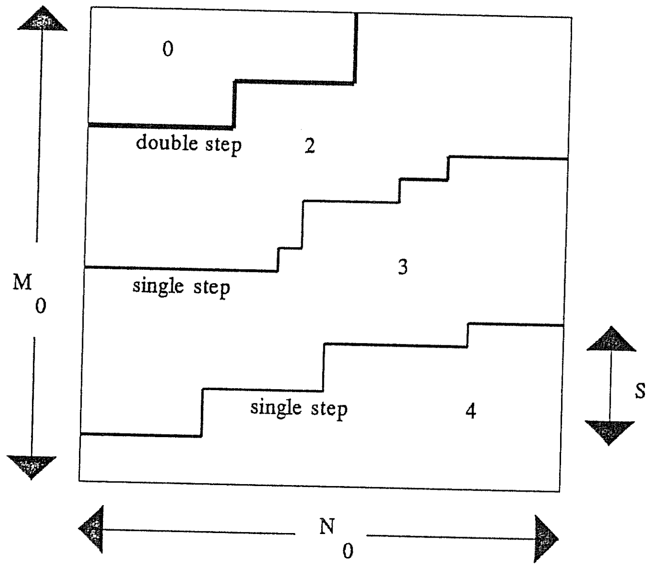

Fig. 3.1: A geometrical arrangement of steps. The terrace levels are indicated by continuous curves.

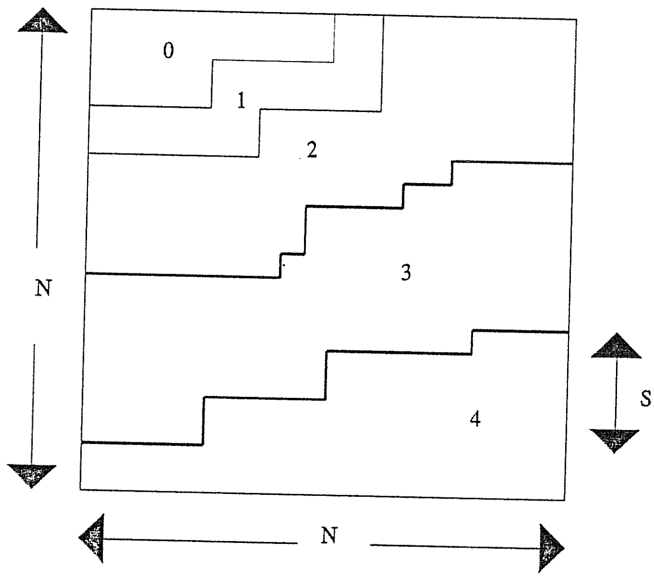

Fig. 3.2: Same as Fig. 3.1, after applying the sliding procedure described in the text to eliminate multiple steps. This example corresponds to $N_0 = 63$, $M_0 = 60$, $K_0 = 4$, $S = 16$, $N = 64$, $Q = 1$. $A = 256$, $B = 64$ and $(h,k,l) = (\bar{1}, 4, 60)$.

Assuming that the resulting table is a square of side N, we have $M_0 = N - L$, $N_0 = N - Q$, where $Q = LS/N$. Thus, the Miller indices are given by $h = -Q/u$, $k = L/u$ and $l = (N - L)/u$, where u is the largest common factor of Q, L and $N - L$. The steps as formed can now be identified with the lines of the line representation of the six-vertex model[5]. However, after the sliding procedure described above, no touching of lines will occur. Thus, vertex two is actually absent and we are left with a five-vertex model.

In the BCSOS mapping, the slope of the surface is equal to the vertical and horizontal polarizations of the vertex model defined in Eq. (2.43) and (2.56). In the GLT mapping scheme this is not the case. The inclination of the corresponding surface is actually equal to $P_v = (n_3 + n_5)/N$ and $P_h = (n_4 + n_5)/N$. Using the definition of p_v and p_h, from Eqs. (2.43) and (2.56) the results

$$P_v = \frac{1 - p_v}{2} , \quad P_h = \frac{1 - p_h}{2} , \tag{3.36}$$

are immediately obtained. Thus, the height difference which gives an inclination equal to P_v is

$$h_j - h_0 = \sum_{j'}^{j} \frac{1 - \sigma_{j'}}{2} . \tag{3.37}$$

The height-height correlation in a row defined in Eq. (3.28), for e.g. up arrows and after some algebra, becomes

$$\begin{aligned} g_j &= \frac{1}{4} \langle \sum_{j',j''=1}^{j} (1 - \sigma_{j'})(1 - \sigma_{j''}) \rangle ; \\ &= \frac{1}{4} \sum_{j'=1}^{j} \sum_{l=1-j'}^{j-j'} \langle \sigma_0 \sigma_l \rangle ; \\ &= \frac{1}{4} j + \frac{1}{2} \sum_{l=1}^{j-1} (j - l) \langle \sigma_0 \sigma_l \rangle . \end{aligned} \tag{3.38}$$

The first summation from Eq. (3.38), as in the six-vertex case, in the asymptotic regime will give $j/2 \sum_{l=1}^{\infty} \langle \sigma_0 \sigma_l \rangle = -j/4$, which cancels the first term of Eq. (3.38). The asymptotic form of the remaining last term from Eq. (3.38) using Eq. (3.12) is

$$g_j \;=\; \frac{1}{2}\, K \int_1^j \frac{1}{l}\, dl \;-\; \frac{1}{2}\, K' \int_1^j \frac{\cos(\pi l)\cos(\pi l p_v)}{l^{\theta-1}}\, dl \quad . \tag{3.39}$$

In this case also, the second integral from Eq. (3.39) gives [33] in the $j \to \infty$ limit a non-divergent function of θ. The first integral will dominate, yielding

$$g_j \;=\; \frac{1}{2}\, K\, \ln j \quad . \tag{3.40}$$

Obviously, the K roughness constant, for this case is given by Eq. (3.26), the analysis of which will be given in the next paragraph. If we are close to the ferroelectric phase, i.e. $p_v = 1$, then $\theta = 2$ and $K = -K'$ [55,56]. Thus both terms of Eq. (3.39) will contribute giving

$$g_j \;=\; K\, \ln j \quad . \tag{3.41}$$

3.3 The Roughening Transition

The roughening transition of a crystal surface is characterized macroscopically by the disappearance of a facet of a given orientation from the equilibrium crystal shape [62]. This corresponds to the disappearance of a cusp in the Wulff plot. If we consider the GLT model, from Eq. (3.36) it is clear that we can interpret the polarizations P_v and P_h of the five-vertex model as the height differences per unit length, or the slope of the surface. Thus, as in the case of the BCSOS model [62], we can directly translate the calculated quantities of the five-vertex model into the corresponding quantities of the GLT model. The only difference between the correspondences of models: six-vertex with BCSOS and five-vertex with GLT is that for the later p_v and p_h must be changed with P_v and P_h.

Microscopically the roughening transition will be characterized by the emergence of strong height fluctuations on the facets, however, we will also show in § **3.4** that this implies that the free energy of a step on the facet is vanishing. We are mainly interested in the **FeI** and **FeII** phases of Fig. 2.3, as they are appropriate for the GLT model. However, as we will see later, the **c** transition curve behaves similarly to the **b** line.

3.3.1 The (100) surface

The **FeI** phase from Fig. 2.3 is a frozen-in ferroelectric phase, whose free energy is equal to ε_1. This phase via the GLT mapping corresponds to a *(100)* surface of a sc crystal, as $P_v = 0$ and $P_h = 0$. The transition temperature, as we have calculated in § **2.7** is given by $y = 1 + x$, i.e.

$$\exp(\frac{\varepsilon_5 - \varepsilon_4}{k_B T_c}) = 1 + \exp(\frac{\varepsilon_5 - \varepsilon_1}{k_B T_c}) \quad , \qquad (3.42)$$

where $\varepsilon_3 = \varepsilon_4$ and $\varepsilon_5 = \varepsilon_6$. For $T > T_c$ the inclination of the surface is changing because the polarizations p_v and p_h, that is P_v and P_h are continuously varying with x and y, see also Fig. 2.4. This property will be further used in § **3.4**. At the moment we are interested if the surface *(100)* exhibits a roughening transition or not. For this, we include the external field. If no external field is applied, as soon as the **b** transition line is reached, p_v, i.e. the orientation of the surface begins to vary with temperature, which is not physical. We impose V to be such that the inclination of the surface is constant. At the beginning let us consider the non-interacting, $y = 1$ case. Using Eq. (2.114) the values of V for which p_v and

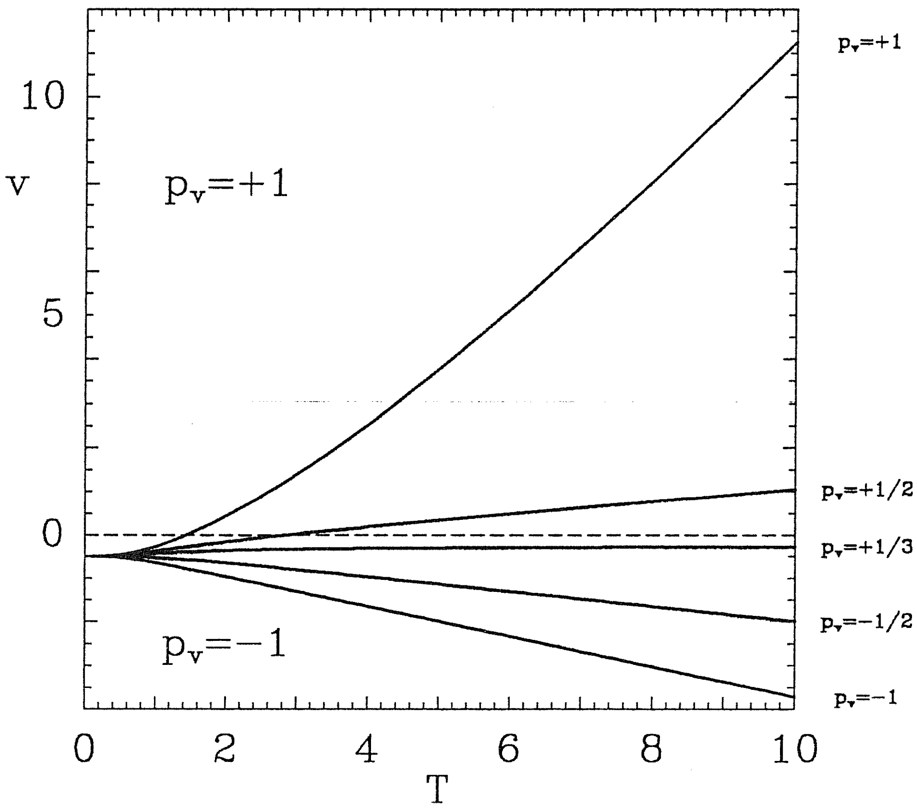

Fig. 3.3: The phase diagram of the modified KDP model in external field. The continuous curves corresponds to constant values of the vertical polarization. The dashed line is guide for the eye.

p_h are constants are easily obtained. The phase diagram versus the temperature is given in Fig. 3.3. Note, the $p_v = 0$ phase, existing in the case of the six-vertex model, shrinks to a point. As it can be seen from Eq. (2.114), fixing the polarizations at a constant value, we must fix also the value of Q_0. The transition given by the $Q_0 = 0$ condition, i.e. curve **b** of Fig. 2.3 or 2.13 will not appear. Thus, for $V = x - 1$, that is $p_v = 1$ the system is built up by only vertices one.

This means that the (*100*) surface is smooth, see Eq. (3.10) from $T = 0$ up to the infinite temperature point. For any value of V for which $p_v < 1$, but constant, the corresponding surface is rough from $T = 0$ up to the infinite temperature point. Interestingly, the roughness constant, K will not vary with the temperature, being $K = 2/\pi^2$ for the whole temperature range.

If we leave behind the non-interacting case, the situation will not change. The transition temperature, Eq. (3.42) is given by the $Q_L = 0$ condition. An external field which varies like

$$V \;=\; \frac{x\,(x-y)}{\sqrt{(y^2-1)\,(y^2-2xy-1)\;+\;x^2y^2}} \quad , \tag{3.43}$$

causes Q_L to vanish and fixes the polarizations to the $p_v = 1$ and $p_h = 1$ values. Thus, the free energy will be $f_L = \varepsilon_1 - v$ and the system will exhibit a frozen-in ferroelectric phase. Being so, the corresponding (*100*) surface will be smooth at any temperature. Fixing the polarizations at any other constant value $p_v \neq 1$, the corresponding surface will be rough at any temperature, with the roughness constant K given in the first equation from Eq. (3.26).

As an example, let us consider the $p_v = 0$ case, which has implications also for the **c** transition curve. For this case $Q_L = \pi$ and the external field which ensures this value for the polarization is

$$V \;=\; \frac{x\,(x+y)}{\sqrt{(y^2-1)\,(y^2+2xy-1)\;+\;x^2y^2}} \quad . \tag{3.44}$$

For this specific value of the field the roughness constant from Eq. (3.26) becomes

$$K \;=\; \frac{2}{\pi^2}\,[1 \;\pm\; \frac{\Delta_5}{2}\,\frac{3\;-\;\Delta_5}{1\;-\;\Delta_5}]^2 \quad , \tag{3.45}$$

where the $+,-$ sign refers to $y > 1$ and $y < 1$, respectively. It can be seen from Eq. (3.45) that $K = 2/\pi^2$ at $T = 0$ and increases as T is increased. Thus, no roughening transition between the **FeI** and **FiI** phases of the phase diagram, Fig. 2.3 is present.

The **FiII** phase is not suitable for a GLT mapping scheme, however, from the previous example we can see that in this case also, any external field which fixes the polarization, fixes in the same manner the value of Q_L, and by this the transition is lost.

3.3.2 The (110) surface

The second frozen-in ferroelectric phase present in the phase diagram from Fig. 2.3 is the **FeII** phase. The **FeII** phase is built up with vertices four (or three, being symmetry breaking, however, as the two cases are similar we will deal with only one). This phase via the GLT mapping corresponds to a *(110)* surface of a sc crystal, as $P_v = 0$ and $P_h = 1$. The case of vertex three would correspond to a $(\bar{1}01)$ surface, with $P_v = 1$ and $P_h = 0$. The transition temperature, as we have calculated in § **2.7** is given by $x = y - 1/y$, i.e.

$$\exp(\frac{\varepsilon_5 - \varepsilon_1}{k_B T_c}) = \exp(\frac{\varepsilon_5 - \varepsilon_4}{k_B T_c}) - \exp(\frac{\varepsilon_4 - \varepsilon_5}{k_B T_c}) \quad , \qquad (3.46)$$

where $\varepsilon_3 = \varepsilon_4$ and $\varepsilon_5 = \varepsilon_6$.

The *(110)* surface corresponding to the **FeII** phase is a perfectly smooth surface. Past a first order phase transition at T_c given in Eq. (3.46) the free energy is given by Eq. (2.76). The variation of the vertical polarization is given in Fig. 2.4. As in the previous paragraph, we want the surface inclination to be the same after the transition. Thus, we apply an external field in order to make $p_v \to 1$ in the **FiI** phase close to the **a** transition line. The difference from the case of the previous paragraph is that in the present case case Q_L is not vanishing.

Thus, from Eq. (2.118) we obtain for Q_L the equation

$$2Q_L(V) \; + \; \frac{\partial Q_L(V)}{\partial V} \; lnV \; = \; 0 \quad , \tag{3.47}$$

whose general solution reads as

$$Q_L(V) \; = \; Q_L(V=0) \; \exp[-2\mathrm{Ei}(lnV)] \quad , \tag{3.48}$$

where Ei is the exponential-integral function [33]. To obtain an analytic result from Eq. (3.48) we move close to the $x = y - 1/y$ line where $v \gg 1$. For this case, using the expression of Q_L given in Eq. (2.117) in leading order we find from Eq. (3.48)

$$V \cong \frac{x}{\sqrt{y^2 \; - \; 1}} \quad . \tag{3.49}$$

Thus, with such an external field we ensured that $p_v = 1$ close to the **a** transition curve. The free energy of the system above T_c is given by

$$\begin{aligned} f_L \; &= \; \varepsilon_1 \; - \; v \; - \; k_B T \frac{Q_L}{\pi} lnV \\ &- \; \frac{k_B T}{2\pi} \int_0^{Q_L} \rho(k) \; \ln[\frac{1}{x^2}(y^2 + \frac{1 - 2y^2 + 2xy\cos k}{x^2 + y^2 - 2xy\cos k}) \; dk \quad , \end{aligned} \tag{3.50}$$

where on the $x = y - 1/y$ curve

$$Q_L \; = \; \cos^{-1}(1 \; - \; \frac{1}{2y^2}) \; , \quad \rho(k) \; = \; \frac{1}{2} \, \frac{1}{\pi \; + \; Q_L} \quad , \tag{3.51}$$

and V from Eq. (3.49) is

$$V \; = \; \sqrt{1 \; - \; \frac{1}{y^2}} \quad . \tag{3.52}$$

According to Eq. (3.41) the corresponding surface is rough. We recall that within the **FiI** phase we must make the $p_v \to 1$ limit, which for the roughness constant, from Eq. (3.26) gives a constant value of $K \; = \; 2/\pi^2$ as for the non-interacting system. Thus, the *(110)* surface, indeed exhibits a roughening transition which, interestingly, turns out to be of the first order type.

In the case, when the **FeII** phase is built up with vertices three, the $p_v \to -1$ limit should be performed, which also gives a rough surface according to Eq. (3.41) with the roughness constant having the same $K = 2/\pi^2$ value.

In the **FiI** phase any inclination of the surface can be achieved by an external field. The trivial case is when $p_v = 0$ is enforced with a field given in Eq. (3.44). However, in this case, crossing the **a** transition curve not only the surface becomes rough, but also its inclination changes (unless the field changes).

Closing this paragraph, we mention that this behaviour is not specific to the f_L term studied in § **2.7**. The second free energy term $f_{M'}$ analyzed in § **2.8** also gives such a roughening transition. In the case of the $f_{M'}$ term and without external field the **a** transition curve turns out to be of the second order type. However, in the presence of an external field, as the transition curve **a** will be still given by the $\Delta_5 = 1$ condition, it changes to a first order transition.

3.4 Vicinal Areas

Facets and curved regions when they meet at edges can exhibit two types of behaviour: sharp edges with slope discontinuity, or (rounded) smooth edges with no slope discontinuity. Sharp edges correspond to first order transitions and smooth edges to second order phase transitions[62,64] or see Ref. [67].

Both behaviours can be found in the phase diagram from Fig. 2.3. Transition curve **a** corresponds to sharp edges, as the value of the polarizations has a jump at the transition and indeed represents a first order transition. The schematic plot of such a situation is presented in Fig. 3.4. The concrete $\tan\alpha$ values for the

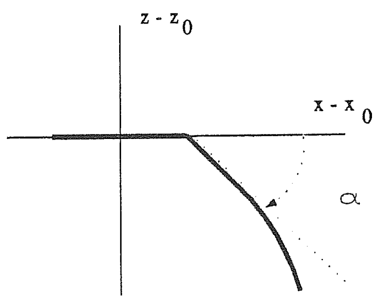

Fig. 3.4: Schematic plot of sharp edges.

$x = y - 1/y$, i.e. a transition curve are given in Fig. 3.5. Curve b of Fig. 2.3,

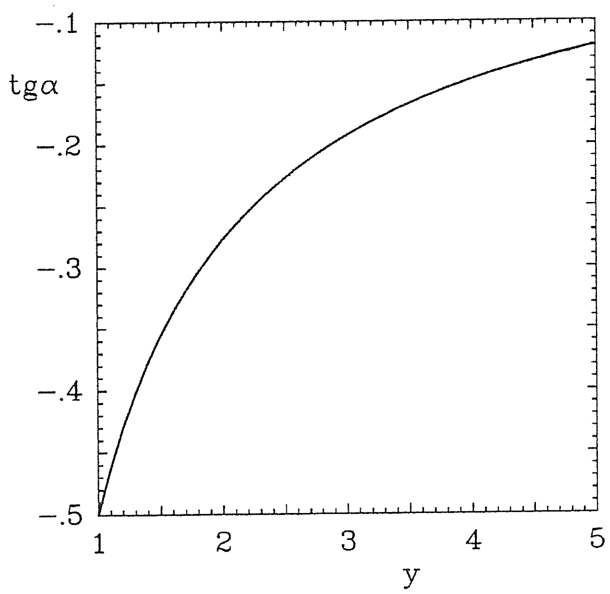

Fig. 3.5: The value of tgα corresponding to sharp edges (see Fig. 3.4) as a function of y for the *a* first order transition curve of Fig. 2.3.

where a smooth change of slope exists, i.e. a smooth variation of the inclination of the corresponding facet, represents a second order transition.

The behaviour, near smooth edges, of the shape of the curved interface must be critical. Thus, it can be given in the form

$$z - z_0 \;=\; A\,(x - x_0)^\alpha \quad , \tag{3.53}$$

where α is a critical exponent. In order to calculate α we are looking for an expansion of the free energy of the form

$$f_L \;=\; f_L(P_v = 0) \;+\; P_v\, f_L^{[s]} \;+\; P_v^2\, f_L^{[2]} \;+\; P_v^3\, f_L^{[3]} \;+\; \ldots \quad . \tag{3.54}$$

We place ourselves near the **b** transition line. Being so, such an expansion can be made from two directions. One is the $T > T_c$ limit. We approach the transition from a rough surface, thus we obtain

$$f_L \;=\; f_L(P_v = 0) \;+\; k_B T\,(\frac{\pi}{2})^2\, f_L(x, y, V)\, P_v^2 \;+\; \ldots \quad , \tag{3.55}$$

where $f_L(x, y, V)$ represents a rather complicated function of the variables x, y and V. Compared with Eq. (3.54) it can be seen that the linear term $f_L^{[s]}$ is missing in Eq. (3.55), thus the step free energy is zero, which is natural for a rough surface. The $f_L(x, y, V)$ function simplifies considerably for $V = 1$, $f_L(x, y, V = 1) = y$, which equals unity in the non-interacting limit.

In order to see the critical behaviour at the smooth edges the expansion from Eq. (3.54) must be done from the side of the smooth surface. In our case this means from the **FeI** phase. This amounts to perturb the smooth, frozen-in surface by introducing a small step density (given by a small P_v) and computing the effect on the free energy. The term linear in P_v gives the step energy, the quadratic and higher-order terms give the step interaction. As the calculation is rather involved, we restrict ourselves to the non-interacting case, i.e. modified KDP model, whose free energy is given in Eq. (2.70). Being at $T < T_c$, or $x > 2$ we take $Q_0 = \pi P_v \ll 1$. Using the expansion [33] of Clausen's integrals for small arguments, $Cl_2(x) \sim x$, the free energy becomes

$$f_L = \varepsilon_1 + \frac{k_B T \ ln x}{\pi} \arctan \frac{\sin \pi P_v}{\cos \pi P_v - 1/x} . \tag{3.56}$$

Expanding Eq. (3.56) we obtain

$$f_L = \varepsilon_1 + 2ln2 \ k_B T_c \ P_v - \frac{3ln2}{\pi^2} k_B T_c \ P_v^3 + \dots . \tag{3.57}$$

The last term can be interpreted as an effective entropic intercation between steps. Note that, the same form of the surface energy is obtained considering elastic interaction between steps [68]. Using the expression of the crystal shape in the (X, Y, Z) plane from the Wulff construction [62] with the obvious change $p_v \leftrightarrow P_v$ we obtain from Eq. (3.57)

$$\begin{aligned} Z &= Z_0 + \frac{6ln2}{\pi^2} k_B T_c \ P_v^3 \ ; \\ X &= X_0 + \frac{9ln2}{\pi^2} k_B T_c \ P_v^2 \ . \end{aligned} \tag{3.58}$$

Eqs. (3.58) can be reduced to a form of Eq. (3.53)

$$Z - Z_0 = \frac{2 \ \pi}{9\sqrt{\varepsilon_5 - \varepsilon_1}} (X - X_0)^{3/2} . \tag{3.59}$$

This is nothing else than the Pokrovsky-Talapov [69] or Gruber-Mullins [70] universality class.

Conclusions

The present thesis shows that the Bethe Ansatz provides an exact eigenfunction also for the five-vertex model. As the analysis of the eigenvalues and eigenfunction given, in Chap. **2**, demonstrates the model turns out to be easily integrable, due to the the presence of a degenerate kernel. The phase diagram obtained in the thermodynamic limit contains both first order transitions and continuous transitions of second order. Several aspects of the phase diagram are unusual and can be related to the symmetry-breaking property induced by the absence of vertex two. Even the second order phase transitions are of unusual type, because the order parameter is equal to unity on both sides of the transition, instead of vanishing as in the Curie point of a ferromagnet. However, further analysis is needed for a complete knowledge of the behaviour of the system. A simple type of correlations (along a row) has been evaluated, for all distances in the non-interacting case and asymptotically for the general case. Calculating more general correlations might be useful.

The model, exhibiting two frozen-in ferroelectric phases, is suitable for the Garrod, Levi and Touzani mapping procedure to describe perfectly smooth surfaces of a simple cubic crystal. Two possible surfaces can be obtained from the mapping. The (100) surface shows no roughening transition up to infinite temperatures. However, it has the property of exhibiting rounded edges for the vicinal areas. The step energy has been calculated and the result has the form known from the elastic interaction theories, showing also a behaviour belonging to the Pokrovsky-Talapov universality class.

The second surface obtained from the mapping is (110). Its behaviour is rather unusual: it undergoes a first order roughening transition. The vicinal areas exhibit sharp edges. Obviously, these interesting properties need further study, which will reveal the exact form of the step free energy and of the interaction between two steps.

Acknowledgements

I would like to express my cordial thanks to Professors Erio Tosatti and Andrea Levi for suggesting me this problem, for introducing me to this field of research, and mainly for the continuous encouragement and stimulating discussions throughout the course of this work, without which this work would have not been accomplished.

I am very grateful to Drs. Goranka Bilalbegović and Giancarlo Jug, who advised me and often responded to my elementary questions without reluctance. I have appreciated fruitful discussions at every stage of this work with Giorgio Mazzeo. I express my gratitude to Drs. M'hammed Touzani and Mirek Kotrla for the discussions and useful comments on this work.

I wish to express my thanks to Dr. Furio Ercolessi and Pasquale Pavone in sharing a small part of their knowledge in using computers. Although I do not write down their names, I express my gratitude to many researchers and colleagues who discussed with me and made useful comments on this work.

Bibliography

[1] E. H. Lieb, Phys. Rev. **162**, 162 (1967); Phys. Rev. Lett. **18**, 1046 (1967) and *ibid.* **19**, 108 (1967).

[2] C. P. Yang, Phys. Rev. Lett. **19**, 586 (1967) and B. Sutherland, C. N. Yang and C. P. Yang, *ibid.* **19**, 588 (1967).

[3] N. A. Gjostein, in *Surfaces and interfaces : chemical and physical characteristics*, edited by J. J. Burke, N. L. Reed, and V. Weiss, Syracuse University Press, 1967.

[4] C. Garrod, A. C. Levi and M. Touzani, Solid State Commun. **75**, 375 (1990) and C. Garrod, Phys. Rev. A**41**, 4195 (1990).

[5] R. J. Baxter, *Exactly Solved Models in Statistical Mechanics*, Academic Press, 1990 and in *Fundamental Problems in Statistical Mechanics*, vol. V, ed. E. G. D. Cohen, North-Holland, 1980.

[6] E. H. Lieb and F. Y. Wu, in *Phase Transition and Critical Phenomena*, vol. 1, eds. C. Domb and N. S. Green, Academic Press, 1972.

[7] F. Y. Wu, Phys. Rev. Lett. **18**, 605 (1967) and Phys. Rev. **168**, 539 (1967).

[8] P. W. Kasteleyn, Physica **21**, 1209 (1961) and J. Math. Phys. **4**, 287 (1963).

[9] M. E. Fisher, Phys. Rev. **124**, 1664 (1961).

[10] C. Garrod, J. Stat. Phys. **63**, 882 (1991).

[11] L. Onsager, Phys. Rev. **65**, 117 (1944) and in *Critical Phenomena in Alloys, Magnets and Superconductors*, ed. R. E. Mills, E. Ascher and R. I. Jaffe, McGraw-Hill Press, 1971.

[12] T. H. Berlin and M. Kac, Phys. Rev. **86**, 821 (1952).

[13] R. J. Baxter, Phys. Rev. Lett. **26**, 832 (1971); Ann. Phys. (N.Y.) **70**, 193, 229 (1972) and *ibid.* **76**, 1, 25, 48 (1973).

[14] R. J. Baxter and F. Y. Wu, Phys. Rev. Lett. **31**, 1294 (1973) and Aust. J. Phys. **27**, 357 (1974).

[15] R. J. Baxter, J. Phys. C**6**, L445 (1973); R. J. Baxter, S. B. Kellhand and Y. F. Wu, J. Phys. A**9**, 397 (1976) and R. J. Baxter, Proc. Roy. Soc. London A**383**, 43 (1982).

[16] R. J. Baxter, J. Phys. A**13**, L61 (1980); J. Stat. Phys. **26**, 427 (1981) and R. J. Baxter and P. A. Pearce, J. Phys. A**15**, 897 (1982).

[17] A. B. Zamolodchikov, Zh. Eksp. Teor. Fiz. **79**, 641 (1980) [J. E. T. P. **52**, 325 (1980)] and Commun. Math. Phys. **79**, 489 (1981).

[18] R. J. Baxter, Phys. Rev. Lett. **53**, 1795 (1984).

[19] R. J. Baxter and I. G. Enting, J. Phys. A**9**, L149 (1976).

[20] G. E. Andrews, R. J. Baxter and P. J. Forrester, J. Stat. Phys. **35**, 193 (1984).

[21] H. N. V. Temperley and E. H. Lieb, Proc. Roy. Soc. London A**322**, 251 (1971).

[22] C. Destri, H. J. van Vega and H. J. Giacomini, J. Stat. Phys. **56**, 291 (1989).

[23] M. Suzuki and M. E. Fisher, J. Math. Phys. **12**, 235 (1970).

[24] F. Y. Wu, Phys. Rev. Lett. **22**, 1174 (1969) and *ibid.* **24**, 1476 (1970).

[25] A. A. Litvin and V. B. Priezzhev, J. Stat. Phys. **60**, 307 (1990).

[26] M. Gaudin, *La fondation d'onde de Bethe*, Masson, 1983.

[27] L. D. Faddeev, in *Recent Advances in Field Theory and Statistical Mechanics*, eds. J. -B. Zuber and R. Stora, Elsevier Science Publishers, 1984 and in *Exactly Solvable Problems in Condensed Matter and Relativistic Field Theory*, eds. B. S. Shastry, S. S. Jha and V. Singh, Springer Verlag, 1985.

[28] L. A. Takhatajan, in *Exactly Solvable Problems in Condensed Matter and Relativistic Field Theory*, eds. B. S. Shastry, S. S. Jha and V. Singh, Springer Verlag, 1985 and *Integrable Models in Classical and Qunatum Field Theory*, Proceedings of the International Congress of Mathematicians, August 16-24, 1983, Warszawa, Sec. 13, p. 1331.

[29] C. N. Yang and C. P. Yang, Phys. Rev. **150**, 321, 327 (1966).

[30] B. Sutherland, in *Exactly Solvable Problems in Condensed Matter and Relativistic Field Theory*, eds. B. S. Shastry, S. S. Jha and V. Singh, Springer Verlag, 1985.

[31] B. McCoy and T. T. Wu, Il Nuovo Cimento B**LVI**, 311 (1968).

[32] B. Sutherland, J. Math. Phys. **11**, 3183 (1970).

[33] I. S. Gradshteyn and I. M. Ryzhik, *Table of Integrals, Series and Products*, Academic Press, 1980.

[34] L. A. Takhatajan and L. D. Faddeev, Russ. Math. Surv. **34**, 11 (1979).

[35] C. Destri, H. J. de Vega and H. J. Giacomini, J. Stat. Phys. **56**, 291 (1989).

[36] C. N. Yang, Phys. Rev. Lett. **19**, 1312 (1967).

[37] Yu. G. Stroganov, Phys. Lett. A**74**, 116 (1979) and R. Shanker, Phys. Rev. Lett. **47**, 1177 (1981).

[38] H. J. Hilhorst, M. Schick and J. M. J. van Leeuwen, Phys. Rev. B**19**, 2749 (1979) and M. T. Jaekel and J. M. Maillard, J. Phys. A**15**, 1309 (1982).

[39] R. J. Baxter and P. J. Forrester, J. Phys. A**18**, 1483 (1985).

[40] A. P. Prudnikov, Yu. A. Brychkov and O. I. Marichev, *Integrals and Series*, vol. 1, Gordon and Breach Publishers, 1986.

[41] C. Fan and F. Y. Wu, Phys. Rev. B**2**, 723 (1970).

[42] The norm of the Bethe Ansatz wave function is given, without any derivation in M. Gaudin, Ph.D. Thesis, Univ. de Paris, 1967, see Refs. [28,30]

[43] B. McCoy, T. T. Wu and M. Gaudin, Phys. Rev. D**23**, 417 (1980)

[44] V. E. Korepin, Commun. Math. Phys. **86**, 391 (1982).

[45] B. Sutherland, Phys. Lett. A**26**, 532 (1968).

[46] A. L. Fetter and J. D. Walecka, *Quantum Theory of Many-Particle Systems*, McGraw-Hill, Inc., 1971.

[47] J. D. Johnson, S. Krinsky and B. McCoy, Phys. Rev. A**8**, 2526 (1973).

[48] T. D. Schultz, D. C. Mattis and E. H. Lieb, Rev. Mod. Phys. **36**, 856 (1964).

[49] A. Luther and I. Peschel, Phys. Rev. B**9**, 2911 (1974) and *ibid.* B**12**, 3908 (1975).

[50] H. C. Fogedby, J. Phys. C**11**, 4767 (1978).

[51] For a review, see J. L. Cardy, in *Phase Transition and Critical Phenomena*, eds. C. Domb and J. L. Lebowitz, vol. 11, Academic Press, 1987; C. Itzykson, H. Saleur and J.-B. Zuber, *Conformal Invariance and Applications to Statistical Mechanics*, World Scientific, 1988 and C. Itzykson and J.-M. Drouffe, *Statistical Field Theory*, Cambridge University Press, 1989.

[52] L. P. Kadanoff and A. C. Brown, Ann. Phys. (N.Y.) **121**, 318 (1979); M. P. M. den Nijs, Phys. Rev. B**23**, 6111 (1981); B. Nienhuis, J. Stat. Phys. **34**, 731 (1984); F. C. Alcaraz, M. N. Barber and M. T. Batchelor, Phys. Rev. Lett. **58**, 771 (1987) and M. N. Barber and M. T. Batchelor, Int. J. Modern

Phys. B4, 253 (1990).

[53] J. L. Cardy, Nucl. Phys. B**270**, 186 (1986) and H. J. de Vega and M. Karowski, Nucl. Phys. B**285**, 619 (1987).

[54] A. A. Belavin, M. M. Polyakov and A. B. Zamolodchikov, J. Stat. Phys. **34**, 763 (1984) and Nucl. Phys. B**241**, 333 (1984).

[55] V. E. Korepin, Theor. Math. Phys. **41**, 953 (1979) [Teor. Mat. Fiz. **41**, 169 (1978)].

[56] A. G. Izergin and V. E. Korepin, Commun. Math. Phys. **94**, 67 (1984); V. E. Korepin, *ibid.* **94**, 93 (1984); A. G. Izergin and V. E. Korepin, *ibid.* **99**, 271 (1985) and N. M. Bogoliubov, A. G. Izergin and V. E. Korepin, Nucl. Phys. B**275**, 687 (1986).

[57] R. W. Youngblood, J. D. Axe and B. M. McCoy, Phys. Rev. B**21**, 5212 (1980) and R. W. Youngblood and J. D. Axe, *ibid.* B**23**, 232 (1981).

[58] S. T. Chui and J. D. Weeks, Phys. Rev. B**14**, 4978 (1976); T. Ohta and K. Kawasaki, Prog. Theor. Phys. **60**, 365 (1978) and J. D. Weeks, in *Ordering in Strongly Fluctuating Condensed Matter Systems*, ed. T. Riste, Plenum Pblishing, 1979.

[59] V. L. Berezinskii, Sov. Phys. JETP **32**, 493 (1971) [Zh. Eksp. Teor. Fiz. **59**, 907 (1970)].

[60] W. K. Burton and N. Cabrera, Disc. Fraday Soc **5**, 40 (1949) and W. K. Burton, N. Cabrerea and F. C. Frank, Phil. Trans. Roy. Soc. London A**243**, 299 (1951).

[61] E. H. Hauge and P. C. Hemmer, Physica Norvegica **5**, 209 (1974) and C. Deutsch and M. Lavaud, Phys. Rev. A**9**, 2598 (1974).

[62] D. B. Abraham, in *Phase Transition and Critical Phenomena*, eds. C. Domb

and J. L. Lebowitz, vol. 10, Academic Press, 1986; B. Nienhuis, in *ibid.*, vol. 11, Academic Press, 1987; H. van Beijeren and I. Nolden, in *Topics in Currect Physics*, eds. W. Schommers and P. von Blanckenhagen, vol. 43, Springer, 1987 and I. Nolden, Ph.D. Thesis, Univ. of Utrecht, 1990.

[63] H. van Beijeren, Phys. Rev. Lett. **38**, 993 (1977).

[64] C. Jayaprakash and W. F. Saam, Phys. Rev. B**30**, 3917 (1984).

[65] A. Trayanov, A. C. Levi and E. Tosatti, Surf. Sci. **233**, 184 (1990).

[66] A. C. Levi, Surf. Sci. **137**, 385 (1984).

[67] C. Jayaprakash, W. F. Saam and S. Teitel, Phys. Rev. Lett. **50**, 2017 (1983); C. Jayaprakash, C. Rottman and W. F. Saam, Phys. Rev. B**30**, 6549 (1984); H. J. Schulz, J. Phys. (Paris) **46**, 257 (1985); V. Elser, J. Phys. A**18**, 857 (1985) and J. J. Saenz and N. Garcia, Surf. Sci. **155**, 24 (1985).

[68] D. J. Srolovitz and J. P. Hirth, Surf. Sci. **255**, 111 (1991).

[69] V. L. Pokrovsky and A. L. Talapov, Phys. Rev. Lett. **42**, 65 (1979), and Zh. Eksp. Teor. Fiz. **78**, 269 (1980) [Sov. Phys. JETP **51**, 134 (1980)].

[70] E. E. Gruber and W. W. Mullins, J. Phys. Chem. Solids **28**, 875 (1967).

Appendix A

Eigenvalues of the General Six-Vertex Model

The maximum number of vertices which can be solved by the algebraic Bethe Ansatz is six. Combinations of higher numbers of vertices can be solved by the so-called generalized (or nested) algebraic Bethe Ansatz. As defined in Chapter 1, the lattice has M rows and N columns, and there are imposed cyclic (i.e. toroidal) boundary conditions. The eigenvalue equation which is to be solved is

$$\Lambda\ g(X) = \sum_{Y} V(X,Y)\ g(Y) \quad , \tag{A.1}$$

where $X = \{x_1, \ldots, x_n\}$, with $x_1, \ldots, x_n$ being the positions of the lines, ordered so that

$$1 \leq x_1 < x_2 < \ldots < x_{n-1} < x_n \leq N \quad , \tag{A.2}$$

and

$$V(X,Y) = \sum \omega_1^{m_1}\, \omega_2^{m_2}\, \omega_3^{m_3}\, \omega_4^{m_4}\, \omega_5^{m_5}\, \omega_6^{m_6} \quad , \tag{A.3}$$

is the $2^N \times 2^N$ transfer matrix, with $m_1, \ldots, m_6$ being the numbers of intervening vertices of types 1, ..., 6. We are using the line representation of the vertices shown in Fig. 1.1. However, the method can be directly applied to down (up) arrows, as it is done for the Heisenberg-Ising (XXZ) chain, giving exactly same result. The Hubbard chain solution is slightly different. We will use the same notations as Baxter [5] is using for the solution of the symmetric six-vertex model. The following discussion is basically identical to that given by Baxter [5], except that we keep all the ω's different.

The trivial case is when there is no vertical line (down arrows) between two successive rows. This means $n = 0$, thus the rows are built up by ω_1 and ω_4.

$$\Lambda \;=\; \omega_1^N \;+\; \omega_4^N \quad . \tag{A.4}$$

Let us consider one down arrow ($n = 1$), i.e. one overturned *spin*. The four possible cases are shown in Fig. A.1. The corresponding weights are

$$\begin{aligned}
&\text{case a)} \quad \omega_1^{N-1}\omega_3 \quad , \\
&\text{case b)} \quad \omega_2\omega_4^{N-1} \quad , \\
&\text{case c)} \quad \sum_{Y=X+1}^{N} \omega_1^{N+X-Y-1}\omega_4^{-X+Y-1}\omega_5\omega_6 \quad , \\
&\text{case d)} \quad \sum_{Y=1}^{X-1} \omega_1^{X-Y-1}\omega_4^{N-X+Y-1}\omega_5\omega_6 \quad .
\end{aligned} \tag{A.5}$$

For a solution of the

$$g(X) \;=\; z^X \tag{A.6}$$

form, with complex z, Eq. (A.1) becomes

$$\begin{aligned}
\Lambda\, z^X \;=&\; \omega_1^{N-1}\omega_3 z^X \;+\; \omega_2\omega_4^{N-1} z^X \\
&+ \sum_{Y=1}^{X-1} \omega_1^{X-Y-1}\omega_4^{N-X+Y-1}\omega_5\omega_6 z^Y \\
&+ \sum_{Y=X+1}^{N} \omega_1^{N+x-Y-1}\omega_4^{-X+Y-1}\omega_5\omega_6 z^Y \quad .
\end{aligned} \tag{A.7}$$

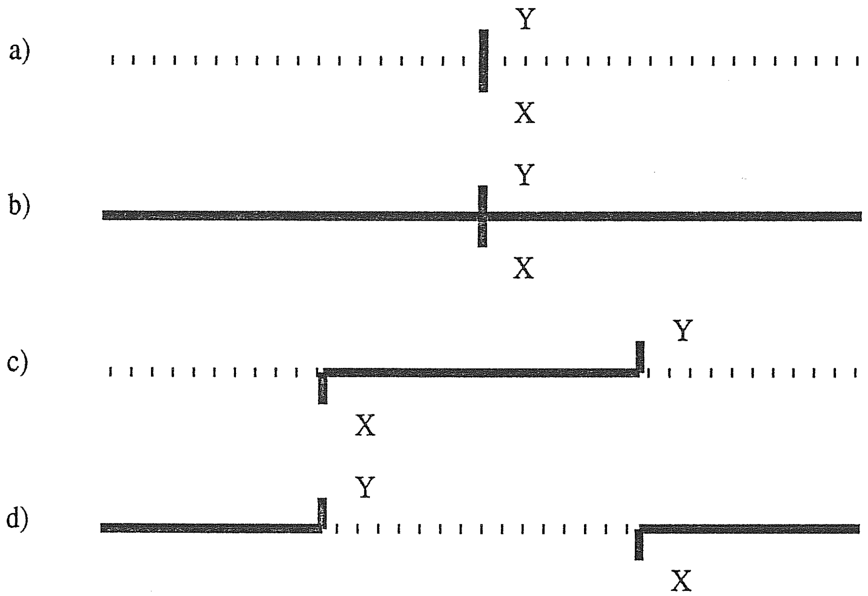

Fig. A.1: The four possible arrangements of lines in adjacent rows for $n = 1$

Summing up the geometric progression $[\sum_{i=1}^{I} x^i = (1 - x^{I+1}) \,/\, (1 - x)]$, Eq. (A.7) can be given in the form

$$\begin{aligned} \Lambda\, z^X &= \omega_1^N z^X L(Z) + \omega_4^N z^X M(z) \\ &+ \omega_1^{X-1} \omega_4^{N-X} \omega_5 \omega_6 [z - z^{N+1}] \frac{1}{\omega_1 - \omega_4 z} \quad . \end{aligned} \tag{A.8}$$

The following notation was used

$$L(z) = \frac{\omega_1\omega_3 + (\omega_5\omega_6 - \omega_3\omega_4)z}{\omega_1(\omega_1 - \omega_4 z)} \quad , \tag{A.9.1}$$

$$M(z) = \frac{\omega_1\omega_2 - \omega_5\omega_6 - \omega_2\omega_4 z}{\omega_4(\omega_1 - \omega_4 z)} \quad . \tag{A.9.2}$$

As it can be seen from Eq. (A.8), the eigenvalue turns out to be of the same form as in Eq. (A.4) if the third term vanishes. That is why this term is called *unwanted*

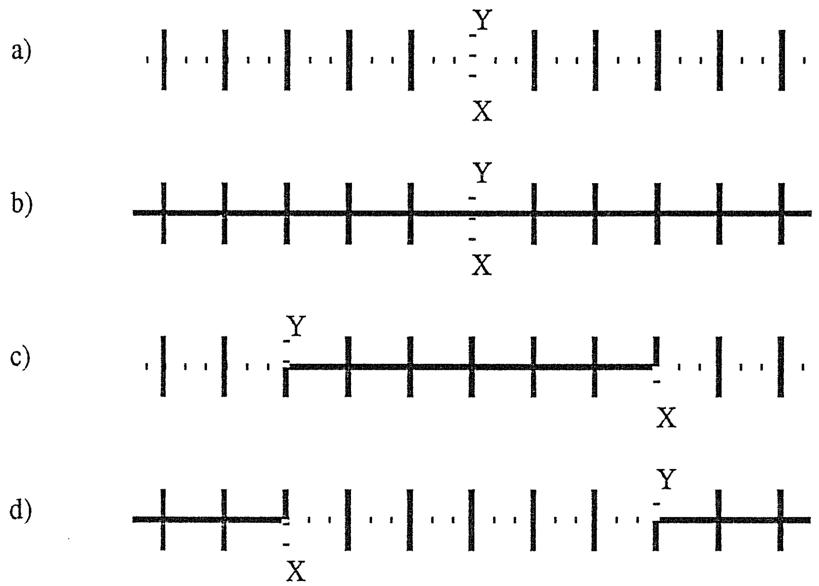

Fig. A.2: The four possible arrangements of lines in adjacent rows for one overturned arrow in a reference state built up by down pointing arrows.

term. It turns out, that if we impose the boundary condition, i.e. by choosing $z^N = 1$, this term is zero. Due to this it is called *boundary* term or *unwanted external* term. Thus for one overturned *spin*, the eigenvalue is given by

$$\Lambda \;=\; \omega_1^N \; L(z) \;+\; \omega_4^N \; M(z) \quad . \tag{A.10}$$

Before passing to the $n = 2$ case, we briefly present the situation where the reference state is taken to be the state with all spins down. The eigenvalue of the transfer matrix will be

$$\Lambda \;=\; \omega_2^N \;+\; \omega_3^N \quad . \tag{A.11}$$

For one overturned arrow, the four possible cases are presented in Fig. A.2. While the corresponding weights are

$$
\begin{aligned}
&\text{case a)} \quad \omega_1 \omega_3^{N-1} \quad , \\
&\text{case b)} \quad \omega_2^{N-1} \omega_4 \quad , \\
&\text{case c)} \quad \sum_{Y=1}^{X-1} \omega_2^{X-Y-1} \omega_3^{N-X+Y-1} \omega_5 \omega_6 \quad , \\
&\text{case d)} \quad \sum_{Y=X+1}^{N} \omega_2^{N+X-Y-1} \omega_3^{-X+Y-1} \omega_5 \omega_6 \quad .
\end{aligned}
\tag{A.12}
$$

Summing up the geometric progressions and imposing the boundary condition the eigenvalue becomes

$$
\Lambda = \omega_2^N L(z) + \omega_3^N M(z) \quad , \tag{A.13}
$$

where in this case

$$
L(z) = \frac{\omega_2 \omega_4 + (\omega_5 \omega_6 - \omega_3 \omega_4) z}{\omega_2 (\omega_2 - \omega_3 z)} \quad , \tag{A.14.1}
$$

$$
M(z) = \frac{\omega_1 \omega_2 - \omega_5 \omega_6 - \omega_1 \omega_3 z}{\omega_3 (\omega_2 - \omega_3 z)} \quad . \tag{A.14.2}
$$

We conclude, that the change in the reference state implies the changes $\omega_1 \leftrightarrow \omega_2$ and $\omega_3 \leftrightarrow \omega_4$ in the expression of the eigenvalue.

The $n = 2$ case contains two lines, i.e. down arrows, or overturned *spins*, at the locations X_1, X_2 in the lower row and Y_1, Y_2 in the upper row. The ice-rule ensures that Y_1 and Y_2 must satisfy

$$
X_1 \le Y_1 \le X_2 \le Y_2 \qquad \text{(Fig. A.3)} \quad , \tag{A.15}
$$

and

$$
Y_1 \le X_1 \le Y_2 \le X_2 \qquad \text{(Fig. A.4)} \quad , \tag{A.16}
$$

The different weights (without writing the summation over the positions of the vertical lines) corresponding to all the line configurations for Fig. A.3 are the following :

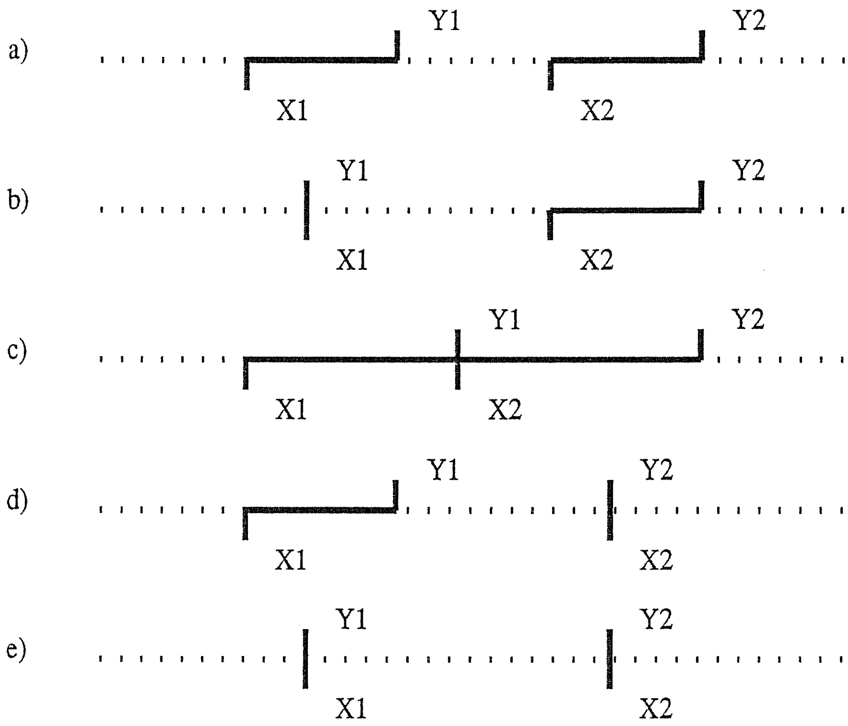

Fig. A.3: The five possible arrangements of lines in adjacent rows for $n = 2$ and $X_1 \le Y_1 \le X_2 \le Y_2$.

$$
\begin{aligned}
&\text{case a)} \quad \omega_1^{X_1-1}\omega_5\omega_4^{-X_1+Y_1-1}\omega_6\omega_1^{X_2-Y_1-1}\omega_5\omega_4^{-X_2+Y_2-1}\omega_6\omega_1^{N-Y_2} \quad ,\\
&\text{case b)} \quad \omega_1^{X_1-1}\omega_3\omega_1^{-X_1+X_2-1}\omega_5\omega_4^{-X_2+Y_2-1}\omega_6\omega_1^{N-Y_2} \quad ,\\
&\text{case c)} \quad \omega_1^{X_1-1}\omega_5\omega_4^{-X_1+Y_1-1}\omega_2\omega_4^{-X_2+Y_2-1}\omega_6\omega_1^{N-Y_2} \quad ,\\
&\text{case d)} \quad \omega_1^{X_1-1}\omega_5\omega_4^{-X_1+Y_1-1}\omega_6\omega_1^{X_2-Y_1-1}\omega_3\omega_1^{N-X_2} \quad ,\\
&\text{case e)} \quad \omega_1^{X_1-1}\omega_3\omega_1^{-X_1+X_2-1}\omega_3\omega_1^{N-X_2} \quad .
\end{aligned}
\tag{A.17}
$$

By symmetry, it can be seen that Fig. A.4 will have the same weights for the different line configurations with the obvious change $X_i \leftrightarrow Y_i$, $\omega_1 \leftrightarrow \omega_4$, $\omega_2 \leftrightarrow \omega_3$

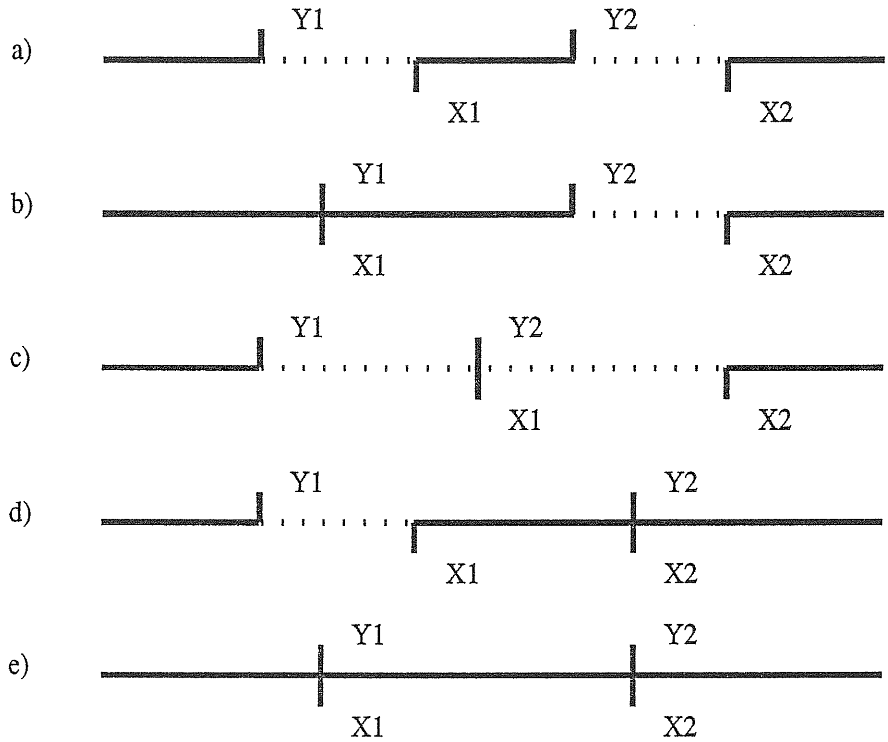

Fig. A.4: The five possible arrangements of lines in adjacent rows for $n = 2$ and $Y_1 \le X_1 \le Y_2 \le X_2$.

and $\omega_5 \leftrightarrow \omega_6$. By introducing the following notations

$$\begin{aligned} D(X,Y)\,[X=Y] &= \frac{\omega_2}{\omega_5} \quad , \\ D(X,Y)\,[X>Y] &= \omega_6\; \omega_1^{X-Y-1} \quad , \\ E(X,Y)\,[X=Y] &= \frac{\omega_3}{\omega_6} \quad , \\ E(X,Y)\,[X<Y] &= \omega_5\; \omega_4^{-X+Y-1} \quad , \end{aligned} \qquad (A.18)$$

and generalizing Eq. (A.6) to

$$g(X_1, X_2) = A_{12}\; z_1^{X_1}\; z_2^{X_2} \quad , \qquad (A.19)$$

the eigenvalue equation, Eq. (A.1) becomes

$$\begin{aligned} \Lambda\ A_{12}\ z_1^{X_1}\ z_2^{X_2} \ &= \ - \text{ Correction Terms} \\ &+ \ A_{12} \sum_{Y_1=X_1}^{X_2} \sum_{Y_2=X_2}^{N} \omega_1^{X_1-1} E(X_1,Y_1) D(Y_1,X_2) E(X_2,Y_2) \omega_6 \omega_1^{N-Y_2} z_1^{Y_1} z_2^{Y_2} \\ &+ \ A_{12} \sum_{Y_1=1}^{X_1} \sum_{Y_2=X_1}^{X_2} \omega_4^{Y_1-1} D(Y_1,X_1) E(X_1,Y_2) E(Y_2,X_2) \omega_5 \omega_4^{N-X_2} z_1^{Y_1} z_2^{Y_2} \quad . \end{aligned} \tag{A.20}$$

The Correction Terms are those which appear due to elimination of the non-allowed states, like $Y_1 = X_2 = Y_2$ and $Y_1 = X_1 = Y_2$. The correction terms corresponding to these are $A_{12}\omega_1^{N+X_1-X_2-1}\omega_2\omega_3\omega_4^{-X_1+X_2-1}(z_1 z_2)^{X_2}$ and $A_{12}\omega_1^{-X_1+X_2-1}\omega_2\omega_3\omega_4^{N+X_1-X_2-1}(z_1 z_2)^{X_1}$. The summation is a little more tedious than for Eq. (A.8) and it gives

$$\begin{aligned} \Lambda\ A_{12}\ z_1^{X_1}\ z_2^{X_2} \ &= \ A_{12}\ \omega_1^{X_1}\ [L(z_1)\omega_1^{-X_1+X_2} z_1^{X_1} \ + \ M(z_1)\omega_4^{-X_1+X_2} z_1^{X_2}] \\ &\times \ [L(z_2)\omega_1^{N-X_2} z_2^{X_2} \ - \ \rho(z_2)\omega_4^{N-X_2} z_2^{N}] \\ &+ \ A_{12}\ \omega_4^{N-X_2}\ [\rho(z_1)\omega_1^{X_1} \ + \ M(z_1)\omega_4^{X_1} z_1^{X_1}] \\ &\times \ [L(z_2)\omega_1^{-X_1+X_2} z_2^{X_1} \ + \ M(z_2)\omega_4^{-X_1+X_2} z_2^{X_2}] \\ &- \ A_{12}\omega_1^{N+X_1-X_2-1}\omega_2\omega_3\omega_4^{-X_1+X_2-1}(z_1 z_2)^{X_2} \\ &- \ A_{12}\omega_1^{-X_1+X_2-1}\omega_2\omega_3\omega_4^{N+X_1-X_2-1}(z_1 z_2)^{X_1} \quad . \end{aligned} \tag{A.21}$$

$L(z_i)$ and $M(z_i)$ are given in Eqs. (A.9), while $\rho(z_i)$ is defined as

$$\rho(z_i) \ = \ \frac{\omega_5 \omega_6 z_i}{\omega_1(\omega_1 - \omega_4 z_i)} \quad . \tag{A.22}$$

Obviously, the last two terms of Eq. (A.21) represent the Correction Terms. The following notation will be further introduced

$$R_i(X_1,X_2) \ = \ L(z_i)\omega_1^{X_2-X_1} z_i^{X_1} \ + \ M(z_i)\omega_4^{X_2-X_1} z_i^{X_2} \quad , \tag{A.23}$$

With this Eq. (A.22) becomes

$$\begin{aligned}\Lambda\ A_{12}\ z_1^{X_1}\ z_2^{X_2} \ &= \ A_{12}\ \omega_1^{X_1}\ R_1(X_1,X_2)\ [L(z_2)\omega_1^{N-X_2}z_2^{X_2} \ - \ \rho(z_2)\omega_4^{N-X_2}z_2^{N}] \\ &+ \ A_{12}\ \omega_4^{N-X_2}\ R_2(X_1,X_2)\ [\rho(z_1)\omega_1^{X_1} \ + \ M(z_1)\omega_4^{X_1}z_1^{X_1}] \\ &- \ A_{12}\omega_1^{N+X_1-X_2-1}\omega_2\omega_3\omega_4^{-X_1+X_2-1}(z_1z_2)^{X_2} \\ &- \ A_{12}\omega_1^{-X_1+X_2-1}\omega_2\omega_3\omega_4^{N+X_1-X_2-1}(z_1z_2)^{X_1} \quad . \end{aligned} \tag{A.24}$$

As it can be seen from Eqs. (A.21) and (A.24), the eigenvalue can be brought at the form of Eqs. (A.4) and (A.10), i.e.

$$\Lambda \ = \ \omega_1^N\ L(z_1)\ L(z_2) \ + \ \omega_4^N\ M(z_1)\ M(z_2) \quad , \tag{A.25}$$

if two terms will cancel. The first one, is the so-called *internal unwanted* term

$$\begin{aligned} &A_{12}\ [M(z_1)L(z_2) \ - \ \frac{\omega_2\omega_3}{\omega_1\omega_4}] \\ &\times\ [\omega_1^{N+X_1-X_2}\omega_4^{-X_1+X_2}(z_1z_2)^{X_2} \ + \ \omega_1^{-X_1+X_2}\omega_4^{N+X_1-X_2}(z_1z_2)^{X_1}] \quad , \end{aligned} \tag{A.26}$$

which arise due to the manipulation with the Correction Terms. While the second term which must vanish, the so-called *external unwanted*, i.e. *boundary* term, is equal to

$$A_{12}\ \omega_1^{X_1}\ \omega_4^{N-X_2}\ [\rho(z_1)R_2(X_1,X_2) \ - \ \rho(z_2)z_2^N R_1(X_1,X_2)] \quad . \tag{A.27}$$

In order to cancel the internal and external unwanted terms, it is necessary to introduce the algebraic Bethe Ansatz form for the wave vector $g(X_1,X_2)$

$$g(X_1,X_2) \ = \ A_{12}\ z_1^{X_1}\ z_2^{X_2} \ + \ A_{21}\ z_2^{X_1}\ z_1^{X_2} \quad . \tag{A.28}$$

It can be seen, that the second term of the algebraic Bethe Ansatz gives the same results as the first one, except that $z_1 \leftrightarrow z_2$ must be considered. Introducing the notation

$$s_{12} \ = \ M(z_1)L(z_2) \ - \ \frac{\omega_2\omega_3}{\omega_1\omega_4} \quad , \tag{A.29}$$

the internal unwanted terms will be become

$$\begin{aligned} & [s_{12}\ A_{12}\ +\ s_{21}\ A_{21}] \\ \times & [\omega_1^{N+X_1-X_2}\omega_4^{-X_1+X_2}(z_1 z_2)^{X_2}\ +\ \omega_1^{-X_1+X_2}\omega_4^{N+X_1-X_2}(z_1 z_2)^{X_1}] \quad , \end{aligned} \qquad (A.30)$$

while the boundary terms will reduce to

$$\omega_1^{X_1}\omega_4^{N-X_2}\ [\rho(z_2)R_1(X_1,X_2)(A_{21}-z_2^N A_{12})\ +\ \rho(z_1)R_2(X_1,X_2)(A_{12}-z_1^N A_{21})] \quad . \qquad (A.31)$$

Clearly these terms vanish if

$$s_{12}\ A_{12}\ +\ s_{21}\ A_{21}\ =\ 0 \quad , \qquad (A.32)$$

and

$$z_1^N\ =\ \frac{A_{12}}{A_{21}} \quad , \qquad z_2^N\ =\ \frac{A_{21}}{A_{12}} \quad . \qquad (A.33)$$

The two particle solution, Eqs. (A.32) and (A.33) contains already the main properties of the solutions for any n. It is instructive to analyze it more carefully. The maximum eigenvalue, due to the Perron-Frobenius theorem, is obtained for $z_1 z_2 = 1$. Expressing the value of s_{ij} from Eq. (A.29) we find

$$\begin{aligned} s_{ij}\ =\ -\ & \frac{\omega_5\omega_6}{\omega_1\omega_2(\omega_1-\omega_4 z_i)(\omega_1-\omega_4 z_j)} \\ & [\omega_1\omega_3\ +\ \omega_2\omega_4 z_i z_j\ -\ (\omega_1\omega_2\ +\ \omega_3\omega_4\ -\ \omega_5\omega_6)z_i] \quad . \end{aligned} \qquad (A.34)$$

The solution for this simple case can be obtained from Eqs. (A.32), (A.33) and (A.34) to be

$$z_1^N\ +\ 1\ =\ \frac{\omega_1\omega_2+\omega_3\omega_4-\omega_5\omega_6}{\omega_1\omega_3+\omega_2\omega_4}\ (z_1^{N-1}\ +\ z_1) \quad . \qquad (A.35)$$

Denoting

$$\tilde{\Delta}\ =\ \frac{\omega_1\omega_2+\omega_3\omega_4-\omega_5\omega_6}{\omega_1\omega_3+\omega_2\omega_4} \quad , \qquad (A.36)$$

and setting $z_1 = \exp(ik)$ and $r = N/2-1$, Eq. (A.35) transforms to the well known equation

$$\tilde{\Delta} = \frac{\cos[(r + 1)\,k]}{\cos(r\,k)} \quad , \tag{A.37}$$

as in the symmetric six-vertex model. Thus if $\tilde{\Delta} < 1$ than Eq. (A.37) has one real solution. If $\tilde{\Delta} > 1$ Eq. (A.37) has one single positive imaginary solution. Both solutions are in the interval $(0, \pi/2r)$. In the solution of the six-vertex model, $\tilde{\Delta}$ was replaced by another quantity, but Eq. (A.37) had the same form.

For $n = 3$ the algebraic treatment becomes already very tedious. The ice-rule allows six regions to exist for $X_1,\ Y_1,\ \ldots,\ X_3,\ Y_3$. Let us consider one, for which

$$X_1 \le Y_1 \le X_2 \le Y_2 \le X_3 \le Y_3 \quad . \tag{A.38}$$

All the possible line configurations can be obtained from Fig. A.3, by adding three more cases to every line. These cases are corresponding to the first three possibilities of Fig. A.1. That is, there are 15 configurations. Thus, the total number of combinations will be 90. The important observation is, that the eigenvalue can be given in a factorized form using the notation of Eq. (A.23). For a choice of the wave function of the $g(X_1, X_2, X_3) = A_{123} z_1^{X_1} z_2^{X_2} z_3^{X_3}$ form, the eigenvalue equation becomes

$$\begin{aligned} \Lambda A_{123} z_1^{X_1} z_2^{X_2} z_3^{X_3} &= -\ \text{Correction Terms} \\ &+ A_{123} \omega_1^{X_1} R_1(X_1, X_2) R_2(X_2, X_3) [L(z_3) \omega_1^{N-X_3} z_3^{X_3} - \rho(z_3) \omega_4^{N-X_3} z_3^{N}] \\ &+ A_{123} \omega_4^{N-X_3} R_2(X_1, X_2) R_3(X_2, X_3) [\rho(z_1) \omega_1^{X_1} + M(z_1) \omega_4^{X_1} z_1^{X_1}] \quad . \end{aligned} \tag{A.39}$$

The eigenvalue will have the form

$$\Lambda = \omega_1^N\, L(z_1)\, L(z_2)\, L(z_3) + \omega_4^N\, M(z_1)\, M(z_2)\, M(z_3) \quad , \tag{A.40}$$

if the unwanted terms are canceling. By inspection of Eq. (A.39) it can be seen that the combinations corresponding to Eqs. (A.26) and (A.27) are of the $A_{123}s_{12}$ and $A_{123}[\rho(z_1)R_2(X_1,X_2)R_3(X_2,X_3) - \rho(z_3)z_3^N R_1(X_1,X_2)R_2(X_2,X_3)]$ type, respectively. That is, in order to cancel these terms the $A_{213}z_2^{X_1}z_1^{X_2}z_3^{X_3}$ and $A_{312}z_3^{X_1}z_1^{X_2}z_2^{X_3}$ combinations must be considered. However, these two new combinations are introducing two other unwanted terms which must be canceled with the introduction of other new combinations. At the end, the unwanted terms are completely canceling with a wave function chosen to be

$$\begin{aligned} g(X_1,X_2,X_3) &= A_{123}z_1^{X_1}z_2^{X_2}z_3^{X_3} + A_{321}z_3^{X_1}z_2^{X_2}z_1^{X_3} \\ &+ A_{213}z_2^{X_1}z_1^{X_2}z_3^{X_3} + A_{312}z_3^{X_1}z_1^{X_2}z_2^{X_3} \\ &+ A_{132}z_1^{X_1}z_3^{X_2}z_2^{X_3} + A_{231}z_2^{X_1}z_3^{X_2}z_1^{X_3} \quad . \end{aligned} \tag{A.41}$$

The conditions corresponding to Eqs. (A.32) and (A.33) are becoming

$$\begin{aligned} s_{12}\ A_{123} + s_{21}\ A_{213} &= 0 \\ s_{23}\ A_{231} + s_{32}\ A_{321} &= 0 \\ s_{31}\ A_{312} + s_{13}\ A_{132} &= 0 \quad , \end{aligned} \tag{A.42}$$

and

$$z_1^N = \frac{A_{123}}{A_{231}} \quad , \qquad z_2^N = \frac{A_{231}}{A_{312}} \quad , \qquad z_3^N = \frac{A_{312}}{A_{123}} \quad . \tag{A.43}$$

Eqs. A.38 is the Yang-Baxter equation in the language of the six-vertex model [5]. Combining these two equations, the *fugacities* z_i can be calculated as

$$\begin{aligned} z_1 &= \frac{s_{21}}{s_{12}}\frac{s_{31}}{s_{13}} \\ z_2 &= \frac{s_{12}}{s_{21}}\frac{s_{32}}{s_{23}} \\ z_3 &= \frac{s_{13}}{s_{31}}\frac{s_{23}}{s_{32}} \quad . \end{aligned} \tag{A.44}$$

At this level, the generalization for any n lines is obvious. The wave function must be of the form of Eq. (A.41) with all the $n!$ possible permutations of z_n to be considered. That is

$$g(X_1, \ldots, X_n) = \sum_P A_{p_1, \ldots, p_n} z_{p_1}^{X_1} \ldots z_{p_n}^{X_n} , \tag{A.45}$$

where the sum is over all permutations $P = \{p_1, \ldots, p_n\}$ of the integers $1, \ldots, n$. The eigenvalue will have the form of Eq. (A.40), that is

$$\Lambda = \omega_1^N \prod_{i=1}^{n} L(z_i) + \omega_4^N \prod_{i=1}^{n} M(z_i) , \tag{A.46}$$

where the fugacities z_i are obtained from the set of equations

$$z_i = (-1)^{n-1} \prod_{j=1}^{n} \frac{s_{ji}}{s_{ij}} , \tag{A.47}$$

which corresponds to Eq. (A.44), with the $j = i$ term also included being equal to unity. Using Eqs. (A.9) and (A.34), the solution of the general six-vertex model becomes

$$\Lambda = \omega_1^{N-n} \prod_{i=1}^{n} [\omega_3 + \frac{\omega_5\omega_6 z_i}{\omega_1 - \omega_4 z_i}] + \omega_4^{N-n} \prod_{i=1}^{n} [\omega_2 - \frac{\omega_5\omega_6}{\omega_1 - \omega_4 z_i}] , \tag{A.48}$$

where

$$z_i^N = (-1)^{n-1} \prod_{j=1}^{n} \frac{\omega_1\omega_3 + \omega_2\omega_4 z_i z_j - (\omega_1\omega_2 + \omega_3\omega_4 - \omega_5\omega_6) z_i}{\omega_1\omega_3 + \omega_2\omega_4 z_i z_j - (\omega_1\omega_2 + \omega_3\omega_4 - \omega_5\omega_6) z_j} . \tag{A.49}$$

Eqs. (A.48) and (A.49) are identical with those given by Gaudin[26] with the obvious change $\omega_3 \leftrightarrow \omega_4$, due to the different notations used. By the name *general six-vertex* model we mean that all the six vertex energies, i.e. all the six Boltzmann weights are independent variables!

Two important things can be obtained from the analysis of the general solution, i.e. Eqs. (A.48) and (A.49), before solving the integral equations. These are connected to the ferroelectric transition and to the symmetry of the solution. As we have shown, the $\widetilde{\Delta}$ generalized asymmetry term controls the type of the solutions. The $\widetilde{\Delta} = 1$ condition, i.e.

$$(\omega_1 - \omega_4)(\omega_2 - \omega_3) = \omega^2 \quad , \tag{A.50}$$

gives the ferroelectric transition, where $\omega_5 = \omega_6 = \omega$ was considered. From Eq. (A.50) the cases for the symmetric[5] and asymmetric[2] six-vertex can be obtained.

Let us introduce the following "coordinates" : $x_1 = \omega_1/\omega$, $x_2 = \omega_2/\omega$, $x_3 = \omega_3/\omega$ and $x_4 = \omega_4/\omega$. The eigenvalue equation, from Eq. (A.46) can be given as

$$\begin{aligned} \Lambda/\omega &= x_1^N \prod_{i=1}^{n} L(x_1, x_3, x_4, z_i) + x_4^N \prod_{i=1}^{n} M(x_1, x_2, x_4, z_i) \\ &= f_L(x_1, x_3, x_4, z) + f_M(x_1, x_2, x_4, z) \quad . \end{aligned} \tag{A.51}$$

If we consider a point $P(x_1, x_2, x_3, x_4)$ in the four dimensional space (x_1, x_2, x_3, x_4), we want to find a transformation

$$f_L(P(x_1, x_2, x_3, x_4), z^{\pm 1}) = f_M(\mathbf{S}P(x_1, x_2, x_3, x_4), z^{\pm 1}) \quad , \tag{A.52}$$

where the $z^{\pm 1}$ means that the choice $z = \exp(\pm ik)$ is arbitrary. Following the usual procedures we find

$$\mathbf{S} = \begin{pmatrix} 0 & 0 & 0 & 1 \\ 0 & 0 & 1 & 0 \\ 0 & 1 & 0 & 0 \\ 1 & 0 & 0 & 0 \end{pmatrix} \quad . \tag{A.53}$$

The points which are left invariant by $\mathbf{S}$ are situated on the hypersurface given by the equation

$$x_1 = x_4 \quad , \qquad x_2 = x_3 \quad . \tag{A.54}$$

That is, S represents a reflection with respect to this hypersurface. In terms of Boltzmann weights, Eq. (A.54) means

$$\omega_1 = \omega_4 \quad , \qquad \omega_2 = \omega_3 \quad . \tag{A.55}$$

The state defined with Eq. (A.55) represents a zero polarization state. In calculating the eigenvalues this symmetry allow to evaluate just one of the functions f_L, or f_M, as it is done by the Yangs [2] for the asymmetric six-vertex case.

For the symmetric six-vertex model, $x_1 = x_2 = x$ and $x_3 = x_4 = y$, we obtain

$$\mathbf{S} = \begin{pmatrix} 0 & 1 \\ 1 & 0 \end{pmatrix} \quad . \tag{A.56}$$

The reflection is made with respect to the $x = y$ plane. Indeed, it is known that the solution of the symmetric six-vertex model is symmetric with respect to the $x = y$ plane.

Appendix B

The Asymmetric Six-Vertex Case

The following derivation is based on the work of the Yangs [2] and Gaudin [26]. The eigenvalue of the general six-vertex model is obtained to be a function of six independent variables, $\omega_1, \ldots, \omega_6$. As mentioned in Chapter 1, there are only four independent energies to consider. The four independent variables used for the asymmetric six-vertex model are defined as follows. First the following set of notations

$$a = \sqrt{\omega_1 \omega_2} \quad , \quad b = \sqrt{\omega_3 \omega_4} \quad , \quad c = \sqrt{\omega_5 \omega_6} \quad , \tag{B.1}$$

is introduced, and two independent variables

$$\eta = \frac{a}{b} \equiv e^{\beta\delta} \quad , \tag{B.2}$$

and

$$\xi = \frac{c^2}{ab} \equiv e^{2\beta\epsilon} \quad . \tag{B.3}$$

are defined. In analogy to the symmetric six-vertex model define

$$\Delta_6 = \frac{a^2 + b^2 - c^2}{2ab} \equiv \frac{1}{2} \left(\eta + \frac{1}{\eta} - \xi\right) \quad . \tag{B.4}$$

The remaining two independent variables are defined as

$$H = e^{2\beta h} = \sqrt{\frac{\omega_1 \omega_3}{\omega_2 \omega_4}} \quad , \quad V = e^{2\beta v} = \sqrt{\frac{\omega_1 \omega_4}{\omega_2 \omega_3}} \quad . \tag{B.5}$$

Using Eq. (A.44) we can derive the eigenvalue, $\Lambda =$

$$
\begin{aligned}
&= \frac{\omega_1^N}{\omega_1^n} \prod_{i=1}^{n} [\omega_3 + \frac{c^2 z_i}{\omega_1 - \omega_4 z_i}] + \frac{\omega_4^N}{\omega_4^n} \prod_{i=1}^{n} [\omega_2 - \frac{c^2}{\omega_1 - \omega_4 z_i}] \\
&= \frac{\omega_1^N}{(\omega_1\omega_4)^n} \prod_{i=1}^{n} [\omega_3\omega_4 - \frac{c^2}{1 - \frac{\omega_1}{\omega_4}\frac{1}{z_i}}] \\
&\quad + \frac{\omega_4^N}{(\omega_1\omega_4)^n} \prod_{i=1}^{n} [\omega_1\omega_2 - \frac{c^2}{1 - \frac{\omega_4}{\omega_1} z_i}] \\
&= \frac{\omega_1^N}{(\omega_1\omega_4)^n} (ab)^n \prod_{i=1}^{n} [\sqrt{\frac{\omega_3\omega_4}{\omega_1\omega_2}} - \frac{\xi}{1 - \frac{\omega_1}{\omega_4}\frac{1}{z_i}}] \\
&\quad + \frac{\omega_4^N}{(\omega_1\omega_4)^n} (ab)^n \prod_{i=1}^{n} [\sqrt{\frac{\omega_1\omega_2}{\omega_3\omega_4}} - \frac{\xi}{1 - \frac{\omega_4}{\omega_1} z_i}] \\
&= \frac{\omega_1^N}{(\omega_1\omega_4)^n} (ab)^n \prod_{i=1}^{n} [\frac{1}{\eta} - \frac{\xi}{1 - \eta H \frac{1}{z_i}}] \\
&\quad + \frac{\omega_4^N}{(\omega_1\omega_4)^n} (ab)^n \prod_{i=1}^{n} [\eta - \frac{\xi}{1 - \frac{1}{\eta H} z_i}] \qquad (B.6) \\
&= (\omega_1\omega_4)^{N/2} (\sqrt{\frac{\omega_2\omega_3}{\omega_1\omega_4}})^n \{ (\eta H)^{N/2} \prod_{i=1}^{n} [\frac{1}{\eta} - \frac{\xi}{1 - \eta H \frac{1}{z_i}}] \\
&\quad + (\eta H)^{-N/2} \prod_{i=1}^{n} [\eta - \frac{\xi}{1 - \frac{1}{\eta H} z_i}] \} \\
&= (ab)^{N/2} (\sqrt{\frac{\omega_1\omega_4}{\omega_2\omega_3}})^{N/2} V^{-n} \{ (\eta H)^{N/2} \prod_{i=1}^{n} [\frac{1}{\eta} - \frac{\xi}{1 - \eta H \frac{1}{z_i}}] \\
&\quad + (\eta H)^{-N/2} \prod_{i=1}^{n} [\eta - \frac{\xi}{1 - \frac{1}{\eta H} z_i}] \} \\
&= (ab)^{N/2} V^{N/2-n} \{ (\eta H)^{N/2} \prod_{i=1}^{n} [\frac{1}{\eta} - \frac{\xi}{1 - \eta H \frac{1}{z_i}}] \\
&\quad + (\eta H)^{-N/2} \prod_{i=1}^{n} [\eta - \frac{\xi}{1 - \frac{1}{\eta H} z_i}] \} \ .
\end{aligned}
$$

Choosing $z_i \to 1/z_i$, which is arbitrary, and defining the vertical polarization as

$p_v = 1 - 2n/N$, Eq. (B.6) gives

$$\Lambda = (ab)^{\frac{N}{2}} \, V^{\frac{N}{2}p_v} \, \{ \, (\eta H)^{\frac{N}{2}} \prod_{i=1}^{n} [\eta^{-1} - \frac{\xi}{1 - \eta H z_i}] + (\eta H)^{-\frac{N}{2}} \prod_{i=1}^{n} [\eta - \frac{\xi}{1 - (\eta H z_i)^{-1}}] \, \} \quad . \tag{B.7}$$

The consistency conditions for the z_i fugacities are obtained in the same way from Eq. (A.45). That is, the numerator and denominator are divided by abH, after which we put $z_i \rightarrow 1/z_i$ and the form used by Yang [2] is obtained. Returning back to the eigenvalue, let us denote

$$\Lambda(n) = (\eta H)^{\frac{N}{2}} \prod_{i=1}^{n} [\eta^{-1} - \frac{\xi}{1 - \eta H z_i}] + (\eta H)^{-\frac{N}{2}} \prod_{i=1}^{n} [\eta - \frac{\xi}{1 - (\eta H z_i)^{-1}}] \, \} \quad . \tag{B.8}$$

The free energy from Eq. (B.7) becomes

$$\begin{aligned} f(\eta, \, \xi, \, h, \, v) &= - \frac{k_B T}{N} \ln \Lambda \\ &= - \frac{k_B T}{N} \ln \Lambda(n) - v \, p_v - \frac{k_B T}{2} \ln(ab) \\ &= f(\eta, \, \xi, \, h) - v \, p_v - \frac{k_B T}{4} \ln(\omega_1 \omega_2 \omega_3 \omega_4) \quad . \end{aligned} \tag{B.9}$$

The $f(\eta, \, \xi, \, h) = -k_B T/N \ln \Lambda(n)$ notation was used. As it can be seen from Eq. (B.9), for a given value of $\omega_1\omega_2\omega_3\omega_4$ the study of the general case, with horizontal and vertical external fields, reduces to the study of the eigenvalues with only horizontal external field. Actually, the symmetry of the $\omega_1, \ldots, \omega_6$ vertices allows to choose $\omega_1\omega_2\omega_3\omega_4 = 1$, as it was done by Yang [2], unless one of the four ω's vanishes. The argument is the following. By putting $\omega_5 = \omega_6$ we are left with five independent variables. From these five independent variables we can obtain four independent variables in two ways : imposing a value to one of the five variables, or imposing a condition to any number (larger than two) of variables. The second way was chosen by Yang[2] due to two reasons. First, by this the vertex energies will conserve the symmetry with respect to the simultaneous reversing of all arrows and the external electric fields. Secondly, by such a condition we can generate a new family of parameters such that the transfer matrix is simpler and commutes with the original one.

Let us calculate these vertex energies. Using Eqs. (B.2), (B.3) and (B.4) we obtain

$$\frac{\omega_1}{\omega_4} = e^{\beta(\delta+2h)} \quad , \quad \frac{\omega_1}{\omega_3} = e^{\beta(\delta+2v)} \quad , \quad \frac{\omega_1}{\omega_2} = e^{2\beta(h+v)} \quad . \tag{B.10}$$

Using the fact that $\omega_i = \exp(-\beta\varepsilon_i)$ we obtain

$$\begin{aligned} \varepsilon_2 &= \varepsilon_1 + 2h + 2v \\ \varepsilon_3 &= \varepsilon_1 + \delta + 2v \\ \varepsilon_4 &= \varepsilon_1 + 2h + \delta \quad . \end{aligned} \tag{B.11}$$

With the two conditions $\omega_5 = \omega_6$ and $\omega_1\omega_2\omega_3\omega_4 = 1$, that is $\varepsilon_5 = \varepsilon_6$ and $\varepsilon_1 + \varepsilon_2 + \varepsilon_3 + \varepsilon_4 = 0$ the results

$$\begin{aligned} \varepsilon_1 &= -\frac{\delta}{2} - h - v \\ \varepsilon_2 &= -\frac{\delta}{2} + h + v \\ \varepsilon_3 &= +\frac{\delta}{2} - h + v \\ \varepsilon_4 &= +\frac{\delta}{2} + h - v \\ \varepsilon_5 &= -\epsilon \\ \varepsilon_6 &= -\epsilon \quad , \end{aligned} \tag{B.12}$$

are immediately obtained. Any other condition of the $\varepsilon_1+\varepsilon_2+\varepsilon_3+\varepsilon_4 = \text{const.}$ type can be made equal to the corresponding ones in Eq. (B.12) by a suitable choice of ϵ

and adding $\pm(\varepsilon_1+\varepsilon_2+\varepsilon_3+\varepsilon_4)/4$ to all vertex energies, as emphasized by Yang. Let us consider for this case $\varepsilon_1+\varepsilon_2+\varepsilon_3+\varepsilon_4=4g$. Then from Eqs. (B.10) and (B.11) the vertex energies, with the conditions $\omega_5=\omega_6$ and $\omega_1\omega_2\omega_3\omega_4=\exp(-4\beta g)$, are

$$\begin{aligned}
\varepsilon_1 &= -\frac{\delta}{2} - h - v + g \\
\varepsilon_2 &= -\frac{\delta}{2} + h + v + g \\
\varepsilon_3 &= +\frac{\delta}{2} - h + v + g \\
\varepsilon_4 &= +\frac{\delta}{2} + h - v + g \\
\varepsilon_5 &= -\epsilon + g \\
\varepsilon_6 &= -\epsilon + g \quad .
\end{aligned} \tag{B.13}$$

However in this case the eigenvalues are not equal with those used by Yang, but the term $(\varepsilon_1+\varepsilon_2+\varepsilon_3+\varepsilon_4)/4=g$ must be added!

By choosing this type of conditions, the symmetry properties of the solution are not changed, see Eq. (A.51). Actually they are the same as for the symmetric ($\omega_1=\omega_2$ and $\omega_3=\omega_4$) six-vertex case, as we will show later with the use of the *rapidities*.

If no conditions are imposed we are left with five independent variables. Denoting $\epsilon'=\epsilon-4(\varepsilon_1+h+v+\delta/2)$, we obtain

$$\begin{aligned}
\varepsilon_1 &= \varepsilon_1 \\
\varepsilon_2 &= \varepsilon_1 + 2h + 2v \\
\varepsilon_3 &= \varepsilon_1 + \delta + 2v \\
\varepsilon_4 &= \varepsilon_1 + 2h + \delta \\
\varepsilon_5 &= -\epsilon' \\
\varepsilon_6 &= -\epsilon' \quad .
\end{aligned} \tag{B.14}$$

In Eq. (B.14) it would be natural to chose $\varepsilon_1 =$ const., e.g. $\varepsilon_1 = 0$. It can be seen that the symmetry properties of the solutions (B.12) and (B.13) are lost if another condition than $\varepsilon_1 + \varepsilon_2 + \varepsilon_3 + \varepsilon_4 =$ const. is chosen.

As it is known, in the thermodynamic limit, solving the eigenvalue equations reduces to solving an integral equation, the kernel of which is usually denoted by $\Theta(p, q)$. An important step in the integrable models is that the kernel always can be written as

$$\Theta(p,q) \;=\; \text{a function only of } (\alpha \;-\; \gamma) \quad , \tag{B.15}$$

where $p = k(\alpha)$ and $q = k(\gamma)$ are functions of the *rapidities* α and γ. If Eq. (B.15) is true, then

$$\frac{d\,p}{d\,\alpha}\,\frac{\partial\Theta(p,q)}{\partial p} + \frac{d\,q}{d\,\gamma}\,\frac{\partial\Theta(p,q)}{\partial q} \;=\; 0 \quad . \tag{B.16}$$

Solving Eq. (B.16) for the asymmetric six vertex model, the well known results

$$H\ e^{ik} \;=\; \begin{cases} \frac{e^{i\mu}-e^{\alpha}}{e^{i\mu+\alpha}-1}\ , & \text{if } \Delta_6 = -\cos\mu\ ; \\ \frac{e^{\lambda}-e^{i\alpha}}{e^{\lambda-i\alpha}-1}\ , & \text{if } \Delta_6 = -\cosh\lambda\ . \end{cases} \tag{B.17}$$

are obtained. The $\exp(ik^0) = H\exp(ik)$ notation (i.e. $z_i^0 = Hz_i$) appears in a natural way in Eq. (B.17). Even at this level the eigenvalue equations are not easy to handle. A second transformation is made for the variable η. From the form of the eigenvalue equation "it becomes natural to define another constant" [5] ϕ, of the algebraic form similar to Eq. (B.17). Thus, "ϕ is defined so that $\alpha = i\phi$ corresponds to $\exp(ik^0) = 1/\eta$" [2]. At this point we fix $\eta > 1$, to be in concordance with Yang [2] and Gaudin [26]. With this definition, from Eq. (B.17) ϕ can easily be obtained

$$\begin{cases} e^{i\phi} \;=\; \frac{1+\eta e^{i\mu}}{e^{i\mu}+\eta}\ , & \text{if } \Delta_6 = -\cos\mu\ ; \\ e^{\phi} \;=\; \frac{1+\eta e^{\lambda}}{e^{\lambda}+\eta}\ , & \text{if } \Delta_6 = -\cosh\lambda\ . \end{cases} \tag{B.18}$$

By performing these transformations, from momenta to rapidities simultaneously we have transformed the value of Δ_6 and the ratio $a/b = \eta$. Using Eq. (B.5), we see that the input parameters a, b and c cannot all be determined, just the ratio of them, which is invariant under these transformations

$$\begin{cases} a:b:c = \sin\frac{\mu+\phi}{2} : \sin\frac{\mu-\phi}{2} : \sin\mu \ , & \text{if } \Delta_6 = -\cos\mu \ ; \\ a:b:c = \sinh\frac{\lambda+\phi}{2} : \sinh\frac{\lambda-\phi}{2} : \sinh\lambda \ , & \text{if } \Delta_6 = -\cosh\lambda \ . \end{cases} \qquad (B.19)$$

Or, we can choose a parametrization

$$\begin{aligned} a &= \rho \begin{cases} \sin\frac{\mu+\phi}{2} \ , & \text{if } \Delta_6 = -\cos\mu \ ; \\ \sinh\frac{\lambda+\phi}{2} \ , & \text{if } \Delta_6 = -\cosh\lambda \ , \end{cases} \\ b &= \rho \begin{cases} \sin\frac{\mu-\phi}{2} \ , & \text{if } \Delta_6 = -\cos\mu \ ; \\ \sinh\frac{\lambda-\phi}{2} \ , & \text{if } \Delta_6 = -\cosh\lambda \ , \end{cases} \\ c &= \rho \begin{cases} \sin\mu \ , & \text{if } \Delta_6 = -\cos\mu \ ; \\ \sinh\lambda \ , & \text{if } \Delta_6 = -\cosh\lambda \ . \end{cases} \end{aligned} \qquad (B.20)$$

We are in the $\eta > 1$ case. In the symmetric case, to study the $\eta < 1$ situation the $\phi \to -\phi$ change should be made. The parameter ϕ is referred to as the spectral parameter and, obviously, the eigenvector cannot depend on it. The parameter ρ as it appears in Eq. (B.20) will contribute to the partition function with ρ^N, that is, $\rho = \sqrt{ab}$. Thus $ab = 1$ implies $\rho = 1$ [26].

Furthermore, we want to transform the eigenvalue, Eq. (B.7) as a function of rapidities. Using Eqs. (B.4) and (B.12), we can immediately write from Eq. (B.7)

$$\Lambda = P_+ \ e^{\beta N(\frac{\delta}{2}+h+vp_v)} + P_- \ e^{\beta N(-\frac{\delta}{2}-h+vp_v)} \quad , \qquad (B.21)$$

where

$$P_\pm = \prod_{i=1}^{n} \frac{z_i^{0\,\pm 1}(2\Delta_6 - \eta^{\pm 1}) - 1}{z_i^{0\,\pm 1} - \eta^{\pm 1}} \quad . \qquad (B.22)$$

Using the definition of ϕ and Eq. (B.18) we observe that z_i^0 is identical with η_i with the obvious $\phi_i \to -\phi_i$ change. Thus $P_\pm$ is equal to

$$P_\pm = (-1)^n \ e^{\pm in\mu} \prod_{i=1}^{n} \frac{e^{i(\phi-\phi_i\mp 2\mu)} - 1}{e^{i(\phi-\phi_i)} - 1} \ , \quad \text{if } \Delta_6 = -\cos\mu \quad , \qquad (B.23)$$

and

$$P_{\pm} \;=\; (-1)^n \; e^{\pm n\lambda} \; \prod_{i=1}^{n} \frac{e^{\phi-\phi_i \mp 2\lambda} \;-\; 1}{e^{\phi-\phi_i} \;-\; 1} \;, \quad \text{if} \;\; \Delta_6 \;=\; -\cosh\lambda \;\;, \qquad (B.24)$$

Using Eqs. (B.2), (B.20) and the condition $ab = 1$ we obtain from Eq. (B.21) for the eigenvalue (for simplicity consider n to be even)

$$\begin{aligned} \Lambda \;&=\; e^{\beta N(h+vp_v)} \; \sin^N \frac{1}{2}(\mu+\phi) \prod_{i=1}^{n} \frac{\sin\frac{1}{2}(\phi-\phi_i-2\mu)}{\sin\frac{1}{2}(\phi-\phi_i)} \\ &+\; e^{\beta N(-h+vp_v)} \; \sin^N \frac{1}{2}(\mu-\phi) \prod_{i=1}^{n} \frac{\sin\frac{1}{2}(\phi-\phi_i+2\mu)}{\sin\frac{1}{2}(\phi-\phi_i)} \quad , \end{aligned} \qquad (B.25)$$

for $-1 < \Delta_6 < 1$, and

$$\begin{aligned} \Lambda \;&=\; e^{\beta N(h+vp_v)} \; \sinh^N \frac{1}{2}(\lambda+\phi) \prod_{i=1}^{n} \frac{\sinh\frac{1}{2}(\phi-\phi_i-2\lambda)}{\sinh\frac{1}{2}(\phi-\phi_i)} \\ &+\; e^{\beta N(-h+vp_v)} \; \sinh^N \frac{1}{2}(\lambda-\phi) \prod_{i=1}^{n} \frac{\sinh\frac{1}{2}(\phi-\phi_i+2\lambda)}{\sinh\frac{1}{2}(\phi-\phi_i)} \quad , \end{aligned} \qquad (B.26)$$

if $\Delta_6 < -1$. If we are using the notation

$$\Lambda_L \;=\; \begin{cases} \sin^N \frac{1}{2}(\mu+\phi) \; \prod_{i=1}^{n} \frac{\sin\frac{1}{2}(\phi-\phi_i-2\mu)}{\sin\frac{1}{2}(\phi-\phi_i)} \;, & \text{if } \Delta_6 = -\cos\mu \;; \\ \sinh^N \frac{1}{2}(\lambda+\phi) \; \prod_{i=1}^{n} \frac{\sinh\frac{1}{2}(\phi-\phi_i-2\lambda)}{\sinh\frac{1}{2}(\phi-\phi_i)} \;, & \text{if } \Delta_6 = -\cosh\lambda \;, \end{cases} \qquad (B.27)$$

and

$$\Lambda_M \;=\; \begin{cases} \sin^N \frac{1}{2}(\mu-\phi) \; \prod_{i=1}^{n} \frac{\sin\frac{1}{2}(\phi-\phi_i+2\mu)}{\sin\frac{1}{2}(\phi-\phi_i)} \;, & \text{if } \Delta_6 = -\cos\mu \;; \\ \sinh^N \frac{1}{2}(\lambda-\phi) \; \prod_{i=1}^{n} \frac{\sinh\frac{1}{2}(\phi-\phi_i+2\lambda)}{\sinh\frac{1}{2}(\phi-\phi_i)} \;, & \text{if } \Delta_6 = -\cosh\lambda \;, \end{cases} \qquad (B.28)$$

then the free energy will reduce to

$$\begin{aligned} f(\omega_1,\ldots,\omega_6) \;&=\; f(a,b,c;ab=1) \\ &=\; f(\eta,\xi,h,v) \\ &=\; f_{L(M)}[\phi,\mu(\lambda)] \;\mp h \;-\; vp_v \quad , \end{aligned} \qquad (B.29)$$

where $f_{L(M)} = -k_B T/N \ln \Lambda_{L(M)}$, with $\Lambda_{L(M)}$ defined in Eqs. (B.27) or (B.28).

The consistency conditions of the fugacities are also transformed with the use of Eq. (B.18), to give

$$(H^{-1} \frac{\sin\frac{1}{2}(\mu-\phi_j)}{\sin\frac{1}{2}(\mu+\phi_j)})^N = \prod_{i=1}^{n} \frac{\sin\frac{1}{2}(\phi_j-\phi_i-2\mu)}{\sin\frac{1}{2}(\phi_j-\phi_i+2\mu)} \quad , \tag{B.30}$$

for $-1 < \Delta_6 < 1$, and

$$(H^{-1} \frac{\sinh\frac{1}{2}(\lambda-\phi_j)}{\sinh\frac{1}{2}(\lambda+\phi_j)})^N = \prod_{i=1}^{n} \frac{\sinh\frac{1}{2}(\phi_j-\phi_i-2\lambda)}{\sinh\frac{1}{2}(\phi_j-\phi_i+2\lambda)} \quad , \tag{B.31}$$

if $\Delta_6 < -1$. If we do not restrict n to be even, then $\mu' = \mu - \pi$ and $\lambda' = \lambda - i\pi$ should be used in Eqs. (B.25) - (B.31).

In the asymmetric six-vertex model also the case $\Delta_6 > 1$ is to be analysed[2]. Similarly to Eqs. (B.17) and (B.18), we define the transformation to fugacities and rapidities as

$$z_i^0 = \frac{e^{\nu} - e^{-i\alpha}}{1 - e^{\nu - i\alpha}} \quad , \tag{B.32}$$

and

$$e^{\phi} = \frac{\eta e^{\nu} - 1}{\eta - e^{\nu}} \quad , \tag{B.33}$$

respectively. For this case $\Delta_6 = \cosh\nu$. The Eqs. (B.32) and (B.33) are valid if $\eta > 1$ and $2\beta h < \nu$. Eq. (B.19) becomes

$$a : b : c = \sinh\frac{\phi+\nu}{2} : \sinh\frac{\phi-\nu}{2} : \sinh\nu \quad . \tag{B.34}$$

The eigenvalues are obtained in a similar way as before

$$\begin{aligned} \Lambda &= e^{\beta N(h+vp_v)} \sinh^N \frac{1}{2}(\phi+\nu) \prod_{i=1}^{n} \frac{\sinh\frac{1}{2}(\phi-\phi_i-2\nu)}{\sinh\frac{1}{2}(\phi-\phi_i)} \\ &+ e^{\beta N(-h+vp_v)} \sinh^N \frac{1}{2}(\phi-\nu) \prod_{i=1}^{n} \frac{\sinh\frac{1}{2}(\phi-\phi_i+2\nu)}{\sinh\frac{1}{2}(\phi-\phi_i)} \quad . \end{aligned} \tag{B.35}$$

In this case, however, the consistency conditions are satisfied [26] for any ϕ and ν if we take

$$\phi_k = \pi + i(\phi_0 + k\nu) \quad . \tag{B.36}$$

Furthermore, Gaudin [26] shows that the eigenvalue from Eq. (B.35) reduces to

$$\Lambda = e^{\beta N(h+vp_v)}\, e^{\beta N\delta/2}\, e^{-2\beta nh} - e^{\beta N(-h+vp_v)}\, e^{-\beta N\delta/2}\, e^{2\beta nh} \quad . \tag{B.37}$$

In simple form

$$\Lambda = e^{\beta N[\delta/2+p_v(h+v)]} - e^{-\beta N[\delta/2+p_v(h-v)]} \quad . \tag{B.38}$$

Appendix C

The Six-Vertex Model and the Quantum Spin Chain

The transfer matrix of the general six-vertex model

$$\mathbf{T} \;=\; \mathrm{Tr}\,[\,\prod_{i=1}^{N}\,\mathbf{T}(i)\,] \quad , \tag{C.1}$$

can be related to a one dimensional linear quantum spin Hamiltonian

$$\mathcal{H} \;=\; \sum_{i=1}^{N}\,\mathcal{H}_{i,i+1} \quad . \tag{C.2}$$

Each $\mathbf{T}(i)$ is a 2×2 matrix with operator elements acting on the vertical arrows (spins) at site i, see Barouch [6] and Gaudin [26]

$$\mathbf{T} \;=\; \begin{pmatrix} \frac{\omega_1+\omega_3}{2} \;+\; \frac{\omega_1-\omega_3}{2}\sigma_i^z & \omega\sigma_i^+ \\ \omega\sigma_i^- & \frac{\omega_4+\omega_2}{2} \;+\; \frac{\omega_4-\omega_2}{2}\sigma_i^z \end{pmatrix} \quad , \tag{C.3}$$

where $\omega_5 = \omega_6 = \omega$ was considered. The commutator of $\mathbf{T}$ and $\mathcal{H}$, from Eqs. (C.1) and (C.2) reduces to

$$\begin{aligned}[\mathbf{T},\mathcal{H}] \;=\; \mathrm{Tr}\,\Big[\,\sum_{i=1}^{N}\Big(\ldots \;+\; &\mathbf{T}(i-1)\,\{[\mathbf{T}(i),\mathcal{H}_{i,i+1}]\mathbf{T}(i+1) \\ &+\; \mathbf{T}(i)[\mathbf{T}(i+1),\mathcal{H}_{i,i+1}]\}\;\mathbf{T}(i+2)\;\ldots\Big)\,\Big] \quad .\end{aligned} \tag{C.4}$$

A typical commutator element, $\{[\mathbf{T}(i), \mathcal{H}_{i,i+1}]\mathbf{T}(i+1) \;+\; \mathbf{T}(i)[\mathbf{T}(i+1), \mathcal{H}_{i,i+1}]\}$ is never zero. However, if there exists a 2×2 matrix $\mathbf{Q}(i)$ with the property that

$$\{[\mathbf{T}(i), \mathcal{H}_{i,i+1}]\mathbf{T}(i+1) \;+\; \mathbf{T}(i)[\mathbf{T}(i+1), \mathcal{H}_{i,i+1}]\} \;=\; \mathbf{T}(i)\mathbf{Q}(i+1) \;-\; \mathbf{Q}(i)\mathbf{T}(i+1) \quad , \tag{C.5}$$

then $[\mathbf{T}, \mathcal{H}]$ from Eq. (C.4) is vanishing. The matrix elements a_{ij}, defined as

$$\begin{pmatrix} a_{11} & a_{12} \\ a_{21} & a_{22} \end{pmatrix} \;=\; [\mathbf{T}(i), \mathcal{H}_{i,i+1}]\mathbf{T}(i+1) \;+\; \mathbf{T}(i)[\mathbf{T}(i+1), \mathcal{H}_{i,i+1}]\} \quad , \tag{C.6}$$

using Eq. (C.3) are

$$\begin{aligned} a_{11} \;=\;& \frac{\omega_1^2 - \omega_3^2}{4}([\sigma_i^z, \mathcal{H}_{i,i+1}] \;+\; [\sigma_{i+1}^z, \mathcal{H}_{i,i+1}]) \\ &+\; \frac{(\omega_1 - \omega_3)^2}{4}([\sigma_i^z, \mathcal{H}_{i,i+1}]\sigma_{i+1}^z \;+\; \sigma_i^z[\sigma_{i+1}^z, \mathcal{H}_{i,i+1}]) \\ &+\; \omega^2([\sigma_i^+, \mathcal{H}_{i,i+1}]\sigma_{i+1}^- \;+\; \sigma_i^+[\sigma_{i+1}^z, \mathcal{H}_{i,i+1}]) \quad , \end{aligned} \tag{C.7}$$

$$\begin{aligned} a_{12} \;=\;& \frac{\omega}{2}\{(\omega_4 + \omega_2)[\sigma_i^+, \mathcal{H}_{i,i+1}] \;+\; (\omega_1 + \omega_3)[\sigma_{i+1}^+, \mathcal{H}_{i,i+1}]\} \\ &+\; \omega\frac{\omega_1 - \omega_3}{2}([\sigma_i^z, \mathcal{H}_{i,i+1}]\sigma_{i+1}^+ \;+\; \sigma_i^z[\sigma_{i+1}^+, \mathcal{H}_{i,i+1}]) \\ &+\; \omega\frac{\omega_4 - \omega_2}{2}(\sigma_i^+[\sigma_i^z, \mathcal{H}_{i,i+1}] \;+\; [\sigma_{i+1}^z, \mathcal{H}_{i,i+1}]\sigma_{i+1}^z) \quad , \end{aligned} \tag{C.8}$$

$$\begin{aligned} a_{21} \;=\;& \frac{\omega}{2}\{(\omega_4 + \omega_2)[\sigma_{i+1}^-, \mathcal{H}_{i,i+1}] \;+\; (\omega_1 + \omega_3)[\sigma_i^-, \mathcal{H}_{i,i+1}]\} \\ &+\; \omega\frac{\omega_1 - \omega_3}{2}(\sigma_i^-[\sigma_{i+1}^z, \mathcal{H}_{i,i+1}] \;+\; [\sigma_i^-, \mathcal{H}_{i,i+1}]\sigma_{i+1}^z) \\ &+\; \omega\frac{\omega_4 - \omega_2}{2}(\sigma_i^z[\sigma_{i+1}^-, \mathcal{H}_{i,i+1}] \;+\; [\sigma_i^z, \mathcal{H}_{i,i+1}]\sigma_{i+1}^-) \quad , \end{aligned} \tag{C.9}$$

and

$$\begin{aligned} a_{22} \;=\;& \frac{\omega_4^2 - \omega_2^2}{4}([\sigma_i^z, \mathcal{H}_{i,i+1}] \;+\; [\sigma_{i+1}^z, \mathcal{H}_{i,i+1}]) \\ &+\; \frac{(\omega_4 - \omega_2)^2}{4}([\sigma_i^z, \mathcal{H}_{i,i+1}]\sigma_{i+1}^z \;+\; \sigma_i^z[\sigma_{i+1}^z, \mathcal{H}_{i,i+1}]) \\ &+\; \omega^2([\sigma_i^+, \mathcal{H}_{i.i+1}]\sigma_{i+1}^- \;+\; \sigma_i^+[\sigma_{i+1}^z, \mathcal{H}_{i,i+1}]) \quad . \end{aligned} \tag{C.10}$$

If we use the notation

$$\begin{pmatrix} q^i_{11} & q^i_{12} \\ q^i_{21} & q^i_{22} \end{pmatrix} = \mathbf{Q}(i) \quad , \tag{C.11}$$

then the elements

$$\begin{pmatrix} b_{11} & b_{12} \\ b_{21} & b_{22} \end{pmatrix} = \mathbf{T}(i)\mathbf{Q}(i+1) - \mathbf{Q}(i)\mathbf{T}(i+1) \quad , \tag{C.12}$$

must be equal with the a_{ij}'s from Eqs. (C.7) - (C.10). Computing the matrix products in Eq. (C.12), we find

$$\begin{aligned} b_{11} &= (\frac{\omega_1+\omega_3}{2} + \frac{\omega_1-\omega_3}{2}\sigma^z_i)q^{i+1}_{11} + \omega\sigma^+_i q^{i+1}_{21} \\ &- (\frac{\omega_1+\omega_3}{2} + \frac{\omega_1-\omega_3}{2}\sigma^z_{i+1})q^i_{11} - \omega\sigma^-_{i+1}q^i_{12} \quad , \end{aligned} \tag{C.13}$$

$$\begin{aligned} b_{12} &= (\frac{\omega_1+\omega_3}{2} + \frac{\omega_1-\omega_3}{2}\sigma^z_i)q^{i+1}_{12} + \omega\sigma^+_i q^{i+1}_{22} \\ &- (\frac{\omega_4+\omega_2}{2} + \frac{\omega_4-\omega_2}{2}\sigma^z_{i+1})q^i_{12} - \omega\sigma^+_{i+1}q^i_{11} \quad , \end{aligned} \tag{C.14}$$

$$\begin{aligned} b_{21} &= (\frac{\omega_4+\omega_2}{2} + \frac{\omega_4-\omega_2}{2}\sigma^z_i)q^{i+1}_{21} + \omega\sigma^-_i q^{i+1}_{11} \\ &- (\frac{\omega_1+\omega_3}{2} + \frac{\omega_1-\omega_3}{2}\sigma^z_{i+1})q^i_{21} - \omega\sigma^-_{i+1}q^i_{22} \quad , \end{aligned} \tag{C.15}$$

and

$$\begin{aligned} b_{22} &= (\frac{\omega_4+\omega_2}{2} + \frac{\omega_4-\omega_2}{2}\sigma^z_i)q^{i+1}_{22} + \omega\sigma^-_i q^{i+1}_{12} \\ &- (\frac{\omega_4+\omega_2}{2} + \frac{\omega_4-\omega_2}{2}\sigma^z_{i+1})q^i_{22} - \omega\sigma^+_{i+1}q^i_{21} \quad . \end{aligned} \tag{C.16}$$

At this level of the calculations we must specify the form of the Hamiltonian $\mathcal{H}_{i,i+1}$, which we choose to be of the form

$$\mathcal{H}_{i,i+1} = \Gamma_x\sigma^+_i\sigma^-_{i+1} + \Gamma_y\sigma^-_i\sigma^+_{i+1} + \Gamma_z\sigma^z_i\sigma^z_{i+1} \quad . \tag{C.17}$$

We are using the well-known commutation relations:

$$\begin{aligned} [\sigma^z,\sigma^+] &= +2\sigma^+ \; ; \\ [\sigma^z,\sigma^-] &= -2\sigma^- \; ; \\ [\sigma^+,\sigma^-] &= +4\sigma^z \quad , \end{aligned} \tag{C.18}$$

and the formulas

$$\begin{aligned} \sigma^+\sigma^+ &= \sigma^-\sigma^- = 0 ; \\ \sigma^+\sigma^- &= 2 + 2\sigma^z ; \\ \sigma^-\sigma^+ &= 2 - 2\sigma^z . \end{aligned} \tag{C.19}$$

The commutators entering in Eqs. (C.7) - (C.10), calculated with the use of Eqs. (C.17), (C.18) and (C.19) are

$$\begin{aligned} [\sigma_i^+, \mathcal{H}_{i,i+1}] &= 4\Gamma_y \sigma_i^z \sigma_{i+1}^+ - 2\Gamma_z \sigma_i^+ \sigma_{i+1}^z ; \\ [\sigma_{i+1}^+, \mathcal{H}_{i,i+1}] &= 4\Gamma_x \sigma_i^+ \sigma_{i+1}^z - 2\Gamma_z \sigma_i^z \sigma_{i+1}^+ ; \\ [\sigma_i^-, \mathcal{H}_{i,i+1}] &= -4\Gamma_x \sigma_i^z \sigma_{i+1}^- + 2\Gamma_z \sigma_i^- \sigma_{i+1}^z ; \\ [\sigma_{i+1}^-, \mathcal{H}_{i,i+1}] &= -4\Gamma_y \sigma_i^- \sigma_{i+1}^z + 2\Gamma_z \sigma_i^z \sigma_{i+1}^- ; \\ [\sigma_i^z, \mathcal{H}_{i,i+1}] &= 2\Gamma_x \sigma_i^+ \sigma_{i+1}^- - 2\Gamma_y \sigma_i^- \sigma_{i+1}^+ ; \\ [\sigma_{i+1}^z, \mathcal{H}_{i,i+1}] &= -2\Gamma_x \sigma_i^+ \sigma_{i+1}^- + 2\Gamma_y \sigma_i^- \sigma_{i+1}^+ . \end{aligned} \tag{C.20}$$

By direct calculation, it can be checked easily that

$$\begin{aligned} [\sigma_i^z, \mathcal{H}_{i,i+1}] + [\sigma_{i+1}^z, \mathcal{H}_{i,i+1}] &= 0 ; \\ [\sigma_i^z, \mathcal{H}_{i,i+1}]\sigma_{i+1}^z + \sigma_i^z [\sigma_{i+1}^z, \mathcal{H}_{i,i+1}] &= 0 . \end{aligned} \tag{C.21}$$

The other commutators entering in Eqs. (C.7) - (C.10) are

$$\begin{aligned} [\sigma_i^+, \mathcal{H}_{i,i+1}]\sigma_{i+1}^- + \sigma_i^+ [\sigma_{i+1}^z, \mathcal{H}_{i,i+1}] &= 8\Gamma_y ; \\ [\sigma_i^+, \mathcal{H}_{i,i+1}]\sigma_{i+1}^- + \sigma_i^+ [\sigma_{i+1}^z, \mathcal{H}_{i,i+1}]) &= -8\Gamma_x ; \\ [\sigma_i^z, \mathcal{H}_{i,i+1}]\sigma_{i+1}^+ + \sigma_i^z [\sigma_{i+1}^+, \mathcal{H}_{i,i+1}]) &= 4\Gamma_x \sigma_i^+ - 2\Gamma_z \sigma_{i+1}^+ ; \\ [\sigma_{i+1}^z, \mathcal{H}_{i,i+1}]\sigma_{i+1}^z) + \sigma_i^+ [\sigma_i^z, \mathcal{H}_{i,i+1}] &= 4\Gamma_y \sigma_{i+1}^+ - 2\Gamma_z \sigma_i^+ ; \\ [\sigma_i^-, \mathcal{H}_{i,i+1}]\sigma_{i+1}^z) + \sigma_i^- [\sigma_{i+1}^z, \mathcal{H}_{i,i+1}] &= -4\Gamma_x \sigma_{i+1}^- + 2\Gamma_z \sigma_i^- ; \\ [\sigma_i^z, \mathcal{H}_{i,i+1}]\sigma_{i+1}^-) + \sigma_i^z [\sigma_{i+1}^-, \mathcal{H}_{i,i+1}] &= -4\Gamma_y \sigma_i^- + 2\Gamma_z \sigma_{i+1}^- . \end{aligned} \tag{C.22}$$

By this the expression of a_{11} and a_{22} from Eqs. (C.7) and (C.10) are simplified to

$$a_{11} = 8\Gamma_y \omega^2 (\sigma_i^z - \sigma_{i+1}^z) , \tag{C.23}$$

and

$$a_{22} \ = \ - \ 8\Gamma_x \omega^2 (\sigma_i^z \ - \ \sigma_{i+1}^z) \quad . \tag{C.24}$$

While, the expressions of a_{12} and a_{21} are more involved

$$\begin{aligned} a_{12} \ = \ & \omega[2\Gamma_x(\omega_1 - \omega_3) \ - \ \Gamma_z(\omega_4 - \omega_2)]\sigma_i^+ \\ & + \ \omega[2\Gamma_y(\omega_4 - \omega_2) \ - \ \Gamma_z(\omega_1 - \omega_3)]\sigma_{i+1}^+ \\ & + \ \omega[2\Gamma_x(\omega_1 + \omega_3) \ - \ \Gamma_z(\omega_4 + \omega_2)]\sigma_i^+ \sigma_{i+1}^z \\ & + \ \omega[2\Gamma_y(\omega_4 + \omega_2) \ - \ \Gamma_z(\omega_1 + \omega_3)]\sigma_i^z \sigma_{i+1}^+ \quad , \end{aligned} \tag{C.25}$$

and

$$\begin{aligned} a_{21} \ = \ & - \ \omega[2\Gamma_x(\omega_1 - \omega_3) \ - \ \Gamma_z(\omega_4 - \omega_2)]\sigma_i^- \\ & - \ \omega[2\Gamma_y(\omega_4 - \omega_2) \ - \ \Gamma_z(\omega_1 - \omega_3)]\sigma_{i+1}^- \\ & - \ \omega[2\Gamma_x(\omega_1 + \omega_3) \ - \ \Gamma_z(\omega_4 + \omega_2)]\sigma_i^- \sigma_{i+1}^z \\ & - \ \omega[2\Gamma_y(\omega_4 + \omega_2) \ - \ \Gamma_z(\omega_1 + \omega_3)]\sigma_i^z \sigma_{i+1}^- \quad , \end{aligned} \tag{C.26}$$

The main equation to be solved is given in Eq. (C.5), which with the notations of Eqs. (C.6) and (C.12) reduces to

$$\begin{aligned} a_{11} \ &= \ b_{11} \ ; \\ a_{12} \ &= \ b_{12} \ ; \\ a_{21} \ &= \ b_{21} \ ; \\ a_{22} \ &= \ b_{22} \quad . \end{aligned} \tag{C.27}$$

From the first and fourth equality of Eq. (C.27) we obtain

$$q_{12} \ = \ q_{21} \ = \ 0 \quad . \tag{C.28}$$

This is very a important result, because it follows that the matrix $\mathbf{Q}$ must have a diagonal form. Thus, the b_{ij}'s from Eqs. (C.13) - (C.16) are simplified to

$$\begin{aligned}
b_{11} &= \frac{\omega_1+\omega_3}{2}(q_{11}^{i+1}-q_{11}^{i}) + \frac{\omega_1-\omega_3}{2}(q_{11}^{i+1}\sigma_i^z - q_{11}^{i}\sigma_{i+1}^z)\ ;\\
b_{12} &= \omega_1(b_{22}^{i+1}\sigma_i^+ - b_{11}^{i}\sigma_{i+1}^+)\ ;\\
b_{21} &= \omega_1(b_{11}^{i+1}\sigma_i^- - b_{22}^{i}\sigma_{i+1}^-)\ ;\\
b_{22} &= \frac{\omega_4+\omega_2}{2}(q_{22}^{i+1}-q_{22}^{i}) + \frac{\omega_4-\omega_2}{2}(q_{22}^{i+1}\sigma_i^z - q_{22}^{i}\sigma_{i+1}^z)\quad .
\end{aligned} \tag{C.29}$$

From the properties of the Pauli matrices presented in Eq. (C.18) and (C.19), and the system of equations, Eqs. (C.27) which is to be solved, it follows that the q_{11}^i and q_{22}^i must be of the form

$$\begin{aligned}
q_{11}^i &= B_{11} + B_{12}\,\sigma_i^z\ ;\\
q_{22}^i &= B_{22} + B_{21}\,\sigma_i^z\quad .
\end{aligned} \tag{C.30}$$

Introducing these values in Eqs. (C.29) we construct a system of equations for the B_{ij}'s from Eqs. (C.27). This system of equations turns out to be of Cramer type if all the Boltzmann weights are non-zero. Thus, if the determinant of the system $\sim\ \omega_1\omega_2\omega_3\omega_4$ is non-zero the solutions obtained for the B_{ij}'s are

$$\begin{aligned}
B_{11} &= -\frac{1}{4}[2(\omega_4-\omega_2) - \frac{\omega_1-\omega_3}{2}\frac{\omega_1\omega_2+\omega_3\omega_4-\omega^2}{\sqrt{\omega_1\omega_2\omega_3\omega_4}}]\ ;\\
B_{12} &= -\frac{1}{4}[4(\omega_4+\omega_2) - 2(\omega_4-\omega_2) - \frac{\omega_1+\omega_3}{2}\frac{\omega_1\omega_2+\omega_3\omega_4-\omega^2}{\sqrt{\omega_1\omega_2\omega_3\omega_4}}]\ ;\\
B_{21} &= +\frac{1}{4}[4(\omega_1+\omega_3) - 2(\omega_1-\omega_3) - \frac{\omega_4+\omega_2}{2}\frac{\omega_1\omega_2+\omega_3\omega_4-\omega^2}{\sqrt{\omega_1\omega_2\omega_3\omega_4}}]\ ;\\
B_{22} &= +\frac{1}{4}[2(\omega_1-\omega_3) - \frac{\omega_4-\omega_2}{2}\frac{\omega_1\omega_2+\omega_3\omega_4-\omega^2}{\sqrt{\omega_1\omega_2\omega_3\omega_4}}]\quad .
\end{aligned} \tag{C.31}$$

The constants Γ_x, Γ_y and Γ_z are obtained as

$$\Gamma_x = \frac{1}{2}\sqrt{\frac{\omega_2\omega_4}{\omega_1\omega_3}}\quad , \tag{C.32}$$

$$\Gamma_y = \frac{1}{4\Gamma_x} \quad , \tag{C.33}$$

and

$$\Gamma_z = \frac{1}{2} \frac{\omega_1\omega_2 + \omega_3\omega_4 - \omega^2}{\sqrt{\omega_1\omega_2\omega_3\omega_4}} \quad , \tag{C.34}$$

is identical to the anisotropy constant of the asymmetric six-vertex model, i.e. Δ_6, defined in Eq. (B.4) of Appendix B.

The form of the Hamiltonian from Eq. (C.17) can be put in a symmetric form as it is usually used

$$\mathcal{H}_{i,i+1} = \frac{1}{2} \frac{\omega_1\omega_3 + \omega_2\omega_4}{\sqrt{\omega_1\omega_2\omega_3\omega_4}} \left[(1+\gamma)\sigma_i^+\sigma_{i+1}^- + (1-\gamma)\sigma_i^-\sigma_{i+1}^+ + \tilde{\Delta}\, \sigma_i^z\sigma_{i+1}^z \right] \quad , \tag{C.35}$$

where

$$\gamma = \frac{\omega_2\omega_4 - \omega_1\omega_3}{\omega_2\omega_4 + \omega_1\omega_3} \quad , \tag{C.36}$$

and

$$\tilde{\Delta} = \frac{\omega_1\omega_2 + \omega_3\omega_4 - \omega^2}{\omega_1\omega_3 + \omega_2\omega_4} \quad , \tag{C.37}$$

is the anisotropy constant of the general six-vertex model defined in Eq. (A.32) of Appendix A.

Appendix D

Connection Between the Five-Vertex Model and the Asymmetric Six-Vertex Model

In the asymmetric six-vertex model the following four new variables are defined, see Appendix B or Eqs. (1.7) and (1.8)

$$\eta = \sqrt{\frac{\omega_1\omega_2}{\omega_3\omega_4}} \equiv e^{\beta\delta} \ , \ \xi = \frac{\omega_5\omega_6}{\sqrt{\omega_1\omega_2\omega_3\omega_4}} \equiv e^{2\beta\epsilon} \ , \tag{D.1}$$

and

$$H = \sqrt{\frac{\omega_1\omega_3}{\omega_2\omega_4}} \equiv e^{2\beta h} \ , \ V = \sqrt{\frac{\omega_1\omega_4}{\omega_2\omega_3}} \equiv e^{2\beta v} \ , \tag{D.2}$$

where h and v are the horizontal and vertical field components. The interaction constant is introduced as

$$\Delta_6 = \frac{1}{2}\left(\eta + \frac{1}{\eta} - \xi\right) \ . \tag{D.3}$$

Using these new variables the model is symmetric with respect to reversing all arrows and the external electric field. The textbook solution of the asymmetric six-vertex model runs as follows. In calculating the free energy, with the transformed variables defined in Eqs. (D.1) - (D.3) the rapidity ϕ_0 (see Appendix B) is introduced as

$$\begin{aligned} e^{-\phi_0} &= \frac{1+e^{\lambda}\eta}{e^{\lambda}+\eta}\ , \quad \text{for } \Delta_6 \ < \ -1\ , \quad \Delta_6 \ = \ -\cosh\lambda\ , \quad \lambda \ > \ 0\ ; \\ e^{-i\phi_0} &= \frac{1+e^{i\mu}\eta}{e^{i\mu}+\eta}\ , \quad \text{for } |\Delta_6| \ < \ 1\ , \quad \Delta_6 \ = \ -\cos\mu\ , \quad 0 \ < \ \mu \ < \ \pi\ ; \\ e^{-\phi_0} &= \frac{e^{\nu}\eta-1}{\eta-e^{\nu}}\ , \quad \text{for } \Delta_6 \ > \ 1\ , \quad \Delta_6 \ = \ \cosh\nu\ , \quad \nu \ > \ 0 \quad . \end{aligned} \tag{D.4}$$

The free energy of the asymmetric six-vertex model is given in terms of the rapidity ϕ_0. We note that the parametrization from Eq. (D.4) are for the $\eta \leq 1$ case. For the opposite case $\eta \geq 1$ the $\phi_0 \leftrightarrow -\phi_0$ change should be performed. Combining Eqs. (D.4) with Eqs. (D.1) and (D.3) the products of the Boltzmann weights can be expressed as

$$\begin{aligned} \omega_1\omega_2 &= \sinh^2\frac{1}{2}(\lambda-\phi_0)\ , \quad \Delta_6 \ < \ -1\ ; \\ &= \sin^2\frac{1}{2}(\mu-\phi_0)\ , \quad |\Delta_6| \ \leq \ 1\ ; \\ &= \sinh^2\frac{1}{2}(\nu-\phi_0)\ , \quad \Delta_6 \ > \ 1 \quad , \end{aligned} \tag{D.5}$$

$$\begin{aligned} \omega_3\omega_4 &= \sinh^2\frac{1}{2}(\lambda+\phi_0)\ , \quad \Delta_6 \ < \ -1\ ; \\ &= \sin^2\frac{1}{2}(\mu+\phi_0)\ , \quad |\Delta_6| \ \leq \ 1\ ; \\ &= \sinh^2\frac{1}{2}(\nu+\phi_0)\ , \quad \Delta_6 \ > \ 1 \quad , \end{aligned} \tag{D.6}$$

and

$$\begin{aligned} \omega_5\omega_6 &= \sinh^2\lambda\ , \quad \Delta_6 \ < \ -1\ ; \\ &= \sin^2\mu\ , \quad |\Delta_6| \ \leq \ 1\ ; \\ &= \sinh^2\nu\ , \quad \Delta_6 \ > \ 1 \quad . \end{aligned} \tag{D.7}$$

It can be seen immediately that for any $\omega_1 = a$ finite and $\omega_2 = 0$ Eqs. (D.5) imply $\lambda = \phi_0$ (respectively, $\mu = \phi_0$ or $\nu = \phi_0$) in the three cases. Hence, Eqs. (D.6) and (D.7) yield $\omega_3\omega_4 = \omega_5\omega_6$, which is nothing else than the free fermion condition.